Planar maps and random partitions

Jérémie Bouttier

UNIVERSITÉ PARIS SUD
FACULTÉ DES SCIENCES D'ORSAY
université PARIS-SACLAY

IPhT SACLAY

UNIVERSITÉ PARIS-SUD

École doctorale de mathématiques Hadamard (ED 574)
Institut de Physique Théorique (CEA/DRF/IPhT, CNRS UMR 3681)

Mémoire présenté pour l'obtention du

Diplôme d'habilitation à diriger les recherches

Discipline : Mathématiques

par

Jérémie BOUTTIER

Cartes planaires et partitions aléatoires

Rapporteurs :
CHRISTIAN KRATTENTHALER
JEAN-FRANÇOIS LE GALL
PAUL ZINN-JUSTIN

Date de soutenance : 2 décembre 2019

Composition du jury :

PHILIPPE CHASSAING	(Président)
BERTRAND EYNARD	(Examinateur)
ALICE GUIONNET	(Examinatrice)
CHRISTIAN KRATTENTHALER	(Rapporteur)
JEAN-FRANÇOIS LE GALL	(Rapporteur)
GILLES SCHAEFFER	(Examinateur)

Cartes planaires et partitions aléatoires

Résumé Ce mémoire d'habilitation est une synthèse des travaux de recherche que j'ai effectués entre 2005 et 2019. Il s'organise en quatre chapitres. Les trois premiers portent sur les cartes planaires aléatoires. Le chapitre 1 s'intéresse à leurs propriétés métriques : à partir d'une bijection générale entre cartes et mobiles, on calcule la fonction à trois points des quadrangulations, avant d'évoquer le lien avec les fractions continues. Le chapitre 2 présente la décomposition en tranches, une approche bijective unifiée qui s'applique notamment aux cartes irréductibles. Le chapitre 3 a pour sujet le modèle de boucles $O(n)$ sur les cartes planaires : par une décomposition combinatoire récursive on obtient le diagramme de phase, puis on étudie les statistiques d'emboîtements entre boucles. Le chapitre 4 porte quant à lui sur les partitions aléatoires et processus de Schur, en allant des pavages de dominos pentus aux systèmes fermioniques.

Hormis un avant-propos en français, le document est écrit en anglais. La numérotation des pages de cette version électronique diffère de celle des exemplaires imprimés distribués lors de la soutenance.

Planar maps and random partitions

Abstract This habilitation thesis summarizes the research that I have carried out from 2005 to 2019. It is organized in four chapters. The first three deal with random planar maps. Chapter 1 is about their metric properties: from a general map-mobile bijection, we compute the three-point function of quadrangulations, before discussing the connection with continued fractions. Chapter 2 presents the slice decomposition, a unified bijective approach that applies notably to irreducible maps. Chapter 3 concerns the $O(n)$ loop model on planar maps: by a combinatorial decomposition, we obtain the phase diagram before studying loop nesting statistics. Chapter 4 deals with random partitions and Schur processes, from steep domino tilings to fermionic systems.

The document is written in English, except an introduction in French. The page numbers in this electronic version differ from those of the printed copies given at the defence.

Email : `jeremie.bouttier@ipht.fr`

Affiliations :
Institut de Physique Théorique, Université Paris-Saclay, CEA, CNRS, F-91191 Gif-sur-Yvette
Univ Lyon, Ens de Lyon, Univ Claude Bernard, CNRS, Laboratoire de Physique, F-69342 Lyon

Support :
Agence Nationale de la Recherche (ANR-12-JS02-001-01/Cartaplus, ANR-14-CE25-0014/Graal, ANR-18-CE40-0033/Dimers), Ville de Paris (programme Émergences *Combinatoire à Paris*), CNRS INSMI (PEPS CARMA)

Contents

Preface

This aim of this document is to summarize the research that I have carried out after the completion of my doctoral thesis in 2005. This research has been published in the articles [1–28] [1] [2]. Of course I shall not attempt to be exhaustive, but I will rather try to present how these different papers articulate with one another.

My presentation consists of four chapters, which roughly correspond to four different "threads" of my research. The first three chapters deal with planar maps. Chapter 1 describes results about the metric properties of random planar maps, which form the continuation of the work done during my doctoral thesis. Chapter 2 is devoted to the slice decomposition, an alternate bijective approach for studying planar maps. Chapter 3 deals with the $O(n)$ loop model on random planar maps, a statistical physics model with a rich critical behavior. In the last Chapter 4, we leave the realm of planar maps and enter that of Schur processes, which have been the main topic of my recent research.

Each chapter aims at being as self-contained as possible: it starts with some reminders of the context, then consists of two or three core sections where I highlight one or two main results, and ends with a conclusion discussing perspectives for future research. For convenience I have gathered some common definitions in the mathematical preliminaries at the beginning of the document.

Note that this document is deliberately *not* written in the style of a mathematical paper, as my goal is to narrate stories about my research. Even if I follow the tradition of emphasizing some theorems, definitions and other remarks, I avoided using the proof environment: where relevant I provide some elements of justification in the main text, and in any case the reader is invited to consult the original papers where full proofs are given.

For brevity, I had to exclude several papers from my presentation. The most notable exclusion are the three papers [18, 20, 23] which deal with certain Markov chains whose study was motivated by juggling. But two out of these papers were written with my former student François Nunzi (whom I supervised with Sylvie Corteel), so I may simply point to his thesis [Nun16] for a nice account of this topic.

1. A separate bibliography is provided for these articles, with numbered citations such as [1]. References to works by other authors, or to works done during my doctoral thesis, are given in the general bibliography with "alpha-style" citations such as [Bou05].

2. Due to the important fluctuations of the duration of the refereeing process, these articles are sorted according to the date of their initial posting on arXiv, which is a slightly more accurate indication of the period at which they were conceived.

Avant-propos

> *Mathématiques discrètes et continues se rencontrent et se complètent volontiers harmonieusement* [CF03].

Ce mémoire a pour but de présenter les travaux de recherche que j'ai effectués depuis ma soutenance de thèse de doctorat en 2005. Il s'appuie sur les publications [1–28] [1] dont la liste [2] est donnée un peu plus loin. Il ne s'agit bien sûr pas de donner une présentation exhaustive mais plutôt, au travers de quatre chapitres, de présenter quelques idées et le cheminement qui m'a conduit de l'une à l'autre.

Commençons tout d'abord par tenter d'identifier la démarche générale dans laquelle s'inscrivent mes recherches, qu'on peut situer à l'interface entre la physique statistique, la combinatoire et la théorie des probabilités. Le lien entre physique statistique et combinatoire remonte à Boltzmann lui-même, et à sa célèbre formule $S = k_B \ln W$ qui définit l'entropie microcanonique S d'un système à l'équilibre macroscopique en fonction de son nombre W de micro-états (k_B étant la constante de Boltzmann). Ce lien s'est ensuite particulièrement développé autour des *modèles exactement solubles* [3] : la physique statistique fait grand usage de tels modèles dans lesquelles les grandeurs physiques pertinentes (fonction de partition, fonctions de corrélations...) peuvent être déterminées de manière exacte, au sens où on en a une expression suffisamment explicite pour pouvoir passer à la limite thermodynamique, calculer des exposants critiques, etc. Ce phénomène résulte d'une structure mathématique sous-jacente, appelée généralement *intégrabilité* [4]. L'étude des modèles intégrables discrets amène de nombreuses questions de nature combinatoire. Nous en verrons deux illustrations au cours de ce mémoire, au travers des cartes planaires d'une part, des processus de Schur d'autre part. La théorie des probabilités apporte quant à elle de nouveaux outils, notamment pour l'étude des *limites d'échelle* [5]. En effet, dès lors qu'on s'intéresse aux propriétés macroscopiques des modèles, il est possible d'oublier

1. Afin de différencier ces publications des citations de travaux d'autres auteurs, ou bien de travaux effectués pendant ma thèse de doctorat, j'utiliserai des références numérotées comme [1] pour les premières, et des références dans le style «alpha», comme [Bou05], pour les secondes qui sont listées dans la bibliographie générale à la fin du mémoire.

2. Cette liste est ordonnée selon la date de publication sur arXiv, qui reflète mieux que celle du journal la période de conception des articles.

3. Voir par exemple le livre de Baxter [Bax82] qui traite des modèles sur réseaux bidimensionnels solubles par l'ansatz de Bethe et méthodes liées.

4. Même si cette notion est difficile à définir précisément au-delà du cadre de la mécanique classique.

5. Un autre apport intéressant des probabilités, peu discutée dans ce mémoire, est celle des «limites locales» que l'on peut rapprocher du formalisme des mesures de Gibbs en mécanique statistique. L'idée est alors de décrire directement un système infini sans passer par les systèmes de taille finie. Par bien des aspects, et paradoxalement, cette description peut s'avérer plus simple.

certains de leurs détails microscopiques, et les probabilités fournissent un cadre rigoureux pour ce faire. On arrive parfois ainsi à donner une définition mathématique d'un objet-limite continu capturant l'essence de la physique à grande échelle. Par exemple, la carte brownienne [6] correspond à la limite d'échelle générique des cartes planaires aléatoires non décorées, et le processus d'Airy à celle des processus de Schur autour d'un point générique de la courbe arctique [7]. Cette démarche donne un sens mathématique au phénomène d'*universalité*, puisque différents modèles discrets peuvent avoir une même limite d'échelle continue et donc les mêmes propriétés macroscopiques. En outre, cela justifie la pertinence des modèles exactement solubles : en effet on s'appuie typiquement sur leur intégrabilité afin de les étudier, analyse qui pourra être ensuite étendue au continu et à d'autres modèles par universalité. Comme aboutissement, on arrive à des *résultats rigoureux* qui, au côté des validations expérimentales, permettent de confirmer ou réfuter les prédictions de la physique théorique.

Entrons à présent dans le contenu de ce mémoire. Il est constitué de quatre chapitres principaux, qui sont essentiellement indépendants les uns des autres : chaque chapitre commence par un bref rappel du contexte, comprend ensuite deux ou trois sections présentant certains de mes résultats, et se conclut sur une discussion de quelques pistes de recherche future. Par commodité, quelques définitions communes sont regroupées dans les préliminaires mathématiques en introduction du mémoire.

Les trois premiers chapitres portent sur les cartes planaires, et sont consacrés respectivement aux propriétés métriques des cartes aléatoires, un sujet auquel j'ai continué à m'intéresser après ma thèse de doctorat, à la décomposition en tranches, une nouvelle approche bijective pour l'étude des cartes, et enfin au modèle de boucles $O(n)$ sur les cartes planaires, un modèle de physique statistique au riche comportement critique. Je ne donnerai pas ici de présentation générale du vaste sujet de recherche que sont les cartes, ce qu'on pourra trouver dans d'autres références. Je mentionnerai, entre autres, la revue récente de Gilles Schaeffer [Sch15] pour les aspects relevant de la combinatoire énumérative et bijective, les notes de cours successives de Jean-François Le Gall, Grégory Miermont et Nicolas Curien [LGM12, Mie14, Cur19] pour les aspects probabilistes, le mémoire d'habilitation de Guillaume Chapuy [Cha18] pour une évocation du lien avec les hiérarchies intégrables, et enfin le premier chapitre de ma thèse de doctorat [Bou05] ou la première partie de celle d'Ariane Carrance [Car19] pour une discussion des liens entre cartes et physique théorique.

Dans le quatrième et dernier chapitre, je quitte le monde des cartes planaires pour évoquer mes travaux récents autour des partitions aléatoires, et plus précisément des processus de Schur. Le domaine général est celui des probabilités intégrables auxquelles les notes de cours d'Alexei Borodin et Vadim Gorin [BG16] donnent une bonne introduction. Ma présentation suivra la manière dont j'ai été amené à m'intéresser à ce domaine, en allant des pavages de dominos aux systèmes de fermions à température finie.

6. Voir les références données à la section 1.1.

7. Voir par exemple l'article de Prähofer et Spohn [PS02] qui traite du modèle de croissance polynucléaire (*PNG*), qui se ramène à un processus de Schur. Nous rencontrerons brièvement le noyau d'Airy et son analogue à température finie au chapitre 4.

Dans un souci de concision, j'ai été amené à exclure plusieurs travaux de la présentation qui est faite dans ce mémoire. L'omission la plus importante concerne les trois articles [18, 20, 23] qui portent sur des modèles de jonglage aléatoire. Sur ce sujet, le lecteur pourra consulter la thèse de François Nunzi [Nun16].

Résumé détaillé du mémoire

Le chapitre 1 est consacré aux propriétés métriques des cartes planaires aléatoires. J'y présente quelques résultats issus de travaux poursuivant ceux effectués pendant ma thèse de doctorat. La présentation n'est pas chronologique puisque, après un rappel du contexte dans la section 1.1, je commence par présenter en section 1.2 une bijection obtenue en 2013 avec Éric Fusy et Emmanuel Guitter dans l'article [19]. Il s'agit d'une correspondance entre *cartes convenablement étiquetées* (cartes planaires dont les sommets sont étiquetés par des entiers, de telle sorte que deux sommets adjacents ont des étiquettes consécutives) et *mobiles* (cartes planaires biparties, où les sommets d'un type sont étiquetés par des entiers, et les autres ne sont pas étiquetés mais imposent certaines contraintes sur leurs étiquettes adjacentes). Elle unifie plusieurs constructions antérieures : la célèbre bijection de Cori-Vauquelin-Schaeffer [CV81, Sch98] entre quadrangulations enracinées et arbres bien étiquetés, une première généralisation que nous avions obtenue avec Philippe Di Francesco et Emmanuel Guitter [BDFG04] et qui relie cartes biparties enracinées et mobiles à une face, et une seconde généralisation due à Miermont, Ambjørn et Budd [Mie09, AB13] [8] qui relie quadrangulations convenablement étiquetées et cartes bien étiquetées.

Cette *approche bijective* est particulièrement intéressante pour étudier les distances dans les cartes planaires. En effet, par des choix d'étiquetages judicieux, on peut lire certaines propriétés métriques des cartes dans les mobiles correspondants, qui se trouvent être des arbres ou des cartes à un petit nombre de faces. L'analyse de ces derniers objets peut alors être menée à bien par les différentes méthodes connues pour étudier les arbres : décompositions récursives donnant des équations pour les séries génératrices, codage par des marches permettant de passer à la limite d'échelle, etc.

Dans la section 1.3, je donne un exemple d'une telle analyse pour le calcul de la *fonction à trois points* des quadrangulations, d'après l'article [6] écrit avec Emmanuel Guitter. Le problème est de trouver la série génératrice des quadrangulations ayant trois points marqués à distances prescrites. Par une spécialisation de la bijection présentée en section 1.2, le problème est ramené à celui du comptage de cartes bien étiquetées à trois faces, avec des valeurs prescrites pour les étiquettes minimales incidentes à chaque face. De façon surprenante, ce calcul peut être mené à bien de manière explicite, au sens où on peut donner une formule close pour les séries génératrices correspondantes. Il s'agit d'une manifestation d'un phénomène d'*intégrabilité discrète* que nous avions déjà observé dans le calcul de la fonction à deux points [BDFG03a]. À partir de l'expression exacte discrète, il est facile de passer à la limite d'échelle et calculer ainsi la fonction à trois

8. Voir la remarque 1 dans [19] pour une discussion de l'équivalence entre la formulation de Miermont et celle d'Ambjørn et Budd.

points de la carte brownienne, c'est-à-dire la loi jointe des distances entre trois points tirés au hasard uniformément.

La section 1.4 revient sur le phénomène d'intégrabilité discrète mentionné ci-dessus, dans un cadre légèrement différent : on considère la fonction à deux points seulement, mais dans le contexte plus général des *cartes de Boltzmann*. Avec Philippe Di Francesco et Emmanuel Guitter, nous avions conjecturé une expression exacte pour cette fonction à deux points dans l'article [BDFG03a]. Cette expression a été prouvée quelques années plus tard, dans l'article [10] écrit avec Emmanuel Guitter. Le point de départ de ce travail est l'observation, faite auparavant dans l'article [8], que la fonction à deux points intervient dans le développement en *fraction continue* de la série génératrice des cartes à un bord. Par la théorie générale des fractions continues, on peut donc déduire la première de la seconde, à l'aide de *déterminants de Hankel* qu'on peut identifier à des caractères de groupes orthogonaux ou symplectiques.

Je conclus ce chapitre par la section 1.5 qui évoque quelques questions ouvertes.

Le chapitre 2 est consacré à la *décomposition en tranches* des cartes planaires. Il s'agissait initialement d'une reformulation de la bijection de [BDFG04] évoquée dans les articles [8, 10, 13], mais sa portée plus générale a été comprise dans l'article [16] écrit avec Emmanuel Guitter. En effet, nous y expliquons comment adapter la construction au cas des cartes *irréductibles*, c'est-à-dire des cartes dans lesquelles tout cycle a une longueur au moins égale à un entier $d \geq 0$ fixé, et tout cycle de longueur d est le bord d'une face. Une telle contrainte semble difficile à concilier avec la bijection de la section 1.2.

La section 2.1 rappelle le contexte et notamment le développement du *canevas bijectif* qui vise à unifier les différentes bijections cartes-arbres connues et à en découvrir de nouvelles, en s'appuyant sur la théorie des orientations.

La section 2.2 donne la définition générale des tranches. Il s'agit de cartes avec un bord et trois points marqués A, B, C sur celui-ci, tels que le côté AB est une géodésique entre A et B, et le côté AC est l'unique géodésique entre A et C. Je décris ensuite deux opérations importantes :

— la décomposition d'une tranche en tranches *élémentaires*, qui consiste à découper le long de toutes les *géodésiques gauches* allant des sommets du côté BC vers A,

— l'*enroulement*, qui consiste à identifier les côtés AB et AC, en laissant éventuellement quelques arêtes non identifiées si les longueurs sont différentes : cette opération produit alors des cartes *annulaires* (ayant deux faces marquées).

À l'aide de ces deux opérations, on parvient à exprimer la série génératrice des cartes annulaires en fonction de celle des tranches élémentaires, qui est elle-même égale à celle bien connue des cartes pointées enracinées.

Dans la section 2.3, j'explique comment adapter la décomposition en tranches au cas des cartes irréductibles. La difficulté principale est d'énumérer les tranches élémentaires, qui ne sont plus en bijection avec les cartes pointées enracinées. On est amené à introduire la notion de *quasi-tranche*, en modifiant légèrement la définition des tranches élémentaires : le côté AB n'est plus nécessairement une géodésique entre A et B, mais seulement un chemin de longueur minimale parmi tous les chemins évitant l'arête BC.

Par une nouvelle méthode de décomposition des quasi-tranches, on obtient un système d'équations algébriques qui détermine leurs séries génératrices. On peut alors énumérer les cartes annulaires irréductibles en appliquant l'opération d'enroulement. Celle-ci ne pose pas de difficulté particulière, une fois observé qu'il convient de traiter à part les cycles séparant les deux faces marquées.

Quelques pistes de recherche sont mentionnées en section 2.4.

Au chapitre 3, nous considérons un modèle de physique statistique sur les cartes planaires, le *modèle de boucles* $O(n)$. Les configurations sont des cartes planaires décorées de boucles (cycles disjoints sur la carte duale), chacune recevant un poids n qui joue le rôle d'un paramètre non local.

La section 3.1 passe brièvement en revue la littérature au sujet des modèles de physique statistique sur les cartes. Beaucoup de travaux ont porté sur le modèle de Potts à q états, ses différentes reformulations et ses spécialisations. En particulier, le modèle de boucles $O(n)$ est lié aux points «auto-duaux» du modèle de Potts, avec $q = n^2$. Lorsque n varie dans l'intervalle $[0, 2]$, il existe une famille de points critiques dont les exposants varient continument avec n. On s'attend à ce que la géométrie des cartes sous-jacentes soit affectée par les corrélations à longue échelle aux points critiques, mais cela reste une question largement ouverte.

Les sections 3.2 et 3.3 présentent principalement les résultats de l'article [12] écrit avec Gaëtan Borot et Emmanuel Guitter. Je me concentrerai sur le cas des boucles *rigides* sur les quadrangulations qui est plus simple à analyser. Dans la section 3.2, je présente la décomposition combinatoire dite des *poupées russes*[9] : à une configuration de boucles sur une quadrangulation à un bord, on associe la carte externe formée par les arêtes extérieures à toutes les boucles. Il s'agit d'une carte sans boucles mais pouvant avoir des faces de degrés arbitrairement grands. Nous verrons que cette carte suit la loi d'une carte de Boltzmann, dont les paramètres sont donnés par une équation de point fixe qui donne également la fonction de partition du modèle. J'esquisse ensuite dans la section 3.3 la façon dont l'équation de point fixe peut être résolue, en réécrivant celle-ci sous forme d'une équation fonctionnelle pour la *résolvante*. Cette équation fonctionnelle possède une solution explicite particulièrement simple aux *points critiques non génériques* du modèle. En particulier, on peut voir que, à ces points, la loi du degré d'une face typique de la face externe a une queue lourde. Par des résultats de Le Gall et Miermont [LGM11], la limite d'échelle diffère de la carte brownienne.

La section 3.4 s'inspire de l'article [25] écrit avec Gaëtan Borot et Bertrand Duplantier. On s'y intéresse à la structure des emboîtements entre boucles et, plus précisément, à la *profondeur* d'un sommet marqué, qui est défini comme le nombre de boucles séparant ce sommet du bord. On montre que, à un point critique non générique, la profondeur d'un sommet tiré au hasard croît logarithmiquement avec la longueur du bord (plus précisément, on établit un théorème central limite et un principe de grandes déviations pour cette profondeur). La preuve repose sur le calcul d'une série génératrice raffinée, qu'on parvient à mener à bien en adaptant la méthode utilisée à la section 3.3.

9. Ce terme me semble préférable à celui de *joint de culasse* qui serait la traduction littérale de *gasket*.

La section 3.5 présente quelques perspectives.

Dans le chapitre 4, je quitte le monde des cartes planaires pour évoquer mes travaux récents autour des *processus de Schur*. La section 4.1 présente brièvement le contexte, qui est celui des *probabilités intégrables*. J'y raconte également de quelle manière j'ai été amené à m'intéresser personnellement à ce sujet, par un groupe de travail sur les hiérarchies intégrables où je m'étais familiarisé avec le formalisme des *fermions libres*.

La section 4.2 présente mes premières contributions au domaine, et reprend les articles [21, 24] écrits tous deux avec Guillaume Chapuy et Sylvie Corteel, ainsi que Cédric Boutillier et Sanjay Ramassamy pour le second. Nous définissons la famille des *pavages pentus*, qui sont des pavages du plan par des dominos (rectangles 2×1) obtenus à partir d'un certain pavage fondamental en effectuant une séquence de mouvements élémentaires. Ces pavages sont en bijection avec des configurations de dimères sur un graphe dit en *gare de triage*. Par spécialisation, nous retrouvons plusieurs familles de pavages connues : partitions planes, partitions-pyramides et pavages du diamant aztèque. Nous donnons des expressions explicites pour la série génératrice des pavages pentus, ainsi que pour les *fonctions de corrélation* qui sont les probabilités d'occurrence conjointe de certains types de dominos à des positions prescrites. Nous faisons également un lien avec la théorie de Kasteleyn pour les modèles de dimères.

Dans la section 4.3, je m'intéresse aux pavages pentus avec des *conditions aux bords périodiques ou libres*. Leurs séries génératrices avaient été calculées dans [21], mais nous n'avions pas été alors capables de calculer leurs fonctions de corrélation. C'est un problème sur lequel je suis revenu dans les articles [26, 27] écrits tous deux avec Dan Betea, ainsi que Peter Nejjar et Mirjana Vuletić pour le premier. Nous y calculons les fonctions de corrélation des processus de Schur avec des conditions aux bords respectivement libres et périodiques, via le formalisme des fermions libres [10]. J'esquisse les idées principales de notre approche, qui consiste à considérer des fermions *à température finie* dans le cas périodique, et effectuer une *transformation de Bogolioubov* dans le cas libre.

La section 4.4 porte sur les applications des considérations précédentes. En effet, on s'attend à ce que la modification des conditions aux bords permette d'observer de nouvelles limites d'échelles. Je considère principalement le cas périodique, d'après [27] (le cas libre étant l'objet de travaux en cours). On s'intéresse au cas le plus simple de processus de Schur périodique, qui est une mesure sur les partitions d'entiers appelée *mesure de Plancherel cylindrique*. Cette mesure interpole entre la mesure canonique et la mesure de Plancherel usuelle sur les partitions. On considère la loi de la plus grande part et on montre que, après recentrage et normalisation, celle-ci admet plusieurs limites possibles :

— la loi de Gumbel dans un régime dit de haute température (incluant la mesure canonique),

— la loi de Tracy-Widom de l'ensemble gaussien unitaire (*GUE*) dans un régime dit de basse température (incluant la mesure de Plancherel usuelle),

10. Dans le cas périodique, les fonctions de corrélations avaient précédemment été calculées par Borodin [Bor07] via une autre méthode. La nôtre semble plus simple.

— et enfin, dans un régime intermédiaire, une loi interpolant entre les deux lois précédentes, qui avait précédemment été rencontrée par Johansson dans le cadre des matrices aléatoires.

Du point de vue physique, cette transition de phase peut être expliquée par une compétition entre les fluctuations d'origine thermique et celles d'origine quantique.

Enfin, la section 4.5 indique quelques directions pour le futur.

Remerciements

Je voudrais rendre ici hommage à toutes les personnes qui m'auront amené à présenter ce mémoire d'habilitation, et plus généralement d'avoir la chance et le plaisir d'exercer le métier de chercheur. La liste de ces personnes est longue, et je prie d'avance celles que j'oublierais de citer ici nommément de bien vouloir me pardonner.

Comme d'usage je commencerai par le jury. Merci tout d'abord à Jean-François Le Gall qui a bien voulu être mon rapporteur interne pour l'école doctorale, et m'a permis de passer la première étape de la Commission de la recherche. Merci ensuite à Christian Krattenthaler et Paul Zinn-Justin qui ont accepté d'être mes rapporteurs externes, et ont recommandé de m'autoriser à soutenir. Merci enfin à Philippe Chassaing, Bertrand Eynard, Alice Guionnet et Gilles Schaeffer qui me font l'honneur d'être mes examinateurs.

J'ajoute au passage des remerciements pour Frédéric Paulin, directeur de l'école doctorale, pour ses nombreux conseils tout au cours de la procédure, et au comité *ad hoc* qui a donné tous les avis favorables nécessaires.

Je voudrais ensuite témoigner de ma profonde gratitude envers les institutions de recherche françaises, et envers les personnes qui les font vivre.

En premier lieu vient mon employeur, le Commissariat à l'énergie atomique et aux énergies alternatives, et au sein de celui-ci l'Institut de physique théorique où j'ai le privilège d'être chercheur permanent depuis 2006. Je dois beaucoup à mes chefs d'institut successifs : Henri Orland, Michel Bauer et François David. Henri a pris la décision capitale de m'offrir un poste, Michel et François m'ont soutenu avec énergie dans la suite de ma carrière, y compris pour mes demandes de mobilité hors de l'IPhT. Je remercie également tout le personnel de support : Sylvie Zaffanella qui a traité avec efficacité et gentillesse toutes mes missions et autres demandes, Laure Sauboy qui m'a notamment aidé pour l'organisation de la conférence Itzykson 2015, Anne Angles à qui je souhaite beaucoup de succès dans ses nouvelles fonctions, Emmanuelle de Laborderie, Loïc Bervas, Patrick Berthelot et Laurent Sengmanivanh... Merci enfin à tous mes collègues, parmi lesquels mes commensaux réguliers Jean-Marc Luck, Marc Barthélémy, Cécile Monthus, Jérôme Houdayer et Lenka Zdeborová, pour les nombreuses discussions intéressantes que nous avons eues.

J'ai passé l'année 2011-2012 au Laboratoire d'informatique algorithmique : fondements et applications (LIAFA, devenu depuis IRIF). Je souhaite y remercier notamment son directeur d'alors, Pierre Fraigniaud, qui a bien voulu m'accueillir, Noëlle Delgado qui

a traité mes demandes administratives y compris après mon séjour en raison de l'ANR Cartaplus, et tous les membres de l'équipe Combinatoire et du groupe de lecture.

De 2012 à 2016, j'ai été professeur associé à temps partiel au Département de mathématiques et applications de l'École normale supérieure. Merci à Wendelin Werner et Thierry Bodineau qui ont pensé à moi pour ce poste, à Olivier Debarre et Claude Viterbo qui ont été mes directeurs successifs au DMA, à Bénédicte Auffray et Zaïna Elmir qui m'ont offert leur précieux soutien administratif au laboratoire, à Laurence Vincent puis Albane Trémeau qui ont fait de même côté enseignement, aux collègues de l'équipe Probabilités et statistiques, à Guilhem Semerjian avec qui j'ai eu la chance d'enseigner... sans oublier les élèves avec qui j'ai eu de nombreux échanges enrichissants.

Depuis 2016, je suis mis à disposition du Laboratoire de physique à l'École normale supérieure de Lyon. Je remercie Thierry Dauxois, son directeur, et Jean-Michel Maillet, chef de l'équipe de physique théorique, qui ont appuyé mon «transfert» et plusieurs de mes projets lyonnais. Je salue Grégory Miermont que j'ai eu le plaisir de retrouver à Lyon, ne perdons pas nos bonnes habitudes d'organiser des évènements scientifiques ! Merci également à Laurence Mauduit, Nadine Clervaux et Fatiha Bouchneb pour leur soutien administratif, au secrétariat de l'UMPA qui fait de même lorsque je m'aventure au quatrième étage, à Krzysztof Gawędzki et Giuliano Niccoli qui ont partagé ou partagent leur bureau avec moi, et à Laurent Chevillard avec qui j'échange toujours volontiers au détour d'un couloir.

Je dois ajouter à ma liste d'institutions celles qui financent mes recherches, notamment l'Agence nationale de la recherche et la Ville de Paris. Merci surtout aux porteurs de projets —Cartaplus, Graal, Combinatoire à Paris, Carma et Dimers— pour leurs efforts qui s'avèrent de plus en plus nécessaires pour que nous puissions effectuer nos missions et nous équiper sans contraintes excessives.

Enfin, j'ai débuté ma carrière postdoctorale hors de France, à l'Institut de physique théorique de l'Université d'Amsterdam. Merci à Bernard Nienhuis qui m'a offert un contrat de deux ans, et à tous les collègues que j'ai côtoyés là-bas et que j'ai encore plaisir à recroiser aujourd'hui.

Je me tourne à présent vers mes collaborateurs, compagnons de route qui me sont indispensables comme ma liste de publications peut en témoigner.

Tout d'abord vient Emmanuel Guitter, qui de directeur de thèse est devenu mon principal coauteur et le reste encore à ce jour. Ce fut une grande chance de pouvoir débuter ma carrière avec lui, et d'obtenir tous les résultats qui peuplent l'essentiel des trois premiers chapitres de ce mémoire. Merci également à Philippe Di Francesco, mon autre directeur de thèse, à qui je suis toujours fier de pouvoir raconter mes recherches, lorsque nous parvenons à nous croiser à Saclay.

Je dois beaucoup à Sylvie Corteel, qui m'a proposé de venir passer une année au LIAFA. Cela a eu un grand impact sur ma carrière, et m'a permis m'intéresser à de nouvelles questions qui ont notamment abouti au quatrième chapitre de ce mémoire.

Je suis reconnaissant envers Dan Betea, avec qui j'ai cheminé ces dernières années dans le monde des probabilités intégrables. C'est bien souvent vers lui que je me tourne en premier pour vérifier l'état de l'art ou tester une idée.

Marie Albenque tient une place particulière puisqu'elle a été ma première collaboratrice. J'espère que nous arriverons enfin à «plier» les tranches eulériennes et autres fractions multicontinues ! Merci également à Gaëtan Borot qui m'aura tout appris sur les subtilités du modèle $O(n)$ et qui aura été si patient, à Guillaume Chapuy qui est non seulement un chercheur accompli mais aussi un porteur bienveillant, à Arvind Ayyer qui m'a transmis le goût du jonglage aléatoire, et aussi à Chikashi Arita, Cédric Boutillier, Mark Bowick, Bertrand Duplantier, Éric Fusy, Momo Jeng, Paul Krapivsky, Svante Linusson, Kirone Mallick, Peter Nejjar, Sanjay Ramassamy et Mirjana Vuletić. Je suis heureux d'avoir coencadré les thèses de François Nunzi et Linxiao Chen, avec comme codirecteurs respectifs Sylvie Corteel et Nicolas Curien.

Je terminerai par ma famille qui m'entoure de son affection au quotidien. J'ai le bonheur de pouvoir toujours compter sur le soutien inconditionnel de mes parents, après plus de quarante ans. Merci aussi à Monique et Bernard qui viennent parfois prêter main forte à la maison quand je suis en déplacement, à Mathieu et Mélanie qui sont d'une grande complicité, et à Olivier et Kirsten chez qui j'ai terminé la rédaction de ce mémoire. J'ai une pensée émue pour mes grands-parents, qui m'ont tant donné et que j'aurais aimé pouvoir inviter à ma soutenance. Merci enfin à Sophie qui partage ma vie avec amour. Et, pour conclure, je souhaite beaucoup de joie à mes petits chercheurs en herbe, Chloé et Raphaël, dans leurs découvertes de tous les jours.

List of publications

[1] J. Bouttier, P. Di Francesco, and E. Guitter. Combinatorics of bicubic maps with hard particles. *J. Phys. A*, 38(21) 4529–4559, 2005. arXiv:math/0501344 [math.CO].

[2] J. Bouttier, P. Di Francesco, and E. Guitter. Multicritical continuous random trees. *J. Stat. Mech. Theory Exp.*, P04004, 2006. arXiv:math-ph/0603007 [math-ph].

[3] J. Bouttier, P. Di Francesco, and E. Guitter. Blocked edges on Eulerian maps and mobiles: application to spanning trees, hard particles and the Ising model. *J. Phys. A*, 40(27) 7411–7440, 2007. arXiv:math/0702097 [math.CO].

[4] J. Bouttier, M. Bowick, E. Guitter, and M. Jeng. Vacancy localization in the square dimer model. *Phys. Rev. E*, 76 041140, 2007. arXiv:0706.1016 [cond-mat.stat-mech].

[5] J. Bouttier and E. Guitter. Statistics in geodesics in large quadrangulations. *J. Phys. A*, 41(14) 145001, 2008. arXiv:0712.2160 [math-ph].

[6] J. Bouttier and E. Guitter. The three-point function of planar quadrangulations. *J. Stat. Mech. Theory Exp.*, P07020, 2008. arXiv:0805.2355 [math-ph].

[7] J. Bouttier and E. Guitter. Confluence of geodesic paths and separating loops in large planar quadrangulations. *J. Stat. Mech. Theory Exp.*, P03001, 2009. arXiv:0811.0509 [math-ph].

[8] J. Bouttier and E. Guitter. Distance statistics in quadrangulations with a boundary, or with a self-avoiding loop. *J. Phys. A*, 42(46) 465208, 2009. arXiv:0906.4892 [math-ph].

[9] J. Bouttier and E. Guitter. Distance statistics in quadrangulations with no multiple edges and the geometry of minbus. *J. Phys. A*, 43(20) 205207, 2010. arXiv:1002.2552 [math-ph].

[10] J. Bouttier and E. Guitter. Planar maps and continued fractions. *Comm. Math. Phys.*, 309(3) 623–662, 2012. arXiv:1007.0419 [math.CO].

[11] J. Bouttier. Enumeration of maps. In *The Oxford handbook of random matrix theory*, pages 534–556. Oxford Univ. Press, Oxford, 2011. arXiv:1104.3003 [math-ph].

[12] G. Borot, J. Bouttier, and E. Guitter. A recursive approach to the $O(n)$ model on random maps via nested loops. *J. Phys. A*, 45(4) 045002, 2012. arXiv:1106.0153 [math-ph].

[13] M. Albenque and J. Bouttier. Constellations and multicontinued fractions: application to Eulerian triangulations. In *24th International Conference on Formal Power Series and Algebraic Combinatorics (FPSAC 2012)*, Discrete Math. Theor. Comput. Sci. Proc., AR, pages 805–816. Assoc. Discrete Math. Theor. Comput. Sci., Nancy, 2012. arXiv:1112.6379 [math.CO].

[14] G. Borot, J. Bouttier, and E. Guitter. More on the $O(n)$ model on random maps via nested loops: loops with bending energy. *J. Phys. A*, 45(27) 275206, 2012. arXiv:1202.5521 [math-ph].

[15] G. Borot, J. Bouttier, and E. Guitter. Loop models on random maps via nested loops: the case of domain symmetry breaking and application to the Potts model. *J. Phys. A*, 45(49) 494017, 2012. arXiv:1207.4878 [math-ph].

[16] J. Bouttier and E. Guitter. On irreducible maps and slices. *Combin. Probab. Comput.*, 23(6) 914–972, 2014. arXiv:1303.3728 [math.CO].

[17] J. Bouttier and E. Guitter. A note on irreducible maps with several boundaries. *Electron. J. Combin.*, 21(1) #P1.23, 2014. arXiv:1305.4816 [math.CO].

[18] C. Arita, J. Bouttier, P. L. Krapivsky, and K. Mallick. Asymmetric exclusion process with global hopping. *Phys. Rev. E*, 88 042120, 2013. arXiv:1307.4367 [cond-mat.stat-mech].

[19] J. Bouttier, É. Fusy, and E. Guitter. On the two-point function of general planar maps and hypermaps. *Ann. Inst. Henri Poincaré D*, 1(3) 265–306, 2014. arXiv:1312.0502 [math.CO].

[20] A. Ayyer, J. Bouttier, S. Corteel, and F. Nunzi. Multivariate juggling probabilities. *Electron. J. Probab.*, 20 no. 5, 29, 2015. arXiv:1402.3752 [math.PR].

[21] J. Bouttier, G. Chapuy, and S. Corteel. From Aztec diamonds to pyramids: steep tilings. *Trans. Amer. Math. Soc.*, 369(8) 5921–5959, 2017. arXiv:1407.0665 [math.CO].

[22] D. Betea, C. Boutillier, J. Bouttier, G. Chapuy, S. Corteel, and M. Vuletić. Perfect sampling algorithm for Schur processes. *Markov Processes and Related Fields*, 24 381–418, 2018. arXiv:1407.3764 [math.PR].

[23] A. Ayyer, J. Bouttier, S. Corteel, S. Linusson, and F. Nunzi. Bumping sequences and multispecies juggling. *Adv. in Appl. Math.*, 98 100–126, 2018. arXiv:1504.02688 [math.CO].

[24] C. Boutillier, J. Bouttier, G. Chapuy, S. Corteel, and S. Ramassamy. Dimers on rail yard graphs. *Ann. Inst. Henri Poincaré D*, 4(4) 479–539, 2017. arXiv:1504.05176 [math-ph].

[25] G. Borot, J. Bouttier, and B. Duplantier. Nesting statistics in the $O(n)$ loop model on random planar maps. Preprint, 2016. arXiv:1605.02239 [math-ph].

[26] D. Betea, J. Bouttier, P. Nejjar, and M. Vuletić. The free boundary Schur process and applications I. *Ann. Henri Poincaré*, 19(12) 3663–3742, 2018. Extended abstract in *29th International Conference on Formal Power Series and Algebraic Combinatorics (FPSAC 2017)*, Sém. Lothar. Combin. 78B, Art. 44, 2017. arXiv:1704.05809 [math.PR].

[27] D. Betea and J. Bouttier. The periodic Schur process and free fermions at finite temperature. *Math. Phys. Anal. Geom.*, 22(1) 22:3, 2019. arXiv:1807.09022 [math-ph].

[28] D. Betea, J. Bouttier, P. Nejjar, and M. Vuletić. New edge asymptotics of skew Young diagrams via free boundaries. Extended abstract in *31th International Conference on Formal Power Series and Algebraic Combinatorics (FPSAC 2019)*, Sém. Lothar. Combin. 82B, Art. 32, 2019. arXiv:1902.08750 [math.CO].

Mathematical preliminaries

We gather here for convenience some general terminology, definitions or notations concerning the objects that we encounter in this document. We believe that most of it is either standard or self-explanatory.

Maps A *planar map* is a connected graph drawn on the sphere without edge crossings, considered up to continuous deformation. It consists of *vertices*, *edges*, *faces* and *corners*. In general we allow the graph to have loops and multiple edges; otherwise the map is said *simple*. The *degree* of a vertex or face is its number of incident corners. One usually represents a planar map via a stereographic projection of the sphere into the plane, which amounts to distinguishing an *outer* face containing the "point at infinity", see Figure 0.1. The outer vertices, edges and corners are those incident to the outer face. All the rest are said *inner*. A planar map having only one face is nothing but a (plane) *tree*.

One may consider maps on surfaces other than the sphere, such as closed orientable surfaces of higher genus or even nonorientable surfaces. We will however not do so in this document, hence unless stated otherwise all maps will be assumed to be planar. We might sometimes encounter maps with *boundaries*, which simply means that some faces are distinguished. A (planar) map with one boundary is sometimes called a *disk* or *plane map*—the distinguished face is then taken as the outer face—and a map with two boundaries a *cylinder* or *annular map*.

When enumerating maps, as well as graphs, trees, etc., a slight subtlety concerns the proper treatment of "symmetries". This problem is usually circumvented by considering *rooted* maps. Rooting is traditionally done by marking and orienting an edge, which amounts to distinguishing a *half-edge*; a more recent trend is to do it by marking a

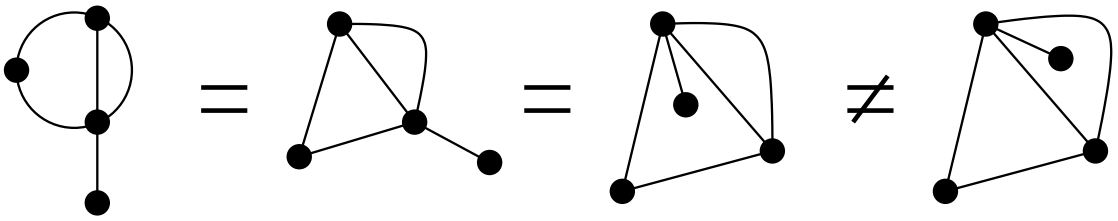

Figure 0.1 – Different drawings of the same graph in the plane. The first three correspond to the same planar map: the first two differ by a simple deformation, and the third by a different choice for the outer face. The fourth corresponds to a different planar map, as may be seen for instance by considering the face degrees.

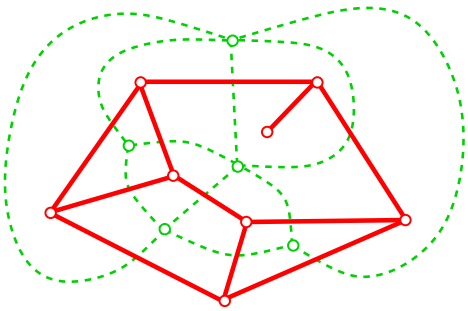

Figure 0.2 – A map and its dual map (drawn with red solid and green dashed edges respectively).

corner. Of course, the two ways are equivalent as there is a one-to-one correspondence between half-edges and corners in a map. Rooting also allows to distinguish one *root vertex* and one *root face*[1], which is usually chosen as the outer face. A *pointed* map has a distinguished vertex called the *origin*. A rooted map is naturally pointed, but in a *pointed rooted* map the origin and the root vertex may differ.

To each map we may associate its *dual map* which, abstractly speaking, is obtained by exchanging the role of vertices and faces. More concretely, to construct the dual map, we add a new dual vertex inside each face of the original (primal) map and, for each primal edge, we consider its two incident faces and draw a dual edge connecting the two dual vertices inside them. See Figure 0.2 for an example. Note that the dual of a simple map is not necessarily simple.

A map is said *bipartite* if its vertex set can be partitioned in two subsets so that no edge has its two endpoints in the same subset. This implies that all the faces have even degrees and, in the planar case, the converse is also true. Through duality we obtain an *Eulerian* map, i.e. a map whose vertices all have even degree. A common combinatorial trick consists in transforming an arbitrary map into a bipartite map by adding a *dummy* vertex in the middle of each edge. The dummy vertices have degree two and form one of the two subsets of the bipartition. In this sense, bipartite (or dually Eulerian) maps appear as "more general" than ordinary maps. A closely related concept is that of *hypermap*, see for instance [LZ04, p. 43].

A *triangulation* is a map all of whose faces have degree three. Similarly a *quadrangulation* has all its faces of degree four. Triangulations and quadrangulations are respectively dual to *cubic* and *quartic* maps, where the degree constraint is on the vertices. In a triangulation or quadrangulation *with a boundary*, we relax the degree constraint on the outer face. A planar quadrangulation (possibly with one boundary) is always bipartite. There is a well-known correspondence between arbitrary maps with n edges and quadrangulations with n faces, see Figure 0.3. This correspondence is two-to-one, since the

1. This is an advantage of corner-rooting where the choice is canonical. For edge-rooting one needs a convention, for instance that the root face is the one on the right of the root edge.

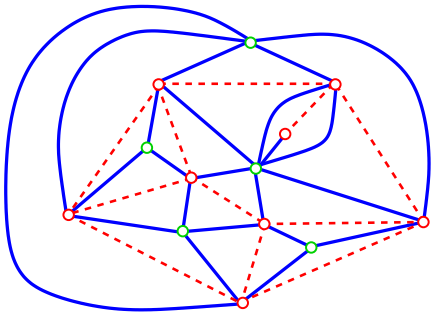

Figure 0.3 – The quadrangulation (blue solid edges) associated with the map of Figure 0.2 (here shown with red dashed edges).

dual map is sent to the same quadrangulation. It becomes one-to-one after rooting, since the quadrangulation has twice as many corners as the original map. The dual of the quadrangulation is sometimes called the *medial graph* (though it is actually a map). A celebrated result of Tutte [Tut63] states that the number of rooted planar maps with n edges, or equivalently the number of rooted planar quadrangulations with n faces, is equal to

$$m_n = \frac{2 \cdot 3^n}{(n+1)(n+2)} \binom{2n}{n} \sim \frac{2}{\sqrt{\pi}} \frac{12^n}{n^{5/2}} \quad (n \to \infty). \tag{0.1}$$

A *well-labeled map* (resp. *suitably labeled map*[2]) is a map whose vertices are labeled by integers, in such a way that the labels of adjacent vertices differ by at most 1 (resp. exactly 1). Note that a suitably labeled map is necessarily bipartite, since vertices with odd labels can only be adjacent to vertices with even labels, and vice versa.

For us, the notions of *path* and *walk* on a map (or graph) are synonymous. The *length* of a path is its number of edges. A path whose two endpoints are equal is said *closed*. A path which never visits the same vertex twice, except possibly at the endpoints, is said *simple* or *self-avoiding*. A simple closed path is called a *cycle*. The *contour* of a face is the closed path formed by its incident edges. A face is said simple if its contour is a cycle (the contour is not a cycle when the face is incident to bridges or "pinch points"). A *geodesic* between two vertices is a path of minimal length connecting them. It is necessarily simple. The *girth* of a map is the length of a shortest cycle. It is infinite in the case of a tree.

Partitions An *integer partition*, hereafter called a *partition* for short, is a way to decompose a nonnegative integer, called the *size* of the partition, as a sum of positive integers. The order of the terms in the sum is disregarded[3], therefore we may order them in weakly decreasing order, and view a partition as a finite nonincreasing sequence of positive integers called *parts*. The number of parts is the *length* of the partition.

2. Or "very well-labeled" map [Arq86]
3. If we do care about the order, we have a *composition*.

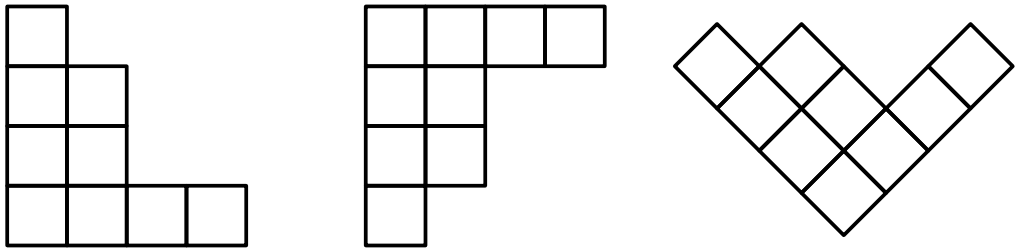

Figure 0.4 – The Young diagram of the partition $(4, 2, 2, 1)$ shown in French (left), English (middle) and Russian (right) conventions. The conjugate partition is $(4, 3, 1, 1)$.

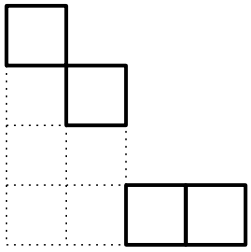

Figure 0.5 – The skew Young diagram of shape $(4, 2, 2, 1)/(2, 2, 1)$, shown in French convention. It is a horizontal strip since no two cells are in the same column.

The tradition is to denote partitions with lower greek letters: λ, μ, ν... Given a partition λ, its size is denoted $|\lambda|$, its length is denoted $\ell(\lambda)$, and its parts are denoted $\lambda_1, \ldots, \lambda_{\ell(\lambda)}$ with $\lambda_1 \geq \cdots \geq \lambda_{\ell(\lambda)}$. It is convenient to set $\lambda_i = 0$ for $i > \ell(\lambda)$. The notation $\lambda \vdash n$ means that λ is a partition of size n. The *empty partition*, denoted $\emptyset$, is the unique partition of size zero.

A well-known graphical representation of partitions is via *Young diagrams*. Trusting that a picture is worth a thousand words, we refer to Figure 0.4 for an example. The small squares are called *cells*. If we reflect the Young diagram of a partition λ along its main diagonal, we obtain the Young diagram of its *conjugate* partition, denoted λ'. In mathematical notation, we have $\lambda'_i = \#\{j : \lambda_j \geq i\}$.

For two partitions λ, μ, we write $\lambda \supset \mu$ if the Young diagram of λ contains that of μ, in other words if we have $\lambda_i \geq \mu_i$ for all i. Such pair (λ, μ) is called a *skew shape*, and is denoted λ/μ. It is represented as a *skew Young diagram*, see Figure 0.5. Its size is $|\lambda/\mu| := |\lambda| - |\mu|$.

The skew shape λ/μ is called a *horizontal strip* if we have

$$\lambda_1 \geq \mu_1 \geq \lambda_2 \geq \mu_2 \geq \cdots \tag{0.2}$$

If so, we write

$$\lambda \succ \mu \tag{0.3}$$

and we say that the partitions λ and μ are (horizontally) *interlaced*. Graphically, this

says that the cells of the skew Young diagram of shape λ/μ lie in different columns, see again Figure 0.5.

If λ and μ are such that their conjugates satisfy $\lambda' \succ \mu'$, then we say that the skew shape λ/μ is a *vertical strip*, that the two partitions are *vertically interlaced*, and we use the alternate notation

$$\lambda \succ' \mu. \tag{0.4}$$

Note that vertical interlacing amounts to the condition that

$$\lambda_i - \mu_i \in \{0, 1\}, \qquad i = 1, 2, \ldots. \tag{0.5}$$

Partitions are classically related with symmetric functions [Mac95]. In Section 4, we will encounter Schur functions. To a skew shape λ/μ we associate the *skew Schur function* $s_{\lambda/\mu}$ that may be defined through the Jacobi-Trudi formula

$$s_{\lambda/\mu}(x_1, \ldots, x_n) = \det_{1 \le i,j \le \ell(\lambda)} h_{\lambda_i - i - \mu_j + j}(x_1, \ldots, x_n) \tag{0.6}$$

where $h_k(x_1, \ldots, x_n)$ is the complete homogeneous symmetric polynomial [4] of degree k, which is conveniently defined by the generating function

$$\sum_{k=0}^{\infty} h_k(x_1, \ldots, x_n) z^k = \prod_{i=1}^{n} \frac{1}{1 - x_i z} \tag{0.7}$$

(with $h_k = 0$ for $k < 0$). The classical Schur function s_λ is obtained by taking μ equal to the empty partition $\emptyset$. It may also be expressed as a ratio of alternants

$$s_\lambda(x_1, \ldots, x_n) = \frac{\det_{1 \le i,j \le n} x_j^{\lambda_i + n - i}}{\det_{1 \le i,j \le n} x_j^{n-i}} \tag{0.8}$$

which may be seen as an instance of the Weyl character formula for the general linear group. In Section 1.4 we will also encounter symplectic and orthogonal Schur functions, corresponding to characters of the respective groups (but we do not give the formulas here for brevity).

It is an elementary exercise to check that the skew Schur function of a single variable x is given by

$$s_{\lambda/\mu}(x) = \begin{cases} x^{|\lambda/\mu|} & \text{if } \lambda \succ \mu, \\ 0 & \text{otherwise.} \end{cases} \tag{0.9}$$

This relation, together with the "branching" relation

$$s_{\lambda/\mu}(x_1, \ldots, x_n) = \sum_{\nu} s_{\lambda/\nu}(x_1, \ldots, x_m) s_{\nu/\mu}(x_{m+1}, \ldots, x_n) \qquad (m \le n) \tag{0.10}$$

4. For simplicity we will ignore the distinction between symmetric polynomials and symmetric functions.

which results from the Jacobi-Trudi formula (0.6) and the Cauchy-Binet formula, yields the expression

$$s_{\lambda/\mu}(x_1,\dots,x_n) = \sum_{\substack{\lambda^{(0)}\prec\lambda^{(1)}\prec\cdots\prec\lambda^{(n)}\\ \lambda^{(0)}=\mu,\ \lambda^{(n)}=\lambda}} x_1^{|\lambda^{(1)}/\lambda^{(0)}|}\cdots x_n^{|\lambda^{(n)}/\lambda^{(n-1)}|} \tag{0.11}$$

which amounts to the combinatorial definition of the Schur functions in terms of semistandard Young tableaux (that are in bijection with the sequences of interlaced partitions on which we sum). For y a variable, the *exponential specialization* ex_y [Sta99, p. 304] is formally obtained by taking $x_1 = \cdots = x_n = \frac{y}{n}$ and letting n tend to infinity. When applied to the skew Schur function $s_{\lambda/\mu}$, it gives

$$s_{\lambda/\mu}(\mathrm{ex}_y) = \lim_{n\to\infty} s_{\lambda/\mu}\Big(\underbrace{\frac{y}{n},\dots,\frac{y}{n}}_{n \text{ times}}\Big) = \frac{\dim(\lambda/\mu)}{|\lambda/\mu|!}y^{|\lambda/\mu|} \tag{0.12}$$

where $\dim(\lambda/\mu)$ is the number of standard Young tableaux of shape λ/μ, i.e. the number of ways to fill the cells of the Young diagram of λ/μ with the numbers $1,\dots,|\lambda/\mu|$ in such a way that cell numbers increase strictly along rows and colums (from left to right and from bottom to top in French convention).

1 Mobiles and distance statistics of random planar maps

The purpose of this chapter is to present some of my contributions to the study of the metric properties of random planar maps. The publications closest to this topic are [5–10, 13, 19]. The general strategy is the following: using a suitable bijection we may translate the problem of determining the distribution of a certain "metric observable" of a map into the problem of counting "mobiles" subject to certain constraints. In several favorable cases, this counting problem may often be solved exactly, and we may then take asymptotics to deduce properties of large random maps.

My presentation will neither be exhaustive nor chronological. After recalling the context in Section 1.1, I will start in Section 1.2 with a general "map-mobile" correspondence taken from [19]. I will then apply two particular cases of this correspondence: in Section 1.3 to compute the three-point function of quadrangulations [6], and in Section 1.4 to study the two-point function of Boltzmann maps and its connection with continued fractions [10]. Perspectives are discussed in Section 1.5.

1.1 Context

The study of the metric properties of random maps has been an exploding topic of research over the last 20 years. To my knowledge, considering the *distance* in 2D quantum gravity was first advocated by Watabiki and his collaborators, see e.g. [AW95] and references therein. In particular, this paper successfully predicted [1] the asymptotic form of the so-called *two-point function* of pure gravity. Coincidentally, Schaeffer introduced in his thesis [Sch98, Chapter 6] one of the most important tools for a rigorous study of distances, namely the bijection between quadrangulations and well-labeled trees. His construction is actually a clever reformulation —which makes the role of distance manifest— of an earlier bijection due Cori and Vauquelin [CV81], hence it is nowadays known as the CVS bijection. It was exploited in [CS04] to prove the first convergence result for a metric-related observable, the radius.

This is the time where I entered into this subject, during my own thesis. This led to several papers written with Philippe Di Francesco and Emmanuel Guitter: in a nutshell we brought the following two main contributions to the field.

1. First, we gave a rigorous derivation of the Ambjørn-Watabiki expression for the

1. It has recently been realized by Timothy Budd that the derivation of [AW95], which is usually regarded as nonrigorous, can be made rigorous if one understands that it actually describes the first passage percolation distance in cubic maps with exponential edge weights [AB16].

two-point function [BDFG03a], relying on an unexpected property of *discrete integrability*. At the time this was a mere observation, but understanding the combinatorial origin of this integrability, as well as working out its applications, has been a major topic of my research in the early period covered by this memoir. This research will be summarized in Sections 1.3 and 1.4.

2. Second, we gave a generalization of the CVS bijection to maps with arbitrary face degrees [BDFG04]. It is now often called the "BDG" bijection but I shall rather use the term *mobile* which we introduced to designate the type of trees produced by our construction. While more elementary than the previous item, it turned out to have important applications as it allows to establish *universality* results: the CVS bijection allows to establish convergence results for distance in quadrangulations, our bijection allows to extend them to triangulations, pentagulations, etc. In Section 1.2, I will give a further extension of the mobile bijection, obtained jointly with Éric Fusy and Emmanuel Guitter [19].

After that, the subject became a major topic in probability theory. Let me highlight some works, without the ambition of being exhaustive. First, Marckert and Mokkadem [MM06] introduced the *Brownian map* describing the scaling limit of quadrangulations. They proved the convergence in a certain weak sense and, in his ICM2006 lecture, Schramm [Sch07, Problem 4.1] asked whether the convergence also holds in the stronger Gromov-Hausdorff sense. This question was addressed in a series of papers mostly by Le Gall and Miermont [LG07, LGP08, Mie08, Mie09, LG10, Mie13, LG13] which ended up with an affirmative answer to Schramm's question. See for instance [Mie14] for a pedagogical presentation. Further developments went in several directions, among which the case of maps of higher genus [CMS09, Bet10, Bet12, Cha16] or on nonorientable surfaces [CD17, Bet15], and proofs of convergence to the Brownian map for various families of maps [BLG13, BJM14, Abr16, ABA17, Mar18b] (some of them not analyzable using the CVS/mobiles bijections). A direction which is still very open is the investigation of families of maps which do *not* converge to the Brownian map, but for instance to the so-called stable maps [LGM11, Mar18a]. We shall return to this question in Chapter 3, where we discuss its connection with the $O(n)$ loop model on random maps.

So far I have only mentioned works that rely on a bijective approach, but further away from the considerations developed in this chapter there are at least two other sides to the story (that were mostly developed after the publications presented in this chapter):

— local limits of planar maps, whose study was initiated by Angel and Schramm [AS03], and which recently brought new insights in the study of distances, see e.g. [CLG15, BC17] and references therein,

— Liouville quantum gravity, whose metric structure and relation with random maps have been recently investigated by Miller, Sheffield and their collaborators in an imposing series of papers including [MS15a, MS15b, MS16a, MS16b, GMS17]. Interestingly, it seems that this approach is able to provide information about families of maps not converging to the Brownian map [GHS17, DG19].

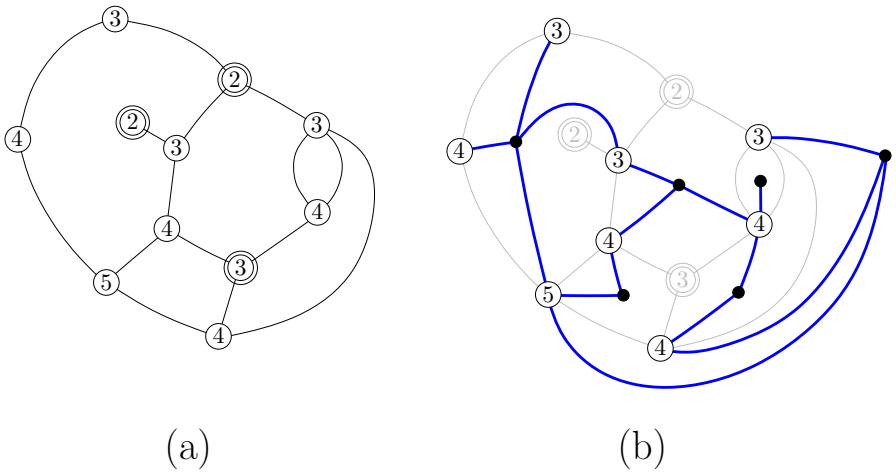

Figure 1.1 – (a) A suitably labeled map (local min are surrounded). (b) Its corresponding mobile (blue edges).

1.2 From maps to mobiles

In this section we present a bijection obtained with Éric Fusy and Emmanuel Guitter in [19]. It may be seen as the "merger" of two generalizations of the CVS bijection: the bijection of [BDFG04] mapping bipartite maps to mobiles, and the Miermont-Ambjørn-Budd bijection [Mie09, AB13] mapping suitably labeled quadrangulations to well-labeled maps. We start by defining the two families related by our bijection.

Recall from the mathematical preliminaries that a *suitably labeled map* is a planar map whose vertices are labeled by integers, in such a way that the labels of adjacent vertices differ by exactly 1. A *local min* is a vertex every neighbor of which has greater label. See Figure 1.1(a) for an example.

A *mobile* is a bipartite planar map where one of the subsets of the bipartition consists of *labeled vertices* which carry an integer label (the vertices in the other subset being *unlabeled*), subject to the constraint displayed on Figure 1.2(a).

To construct a mobile from a suitably labeled map, first add one unlabeled vertex inside each face of the map, then apply the local rule from [BDFG04] shown on Figure 1.2(b), and finally remove the local min which, by construction, are not incident to any edge in the mobile. See Figure 1.1(b) for an example. Note that, in [BDFG04], the construction was restricted to the case where the suitably labeled map is endowed with a "geodesic labeling" (to be defined below), in which case the resulting mobile is a tree. The extension to a general suitable labeling was done in [19], and the mobile is not necessarily a tree anymore. In fact, its number of faces is equal to the number of local min in the suitably labeled map.

Theorem 1.1 (see [19, Theorem 1]). *The construction described above is a bijection between suitably labeled maps and mobiles. Furthermore, we have the following correspondences between their components:*

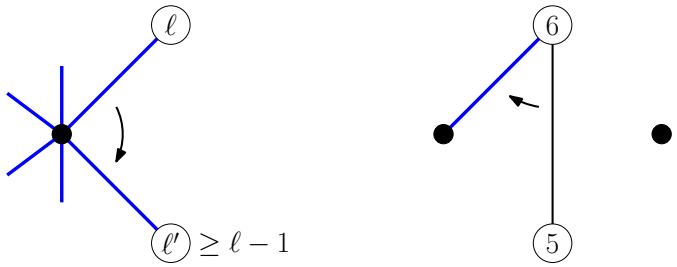

(a) (b)

Figure 1.2 – (a) The constraint on labels in a mobile: around an unlabeled (black) vertex, the labels ℓ, ℓ' of two adjacent vertices that appear consecutively in clockwise order must satisfy $\ell' \geq \ell - 1$. (b) The local rule from [BDFG04]: for each edge of the suitably labeled map, we connect its endpoint with larger label (here equal to 6) to the unlabeled vertex added in the face on the left (when seen from the smaller label, here equal to 5).

suitably labeled map	$\leftrightarrow$	*mobile,*
local min	$\leftrightarrow$	*face,*
non-local min vertex	$\leftrightarrow$	*vertex,*
face of degree $2k$	$\leftrightarrow$	*unlabeled vertex of degree* k*,*
edge with endpoints labeled $\ell/\ell-1$	$\leftrightarrow$	*corner at a vertex labeled* ℓ*.*

We refer to [19] for the proof and a description of the reverse bijection. We now discuss two particular cases.

— When the suitably labeled map is a quadrangulation, then all unlabeled vertices in the mobile have degree two. Consequently we may ignore them, to obtain a well-labeled map [2]. We recover a bijection which appeared in two different forms in [Mie09] and [AB13], see for instance [19, Remark 1] for a discussion of their equivalence.

— When the suitably labeled map has a unique local min, whose label can be taken equal to 0 by a global shift, then it is not difficult to check that the label of any vertex is necessarily equal to its graph distance to the local min. The labeling is then said *geodesic*. The corresponding mobile is a tree, and we recover the bijection from [BDFG04] between pointed bipartite maps and mobiles.

The intersection between these two cases corresponds to the CVS bijection between pointed quadrangulations (endowed with their geodesic labeling) and well-labeled trees.

Remark 1.1. In [BDFG04], we also gave more general constructions dealing with non necessarily bipartite maps. Lifting the bipartiteness assumption is important to study for instance triangulations [LG13, Section 8]. In fact, we may adapt our current construction

2. It is somewhat surprising that well-labeled maps appear both as generalizations of suitably labeled maps and as particular cases of mobiles.

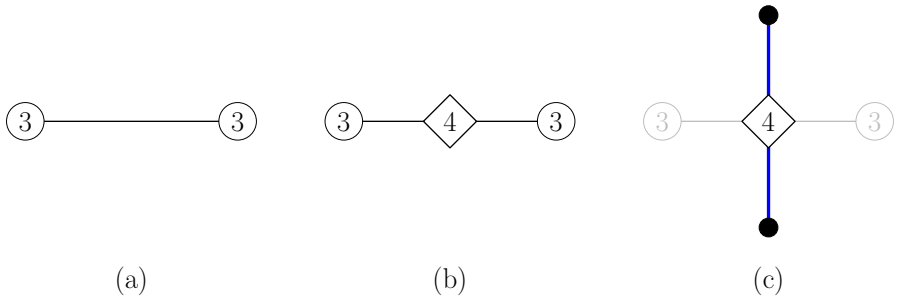

Figure 1.3 – Dealing with frustrated edges: starting with a frustrated edge with endpoints labeled, say, 3 (a), we add in its middle a new "square" vertex with label $3 + 1 = 4$ (b). This square vertex becomes a labeled vertex of degree two in the mobile (c).

as follows: instead of a suitably labeled map, let us start with a well-labeled map. There may then exist some *frustrated* edges whose two endpoints have the same label, and this is unavoidable if the map is not bipartite. We then modify the map by adding new "square" vertices in the middle of frustrated edges, as shown on Figure 1.3: we get a suitably labeled map. We then construct the mobile as before: the square vertices (which cannot be local min) remain of degree two in the mobile. Furthermore, we may check that there is an additional constraint on the mobile: if, on Figure 1.2(a), the vertex with label ℓ' is square, then we must have $\ell' \geq \ell$ (instead of $\ell' \geq \ell - 1$). In the case where the original map had a unique local min, hence was endowed with its geodesic labeling, we recover the construction from [BDFG04, Section 4.2], where square vertices were regarded as "flagged edges" with labels shifted by -1 [3]. It is also possible to recover the most general construction from [BDFG04, Section 3] for Eulerian maps, we leave this as an exercise to the reader.

Remark 1.2. The bijection extends without difficulty to maps of higher genus [19, Section 2.7]. The extension of the CVS bijection to higher genus was done in [CMS09] and that of [BDFG04] in [Cha09].

Theorem 1.1 was used in [19] as the basis for several further correspondences. In particular we adapted a neat idea from [AB13] which consists in composing our bijection with its "mirror". The mirror bijection consists in reversing the rule of Figure 1.2(b): instead of connecting the vertex with larger label to the unlabeled vertex on the left, we connect the two other vertices. And we do so for every edge of the suitably labeled map. In the mirror bijection, it is now the *local max* (rather than local min) which become the faces of the mobile. This has drastic consequences in the case where the suitably labeled map is endowed with its geodesic labeling: there is no reason that there exists a unique local max, unless the map is "causal", which was one the motivations of [AB13]. Therefore, the mirror mobile has in general several faces, but it is possible to show that its labeling is also geodesic in a suitable sense [19, Proposition 2]. From this observation,

3. As observed in [Mie06, Section 3.3], another natural convention consists in labeling the square vertices by half-integers, for instance the square vertex on Figure 1.3 would get label 3.5 instead of 4.

we have been able to compute the two-point function of general maps and other similar families. We do not enter into the details here, but since we have been using the term "two-point function" several times without explaining it, let us try to give a (slightly informal) definition:

Definition 1.1. Let $\mathcal{M}$ be a family of maps, endowed with a *weight function* $w : \mathcal{M} \to \mathbb{R}_+$. Let us denote by $\ddot{\mathcal{M}}$ the set of maps in $\mathcal{M}$ with two marked points and, for $m \in \ddot{\mathcal{M}}$, denote by $D(m)$ the graph distance between the two marked points in m. Then, the (distance-dependent) *two-point function* $(T_d)_{d\geq 0}$ associated with the weighted family $(\mathcal{M}, w)$ is defined by

$$T_d := \sum_{\substack{m\in\ddot{\mathcal{M}} \\ D(m)\leq d}} w(m) \in \mathbb{R}_+ \cup \{+\infty\}. \tag{1.1}$$

Taking $d = \infty$ means that we drop the constraint on $D(m)$ in the sum.

When the weight function is such that $0 < T_\infty < \infty$, then $w(\cdot)/T_\infty$ defines a probability measure on $\ddot{\mathcal{M}}$, and T_d/T_∞ may be interpreted as the distribution function of the random variable D.

Example 1.3. The two-point function of general maps considered in [19] corresponds to taking $\mathcal{M}$ the set of all planar maps, and the weight function $w(m) = t^{E(m)}$, where $E(m)$ denote the number of edges of m and t is a nonnegative real parameter. Here T_d is finite for all d if and only if $t \leq 1/12$, as may be seen from (0.1).

What makes Definition 1.1 slightly informal is the notion of "points": ideally these would be vertices, but then we run into the problem that a map with only two marked vertices may have symmetries. We usually circumvent the problem by considering pointed rooted maps —i.e. we mark one vertex and one corner— at the price of making the definition less symmetric. Such details do not matter much for asymptotics.

It is immediate to extend the definition to an arbitrary number n of marked points: the (full distance-dependent) *n-point function* of $(\mathcal{M}, w)$ depends on $\binom{n}{2}$ parameters, which control the distances between the marked points. These distances should obey the triangular inequalities, which immediately raises the question of a "natural parametrization" of the n-point function. As we shall see in the next section, a very natural parametrization exists for $n = 3$, while the situation remains widely open for $n \geq 4$. Note that, for $n \geq 3$, the problem of symmetries does not occur anymore: a map with 3 marked distinct vertices cannot have symmetries.

1.3 The three-point function of quadrangulations and related results

In this section we restrict to the case of quadrangulations, endowed with the weight function $w(m) = g^{F(m)}$ where $F(m)$ denotes the number of faces of m and g is a nonnegative real parameter smaller than $1/12$. An explicit form for the two-point function

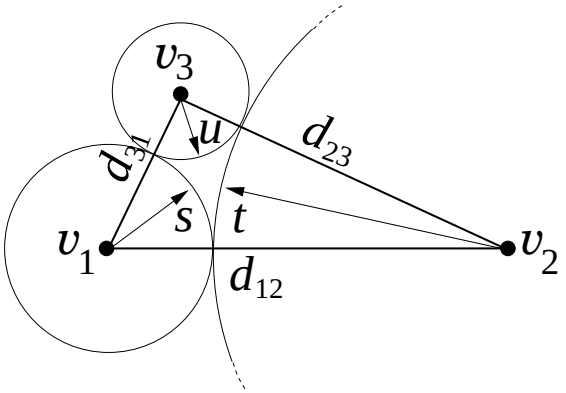

Figure 1.4 – Geometrical interpretation of the parameters s, t, u of (1.2): they correspond to the radii in the "circle packing" consisting of three circles whose centers are at pairwise distances d_{12}, d_{23} and d_{31}.

of quadrangulations was given in [BDFG03a] [4], and a few years later, together with Emmanuel Guitter, we succeeded in computing their three-point function in [6]. This is the story I would like to tell here.

Our inspiration came from the paper of Grégory Miermont [Mie09] [5] containing his generalization of the CVS bijection, mentioned in the previous section. It was then formulated in terms of "sources" and "delays", reflecting his motivations related to Voronoi tessellations. Our key idea was to apply his bijection with a special choice of sources and delays, which we now explain.

Let us consider a quadrangulation with three marked distinct vertices v_1, v_2 and v_3. As mentioned above such a quadrangulation does not possess nontrivial symmetries. We denote by d_{12} the graph distance from v_1 to v_2 in the quadrangulation, and define similarly d_{23} and d_{31}. We then introduce the three parameters s, t, u such that

$$\begin{aligned} d_{12} &= s + t \\ d_{23} &= t + u \\ d_{31} &= u + s \end{aligned} \tag{1.2}$$

i.e. $s = (d_{12} - d_{23} + d_{31})/2$, etc. A geometrical interpretation of these parameters is given on Figure 1.4. The nice thing about s, t, u is that they are "free", unlike d_{12}, d_{23}, d_{31} which are constrained by the triangular inequalities. More precisely we simply have $s, t, u \geq 0$, and at most one of them may vanish due to the constraint that v_1, v_2, v_3 are distinct. The vanishing of one parameters occurs when the points are "aligned": having, say, $u = 0$ simply means that v_3 is on a geodesic between v_1 and v_2. Also, since we are working

4. Note that, though general maps and quadrangulations are in bijection, their metric structures hence their two- or three-point functions are *a priori* different. But, in fact, not too much [19] [BJM14, FG14, Leh19].

5. The preprint was in fact posted in December 2007 on the arXiv. We also had the chance to learn about Grégory's work via the *séminaire Cartes*, which had not yet evolved into the current *journées*.

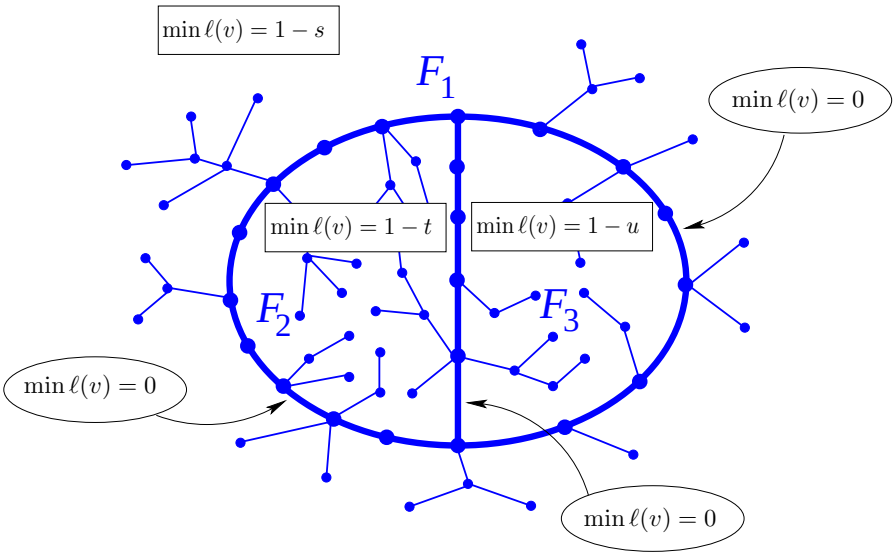

Figure 1.5 – Structure of the well-labeled map in the case $s, t, u > 0$: the map has three faces F_1, F_2, F_3, which are pairwise adjacent. The minimal label among vertices incident to F_1 (resp. F_2, F_3) is $1-s$ (resp. $1-t, 1-u$). The minimal label among vertices incident both to F_1 and F_2 is 0, and the same holds for the two other interfaces.

with (bipartite) quadrangulations, d_{12}, d_{23}, d_{31} are integer numbers whose sum is even. Hence s, t, u are always nonnegative integers.

We now apply the Miermont bijection with the "sources" v_1, v_2, v_3 and the "delays" $-s, -t, -u$. In the language of Section 1.2, this corresponds to endowing the quadrangulation with the suitable labeling defined by

$$\ell(v) = \min\{d(v, v_1) - s, d(v, v_2) - t, d(v, v_3) - u\} \tag{1.3}$$

where v denotes an arbitrary vertex of the quadrangulation. It is not difficult to check that ℓ is indeed a suitable labeling, with generically 3 local min at v_1, v_2, v_3, except in the *aligned case* where there are only 2 (e.g., if $u = 0$ then v_3 is no longer a local min). By Theorem 1.1 (specialized to quadrangulations), we obtain a well-labeled map with respectively 3 or 2 faces. Examining the labels more closely, we find that it has the structure displayed respectively on Figures 1.5 or 1.6. We have reformulated the problem of determining the three-point function of quadrangulations into the problem of counting well-labeled maps with these structures (with now a weight g per edge). We now sketch how to solve this counting problem.

For $d \geq 1$, let us denote by R_d the generating function of well-labeled *trees* with (strictly) positive labels, rooted at a corner labeled d. By shifting, trees with labels (strictly) larger than $-s$ and rooted a corner labeled d have generating function R_{d+s}. From [BDFG03a, BDFG03b], we know that R_d is actually the two-point function of

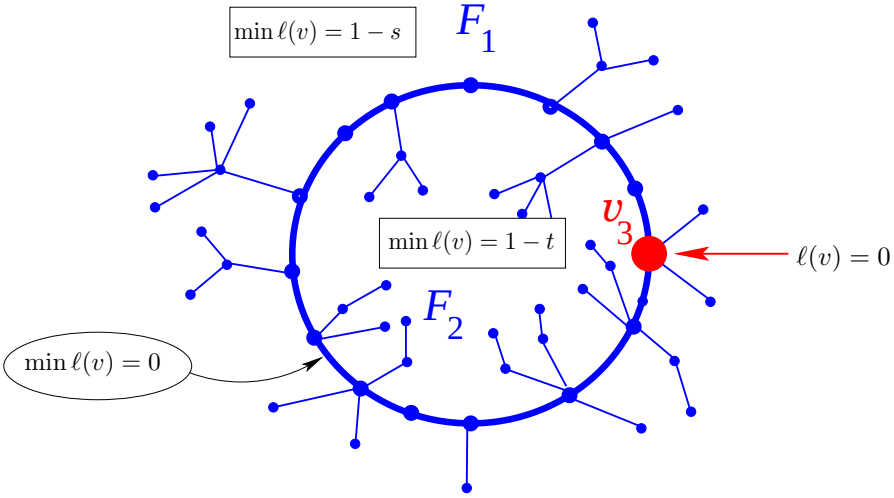

Figure 1.6 – Structure of the well-labeled map in the case $s, t > 0$ and $u = 0$: the map has two faces F_1, F_2, and v_3 is a vertex incident to both. The minimal label among vertices incident to F_1 (resp. F_2) is $1 - s$ (resp. $1 - t$). The minimal label among vertices incident to both faces is 0, and is attained at v_3.

quadrangulations, and is explicitly given by

$$R_d = R\frac{(1-x^d)(1-x^{d+3})}{(1-x^{d+1})(1-x^{d+2})} \tag{1.4}$$

where $R = \frac{1-\sqrt{1-12g}}{6g}$ and x is root of the equation $x + x^{-1} = \frac{1-4gR}{4gR}$ (this equation has two reals roots for $g \leq 1/12$, and we usually pick the root $x \leq 1$ which is analytic at $g = 0$).

The maps of Figures 1.5 or 1.6 are not trees, but since they have few faces it is natural to attempt to decompose them into trees. To remain brief, we only detail the aligned case $u = 0$: as displayed on Figure 1.7, we cut the well-labeled map at v_3, to obtain a *chain*, which may be viewed as a *Motzkin path* with attached subtrees. By a standard combinatorial argument we find that the generating function $X_{s,t}$ of such paths satisfies the recurrence equation

$$X_{s,t} = 1 + gR_sR_tX_{s,t} + g^2R_sR_tX_{s,t}R_{s+1}R_{t+1}X_{s+1,t+1} \tag{1.5}$$

(which uniquely determines $X_{s,t}$ as a power series in g). Remarkably, $X_{s,t}$ admits an explicit expression similar to that of R_d, namely

$$X_{s,t} = \frac{(1-x^3)(1-x^{s+1})(1-x^{t+1})(1-x^{s+t+3})}{(1-x)(1-x^{s+3})(1-x^{t+3})(1-x^{s+t+1})}. \tag{1.6}$$

It is straightforward to check that this is indeed the solution of (1.5), alternatively we give two bijective derivations in [6] (which however take the expression (1.4) for R_d as

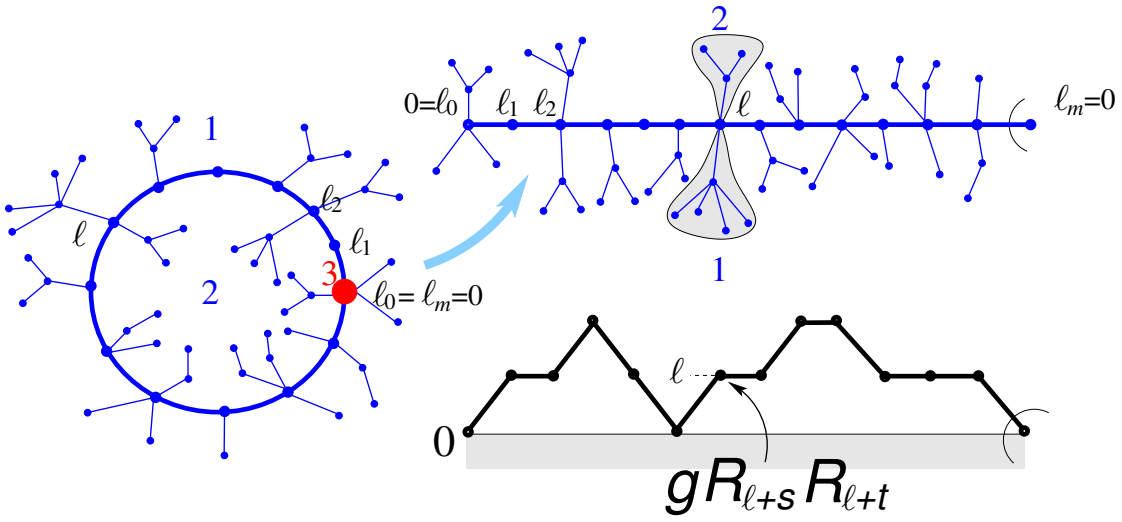

Figure 1.7 – Cutting the well-labeled map of Figure 1.6 into a chain. A chain is a well-labeled tree with two marked vertices with label 0. On the branch between them, the labels remain nonnegative hence form a Motzkin path. Well-labeled subtrees are attached to both sides of the branch, and their labels are at least $1 - s$ and $1 - t$ respectively. Therefore, summing the weights over all possible such subtrees, the global contribution of a step at height ℓ in the Motzkin path is equal $gR_{\ell+s}R_{\ell+t}$. The careful reader might notice the issue that the minima $1-s$ and $1-t$ should be attained in some subtree, this is taken care of by (1.7).

an input). As mentioned in the caption of Figure 1.7, $X_{s,t}$ is not quite the generating function of the maps of Figure 1.6 because the minimal label $1-s$ (resp. $1-t$) should be attained somewhere along F_1 (resp. F_2). But this is easily fixed: the actual generating function for them is

$$\Delta_s\Delta_t X_{s,t} = X_{s,t} - X_{s-1,t} - X_{s,t-1} + X_{s-1,t-1}. \tag{1.7}$$

Here Δ_s denotes the discrete difference operator $\Delta_s f(s) = f(s) - f(s-1)$.

In the generic case $s,t,u > 0$ the decomposition is more involved, see [6, Section 4.3]. Some pieces in the decomposition are the same chains as before, but we also need to introduce so-called *Y-diagrams* whose generating function $Y_{s,t,u}$ depends on the three parameters, and is explicitly given by

$$Y_{s,t,u} = \frac{(1-x^{s+3})(1-x^{t+3})(1-x^{u+3})(1-x^{s+t+u+3})}{(1-x^3)(1-x^{s+t+3})(1-x^{t+u+3})(1-x^{u+s+3})}. \tag{1.8}$$

This expression can be proved by checking that it solves a recurrence equation similar to (1.5), but unlike $X_{s,t}$ we do not know an alternative bijective derivation. Armed with these notations, we may now state the main result of this section:

Theorem 1.2 (see [6])**.** *The three-point function of planar quadrangulations, which counts such maps with three marked distinct vertices at prescribed distances parametrized by s,t,u as in* (1.2)*, is equal to $\Delta_s\Delta_t\Delta_u F_{s,t,u}$ where*

$$F_{s,t,u} := X_{s,t}X_{t,u}X_{u,s}(Y_{s,t,u})^2. \tag{1.9}$$

The role of the discrete difference operators is again to make sure that the minimal labels $1-s, 1-t, 1-u$ are attained somewhere along their respective faces in Figure 1.5, $F_{s,t,u}$ corresponds to a cumulative generating function.

It is natural to consider the "continuum limit" of the three-point function, which corresponds to a certain observable of the Brownian map (precisely, it is the joint law of the distances between three uniform points). The first step consists in letting g tend to the critical value $1/12$ and rescaling jointly the parameters s,t,u via

$$g = \frac{1-\Lambda\epsilon}{12}, \qquad s = \lfloor S\epsilon^{-1/4}\rfloor, \quad t = \lfloor T\epsilon^{-1/4}\rfloor, \quad u = \lfloor U\epsilon^{-1/4}\rfloor \tag{1.10}$$

where $\epsilon \to 0$ and Λ, S, T, U are kept fixed (Λ plays the role of a "cosmological constant"). Then, under this scaling, it is straightforward to check that

$$F_{s,t,u} \sim \epsilon^{-1/2}\mathcal{F}(S,T,U;\sqrt{3/2}\Lambda^{1/4}) \tag{1.11}$$

where

$$\mathcal{F}(S,T,U;\alpha) := \frac{3}{\alpha^2}\left(\frac{\sinh(\alpha S)\sinh(\alpha T)\sinh(\alpha U)\sinh(\alpha(S+T+U))}{\sinh(\alpha(S+T))\sinh(\alpha(T+U))\sinh(\alpha(U+S))}\right)^2. \tag{1.12}$$

The reader might notice that the nontrivial dependency in S,T,U comes from the factor $(Y_{s,t,u})^2$ in $F_{s,t,u}$, while the X factors contribute a trivial factor 3 at leading order. One

may interpret this as the fact that the Y-diagrams capture all the "mass" in the scaling limit, while the X-chains are negligible. It may be seen [6, 7] that the Y-diagrams correspond in the Brownian map to the two "geodesic triangles", namely the two regions delimited by the three geodesics between the marked points [6]. $\mathcal{F}$ corresponds to the "grand canonical" continuum three-point function, for probabilistic interpretation it is preferable to return to the "canonical" ensemble, i.e. to consider the uniform distribution over quadrangulations with a large but fixed number n of faces. This is done by extracting the coefficient of g^n in the series $F_{s,t,u}$, which may be estimated for large n by a saddle-point analysis, and normalizing it by the total number $\frac{3^n}{2}\binom{2n}{n}$ of quadrangulations with three marked distinct vertices. The end result [6] is that, upon replacing ϵ by $1/n$ in the scaling (1.10) for s, t, u, we have

$$\lim_{n\to\infty} \frac{[g^n]F_{s,t,u}}{\frac{3^n}{2}\binom{2n}{n}} = \frac{2}{i\sqrt{\pi}} \int_{-\infty}^{\infty} d\xi \xi e^{-\xi^2} \mathcal{F}(S, T, U; e^{-\mathrm{sgn}(\xi) i\pi/4}\sqrt{3\xi/2}). \tag{1.13}$$

This integral is real and easy to evaluate numerically, see Figure 1.8 for some plots.

To conclude this section, let us briefly my other results in the same vein, all obtained jointly with Emmanuel Guitter. Before the three-point function, we had considered in [5] the statistics of the number of geodesics between two points in a quadrangulation. These can be viewed as discrete enumerative counterparts of the results of Miermont [Mie09] and Le Gall [LG10] about geodesics in the Brownian map. In [7], we refined the computation of the three-point function by taking into effect the phenomenon of "confluence" of geodesics, evidenced by Le Gall [LG10]. The full three-point function depends on 6 distance parameters, corresponding to the lengths of the common and proper parts of the three geodesics between the three marked points. We also obtain similar results for minimal separating loops. In [8], we considered quadrangulations with a boundary, and studied variants of the two-point function where either one or both marked points are on the boundary. Our work was an early attempt at considering the rich possible scaling limits of quadrangulations with a boundary, now studied in much greater detail in [BM17, BMR16]. Also, we first noticed there [8, Equation (7.1)] the connection with continued fractions, on which we will return in the next section. Finally, we considered in [9] the two-point function of quadrangulations without multiple edges, which we related to the physical concept of "minimal neck baby universes" (minbus). On the combinatorial side, we understood how multiple edges can be eliminated at the level of the CVS bijection, via the notion of "well-balanced tree", and of the two-point function, via a substitution scheme. More involved substitution schemes will be discussed in Chapter 2.

6. These two regions are well-defined almost surely by the sphericity of the Brownian map [LGP08, Mie08] and the uniqueness of the geodesic between almost every pair of points [Mie09].

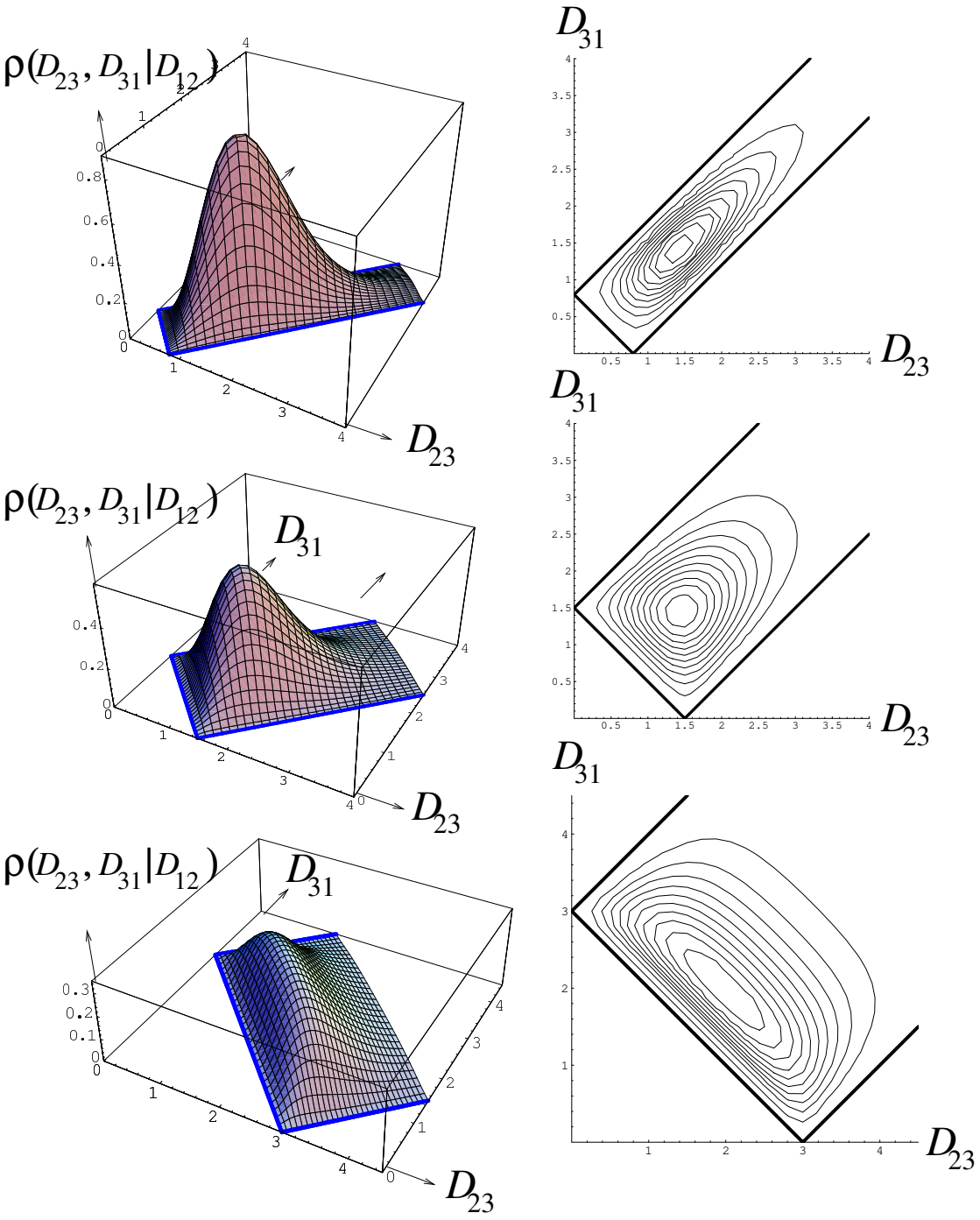

Figure 1.8 – Plots of the probability density of (D_{23}, D_{31}) conditionally on D_{12}, for $D_{12} = 0.8$, 1.5 and 3 (top to bottom). Here $D_{12} = S + T$, $D_{23} = T + U$ and $D_{31} = U + S$ denote the distances between three uniform points in a random quadrangulation with a large number n of faces, rescaled by a factor $n^{-1/4}$.

1.4 From the two-point function of Boltzmann maps to continued fractions

In this section we consider the family of (face-weighted) *Boltzmann maps*, obtained by endowing the set of all planar maps with the weight function

$$w(m) = \prod_{f \text{ face of } m} g_{\text{degree}(f)} \tag{1.14}$$

where $(g_k)_{k\geq 1}$ is a given sequence of nonnegative real numbers. This setting encompasses quadrangulations (take $g_k = g$ if $k = 4$ and 0 otherwise), edge-weighted general maps (take $g_k = t^{k/2}$ for all k), triangulations, etc. For simplicity, we restrict here to the bipartite case, i.e. we assume that $g_k = 0$ if k is odd (see Remark 1.4 below for a brief discussion of the general case). Also, some of our formulas hold only in the case of *bounded degrees*, i.e. when the set of k's such that $g_k \neq 0$ has a maximal element, which we denote by M.

The two-point function of Boltzmann bipartite maps with bounded degrees was considered in [BDFG03a], where we *guessed* its general formula by inferring it from the small values of M (e.g. 4 or 6) which we could solve explicitly. Our original approach was based on a certain "integrable" recurrence equation obeyed by the two-point function. Here I will present a rigorous proof of our formula, which was obtained several years later with Emmanuel Guitter in [10]. Our proof is based on the beautiful combinatorial theory of continued fractions, developed notably by Flajolet [Fla80] and Viennot [Vie84].

Let us first set up some conventions and notations. Here, the two-point function R_d is precisely defined as the generating function of pointed rooted bipartite maps where both endpoints of the root edge are at distance at most d from the origin (since the map is bipartite, one of the endpoints is strictly further from the origin than the other, and we assume that the root edge is oriented towards it). We conventionally set the constant term of R_d to 1, which makes the forthcoming expressions nicer. By Theorem 1.1 specialized to the geodesic labeling, we find that R_d is equal to the generating function of (one-face) mobiles whose labels are all positive, and which are rooted on a corner at a vertex labeled d. The Boltzmann weight (1.14) simply amounts to weighting unlabeled vertices in the mobile (an unlabeled vertex of degree k has weight g_{2k}). For $d = \infty$, the two-point function reduces to the generating function R of pointed rooted maps (or mobiles without the positivity constraint), which is the smallest positive, possibly infinite, root of the equation

$$R = 1 + \sum_{k=1}^{\infty} \binom{2k-1}{k} g_{2k} R^k. \tag{1.15}$$

From now on we assume that the weights $(g_{2k})_{k\geq 0}$ are such that $R < \infty$.

Theorem 1.3 (see [BDFG03a] and [10]). *The two-point function of Boltzmann bipartite maps with degrees bounded by $M = 2p + 2$ is given by*

$$R_d = R \frac{u_d u_{d+3}}{u_{d+1} u_{d+2}} \tag{1.16}$$

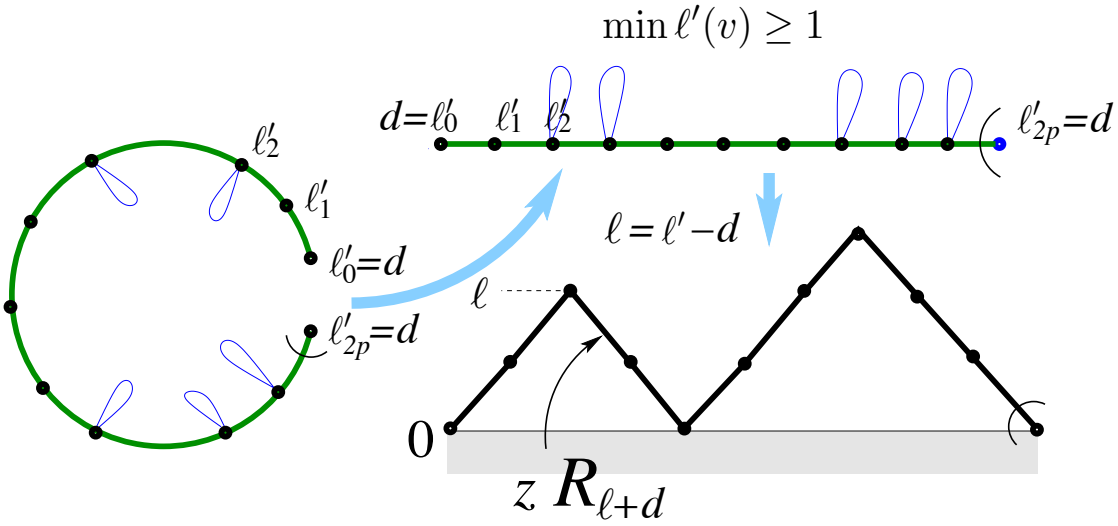

Figure 1.9 – The decomposition of the mobile associated with a map with a boundary counted by W_d. The sequence of labels around the special unlabeled vertex (coming from the root face) is coded by a Dyck path, whose down-steps correspond to the subtrees of the mobile. The global contribution of all possible subtrees for a down-step from height ℓ is $zR_{\ell+d}$. Notice the similarity with Figure 1.7.

where

$$u_d = \det_{1\le i,j\le p}\left(y_i^{d/2+j-1} - y_i^{-d/2-j+1}\right), \tag{1.17}$$

and $y_1, y_1^{-1}, \dots, y_p, y_p^{-1}$ *are the roots of the* characteristic equation

$$1 = \sum_{k=1}^{p+1} g_{2k} R^{k-1} \sum_{m=0}^{k-1} \binom{2k-1}{k-m-1} \sum_{j=-m}^{m} y^j. \tag{1.18}$$

In the case of quadrangulations ($p = 1$), we recover the expression (1.4). An interesting feature of our general expression is that the size of the determinant in (1.17) does not depend on the distance parameter d, which is useful for studying its asymptotic behavior.

In a nutshell, the key observation for proving Theorem 1.3 is that the sequence $(R_d)_{d\ge1}$ arises as the continued fraction expansion of the (well-known) generating function W_0 of maps with a boundary. From the general theory of continued fractions, it follows that R_d admits an expression of the form (1.16) with u_d a Hankel determinant whose entries are given by the series expansion of W_0. We finally use the specific form of these entries to identify the Hankel determinant as a symplectic or odd orthogonal Schur function, which yields (1.17) using the Weyl character formula.

Let us now provide a few more details. As mentioned above, the connection with continued fractions was first observed in [8], as a byproduct of the study of distances in

maps with a boundary [7]. More precisely, let us consider pointed rooted maps and regard the root face as a boundary. Since we wish to control the boundary length (degree) $2n$ separately, we exclude by convention the root face from the product (1.14), and rather assign it a weight z^n with z an extra parameter [8]. We denote by W_d the generating function of such weighted maps in which the distance from the origin to the root vertex is at most d, and no vertex incident to the boundary lies closer to the origin than the root vertex. In particular, for $d = 0$, the origin coincides with the root vertex, hence W_0 can be regarded as the generating function of maps with a boundary. By Theorem 1.1, W_d is also the generating function of certain (one-face) mobiles with positive labels. Using a decomposition of these mobiles illustrated on Figure 1.9 —which is in the same spirit as the decomposition used to arrive at (1.5)— we find that W_d counts certain weighted Dyck paths and, as such, satisfies the recurrence relation

$$W_d = 1 + zR_{d+1}W_dW_{d+1}. \tag{1.19}$$

By iterating this recurrence, we find that W_d admits the Stieljes-type continued fraction expansion

$$W_d = \cfrac{1}{1 - \cfrac{zR_{d+1}}{1 - \cfrac{zR_{d+2}}{1 - \ddots}}} \tag{1.20}$$

and in particular the *whole* sequence $(R_d)_{d\geq 1}$ arises as the *continued fraction expansion* of W_0 with respect to the variable z.

It now follows from the general theory of continued fractions that R_d can be expressed in terms of the Hankel determinants formed with the coefficients of the *power series expansion* of W_0 with respect to the variable z. More precisely, let us denote by w_n the coefficient of z^n in W_0, which counts rooted maps with a boundary of length $2n$ (we have $w_0 = 1$, corresponding to the map reduced to a single vertex). Then, for $n \geq 0$, we form the *Hankel determinants*

$$h_n^{(0)} = \det_{0\leq i,j\leq n} w_{i+j}, \qquad h_n^{(1)} = \det_{0\leq i,j\leq n} w_{i+j+1} \tag{1.21}$$

and we have the relations

$$R_{2n+1} = \frac{h_n^{(1)}/h_{n-1}^{(1)}}{h_n^{(0)}/h_{n-1}^{(0)}}, \qquad R_{2n+2} = \frac{h_{n+1}^{(0)}/h_n^{(0)}}{h_n^{(1)}/h_{n-1}^{(1)}} \tag{1.22}$$

where by convention $h_{-1}^{(0)} = h_{-1}^{(1)} = 1$. See for instance [Vie84] for a nice combinatorial proof of these formulas using nonintersecting lattice paths.

7. The observation was initially made in the case of quadrangulations, but it immediately extends to Boltzmann maps.

8. This is common in the context of Tutte equations, where z appears as the "catalytic variable" [BMJ06].

To proceed further we have to use the specific form of w_n, which is essentially known in the bipartite case since Tutte [Tut62b] [9]. It reads explicitly

$$w_n = R^n \sum_{q\geq 0} a_q \,\mathrm{Cat}(n+q) \tag{1.23}$$

where R is the generating function of pointed rooted maps considered before, $\mathrm{Cat}(n) := \frac{(2n)!}{n!(n+1)!}$ denotes the n-th Catalan number, and

$$a_q := \delta_{q,0} - \sum_{k\geq q+1} \binom{2k-2q-2}{k-q-1} g_{2k} R^k. \tag{1.24}$$

See [10, Section 3] for three different proofs of (1.23) in the more general nonbipartite setting [10]. We now form the Hankel determinants (1.21): first we dispose of the prefactor R^n in w_n, by noting that it just yields a prefactor R in the ratios (1.22). Therefore we find that R_d has the form (1.16), with u_d given by the reduced Hankel determinants

$$u_{2d+1} = \det_{0\leq i,j\leq d-1} \tilde{w}_{i+j}, \qquad u_{2d+2} = \det_{0\leq i,j\leq d-1} \tilde{w}_{i+j+1} \tag{1.25}$$

with $\tilde{w}_n = \sum_{q=0}^{\infty} a_q \,\mathrm{Cat}(n+q)$. This very specific form can be exploited to rewrite the determinants in "Toeplitz-Hankel" form: for ℓ, i, j nonnegative integers, let $p_{i,j}^{(\ell)} := \binom{\ell}{\frac{\ell+i-j}{2}} - \binom{\ell}{\frac{\ell+i+j+2}{2}}$ denote the number of sequences $(i = x_0, x_1, \ldots, x_{\ell-1}, x_\ell = j)$ such that $|x_k - x_{k-1}| = 1$ and $x_k \geq 0$ for all k (we have $\mathrm{Cat}(n) = p_{2n,0,0}$), then it is clear that

$$\begin{aligned} \mathrm{Cat}(i+j+q) &= \sum_{h,h'\geq 0} p_{0,2h}^{(2i)} p_{2h,2h'}^{(2q)} p_{2h',0}^{(2j)}, \\ \mathrm{Cat}(i+j+q+1) &= \sum_{h,h'\geq 0} p_{0,2h+1}^{(2i+1)} p_{2h+1,2h'+1}^{(2q)} p_{2h'+1,0}^{(2j+1)}. \end{aligned} \tag{1.26}$$

This allows to factor out unitriangular matrices from the Hankel matrices, and we obtain the expressions

$$u_{2d+1} = \det_{0\leq i,j\leq d-1} (b_{i-j} - b_{i+j+1}), \qquad u_{2d+2} = \det_{0\leq i,j\leq d-1} (b_{i-j} - b_{i+j+2}) \tag{1.27}$$

where $b_n := \sum_{q\geq 0} a_q \binom{2q}{q+n}$. Note that $b_{-n} = b_n$.

9. We pointed out in [10] that the generating function $W_0 = \sum_{n\geq 0} w_n z^n$ counting maps with a boundary is arguably the most important object in the enumerative theory of planar maps: it plays a fundamental role in Tutte equations, matrix integrals, etc. In some talks, Emmanuel had the idea of picturing it as an iceberg, whose hidden part was the continued fraction expansion.

10. A relatively short derivation of (1.23) is by "depointing" [10, Section 3.1]: let $R(v)$ denote the generating function of pointed rooted maps with an extra weight v per vertex. Then using mobiles one may see that (i) $R(v)$ satisfies the equation obtained from (1.15) by replacing the term 1 in the right-hand side by v and (ii) we have $w_n = \binom{2n}{n} \int_0^1 R(v)^n dv$. From this we get (1.23) through the change of variable $v \to R$.

So far we have not used the assumptions of bounded degrees. When this is the case, taking the maximal degree $M = 2p + 2$ as in Theorem 1.3, then it is clear from (1.24) that $a_q = 0$ for $q > p$, hence $b_n = 0$ for $|n| > p$. Hence, the matrices in (1.27) are banded. Let us consider the characteristic equation

$$\sum_{n=-p}^{p} b_n y^n = 0 \tag{1.28}$$

which may be rewritten in the form (1.18) by simple manipulations: it has $2p$ roots $y_1, y_1^{-1}, \dots, y_p, y_p^{-1}$, and the b_n's, hence the u_d's, are symmetric functions of them. It is then possible to deduce the form of u_d announced in Theorem 1.3 by some algebraic considerations: essentially this boils down to showing that the expressions (1.27) (viewed as polynomials in the y_i's) and (1.17) have the same zeros. But, as pointed out to us by Christian Krattenthaler, our determinants may actually be identified with *odd-orthogonal* and *symplectic Schur functions* of rectangular partitions, namely

$$u_{2d+1} \propto \mathrm{o}_{2p+1}((n+1)^d; y), \qquad u_{2d+2} \propto \mathrm{sp}_{2p}((n+1)^d; y), \tag{1.29}$$

see [10, Section 5] and references therein for more details. The expressions (1.27) correspond to Jacobi-Trudi-type formulas, which express the Schur functions in terms of the elementary symmetric polynomials, while (1.17) corresponds to the Weyl character formula (where the two parities can be put in a common form). Note that there are normalizing constants in (1.29), but they cancel in the ratios (1.22). This completes the proof of Theorem 1.3.

Remark 1.4. In [10] we actually treated the more general case of Boltzmann maps which are not necessarily bipartite. The main complication is that there are now *two* two-point functions to consider: R_d defined as before, and another S_d which essentially counts pointed rooted maps where the root edge is frustrated in the sense of Remark 1.1. The continued fractions that we encounter are of *Jacobi-type* instead of Stieljes-type, the combinatorial reason [Fla80] being that the decomposition illustrated on Figure 1.9 now involves Motzkin paths instead of Dyck paths. We end up with an expression of the form $R_d = R\frac{u_d u_{d+2}}{u_{d+1}^2}$ where u_d is still a rectangular symplectic Schur function, but with a larger number of variables than in the bipartite case ($M - 2$ rather than $(M - 2)/2$). S_d may be expressed in terms of a "nearly-rectangular" symplectic Schur in the same variables. See [10, Section 2] for more details. In the bipartite case there are "miraculous" factorizations [10, Section 5] which lead to the expressions presented here.

Remark 1.5. In the case of quadrangulations, we may provide a combinatorial interpretation of the simplest formula (1.4) via 1D dimers. There is an analogous formula for triangulations. See [10, Section 6] for more details.

1.5 Conclusion and perspectives

To conclude this chapter, let me first make a personal comment: I feel that the results presented or evoked here form the actual completion of the line of research initiated

in [BDFG03a] during my doctoral thesis. With Emmanuel we have obtained exact discrete expressions for several quantities related to the distance, studied their continuum limit, and finally obtained an explanation for the existence of such formulas through the combinatorial theory of continued fractions. Still, our approach left several questions which, to the best of my knowledge, remain open as of today.

First, it is natural to ask for an expression of the three-point function of Boltzmann maps, beyond the case of quadrangulations treated in this chapter and the case of general maps treated in [FG14]. It seems that, at least in the bipartite case, we may still employ the suitable labeling (1.3) and reduce the problem to the enumeration of certain mobiles with three faces. But we do not know how manageable their general structure will be. It seems that the notion of "chains", and the expression for their generating function $X_{s,t}$, extend naturally to the Boltzmann setting. But this is less clear for Y-diagrams. A different but related question is whether we may directly obtain the scaling limit (1.13) of the three-point function by a continuous approach, directly at the level of the Brownian map or why not Liouville quantum gravity/Quantum Loewner Evolution [MS16c]. Let me mention that, for the two-point function, such calculation was essentially done by Delmas [Del03].

Then, we may of course consider the n-point function for $n \geq 4$. As mentioned above, it is already unclear what a natural parametrization of the $\binom{n}{2}$ pairwise distances, generalizing (1.2), would be. We might still renounce to keep track of all distances, but just only consider a subset of them, for instance between the nearest neighbours. This seems similar in spirit to the original idea of Miermont [Mie09] of studying Voronoi-like tessellations on quadrangulations. Let me mention the fascinating recent conjecture of Chapuy [Cha16] concerning the masses of the cells in Voronoi tessellations of Brownian surfaces. The simplest case of this conjecture was proved by Guitter [Gui17] using techniques similar to those presented in this chapter. I cannot help noting that, as apparent on Figure 1.4, our trick for the three-point function involves a circle packing, and we might wonder whether more involved circle packings might play a role for more points.

Finally, several points remain open in the continued fraction approach of Section 1.4. While we have seen that the two-point function appears naturally in this approach, we might ask for a continued fraction interpretation of the three-point function, or of the intermediate quantities $X_{s,t}$ and $Y_{s,t,u}$ encountered in its computation. On the other hand, the generating function W_d of (1.20) corresponds to "truncations" of the continued fractions, but we do not know its general expression beyond the case of quadrangulations [8]. More generally, there is a deep connection between continued fractions and orthogonal polynomials, but the implications of this connection for maps have not been much investigated. Let me mention that the orthogonal polynomials arising from our approach are *different* from those usually considered in matrix models [10, Section 7.2]. Another question concerns the extension of our approach to Eulerian maps, for which it is natural to generalize the Boltzmann weight (1.14) by weighting differently the two types of faces. Rather than continued fractions one should then consider "multicontinued fractions". Together with Marie Albenque, we made a preliminary study of such fractions [13], but much remains to be understood. Let me also mention a work in progress by Bertrand Eynard and Emmanuel Guitter, which should answer some of these questions via the

framework of classical integrability [EG14]. Finally, it would be interesting to analyze the two-point function of Boltzmann maps without the assumption of bounded degrees, in order to deduce the continuum two-point function of stable maps [LGM11]. With Emmanuel Guitter and Grégory Miermont we made a first, but so far unsuccessful, attempt by trying to guess a (pseudo-)differential equation for the continuum one. Another possible way would be to analyze the asymptotics of the Hankel determinants (1.21), which should present all sorts of interesting technical challenges.

This concludes the list of questions that arise in line with the point of view developed in this chapter. The reader is invited to consult the references given in Section 1.1 for the many other approaches to the study of distances in random planar maps that have been developed since, and their current challenges.

2 The slice decomposition of planar maps

In this chapter we return to the enumerative and bijective theory of planar maps. The notions of distances and geodesics will still play an important role, but as technical tools rather than objects of study. The publications closest to this topic are [1, 3, 11, 16, 17], in addition to the papers discussed in Chapter 1 that already contain a fair amount of bijections. Here I will focus on one specific topic, the slice decomposition, which first made brief appearances in [8, 10, 13] as a reformulation of the [BDFG04] bijection, and whose real significance was understood in [16].

My purpose is here to give a "modern" presentation of the subject, with an emphasis on bijections. It is as self-contained as possible, except for some detailed proofs which should be looked for in [16]. After recalling the context in Section 2.1, I will introduce the theory of general slices in Section 2.2. I will then discuss irreducible slices in Section 2.3, before concluding with some perspectives in Section 2.4.

2.1 Context

The enumerative and bijective theory of planar maps has recently been the subject of a very nice review by Gilles Schaeffer [Sch15], containing an extensive bibliography. I feel therefore exempted from having to recall the whole context, and may focus on the more specific line of research motivating this chapter.

While fairly general, the "map-mobile" correspondence presented in Section 1.2 is only one among the many bijections that are known in literature. In particular, it is not well-suited for the study of maps with connectivity or girth constraints, for which specific bijections have been found [JS98, Sch98, DLDRP00, PS03, PS06, Fus07, FSP08, Fus09]. It does not apply either easily to tree-rooted maps [Ber07] [1]. Recently, several authors developed a general "bijective canvas" —this name being borrowed from [Sch15]— which, given a family of maps, splits the task of designing a bijection for it into two, more systematic, subtasks:

1. characterize the family of maps at hand in terms of the existence of certain orientations, following the theory of α-orientations developed by Felsner [Fel04] [2],

1. In [3] we proposed an extension of the bijection of [BDFG04] for maps decorated with spanning trees, Ising spins or hard particles (on bipartite maps), but our construction is arguably complicated. Note that Ising spins and hard particles on nonbipartite maps can be treated through the Eulerian version of the bijection of [BDFG04].

2. See also the earlier work of Propp [Pro93]. Bernardi [Ber07] was one of first to realize the relevance of orientations for the bijective approach, see also [BC11] for the higher genus extension of his bijection.

2. apply to these orientations one of the two known unified constructions: either the Bernardi-Fusy construction which is based on a suitably generalized notion of mobiles [BF12a, BF12b, BF14, BF18], or the Albenque-Poulalhon construction based on blossoming trees [AP15] [3] [4].

Many, if not all, previously known bijections for planar maps may be recovered through the bijective canvas.

In this chapter, we propose another general bijective approach which is based on geodesics rather than orientations. The fundamental idea is that maps can be canonically decomposed along leftmost geodesics, and we call slices the pieces appearing in this decomposition. Initially slices were conceived as a by-product of the CVS/BDG bijection: in the algorithm which produces a map out of a mobile, a slice is the portion of the map which arises from a specific subtree. This follows easily from the well-known observation that the sequence of "successors" of a corner of the mobile forms a leftmost geodesic in the map. We used slices in [10, Appendix A] and [13, Section 4] as a shortcut to reformulate certain combinatorial arguments without resorting to mobiles. But we also realized that slices remain convenient in some situations where mobiles might be impractical. A first example is [8, p. 33], where slices are used to decompose quadrangulations with self-avoiding (simple) boundaries, whose corresponding mobiles are not so easy to characterize. But the virtue of slice decomposition was only fully realized in [16] where we studied "irreducible" maps, which are even less easy to study using mobiles [5]. This shows that slice decomposition is *robust*. It also seems to behave well when passing to the scaling limit: in [LG13], Le Gall used slices (which he calls discrete maps with geodesic boundaries or DMGB) as an important ingredient in his proof. Bettinelli and Miermont use them again to study Brownian disks [BM17].

While it does not seem directly related with the topic of this chapter, I will conclude this overview of the context by mentioning the current common belief that planar maps decorated with models of statistical physics —such as the $O(n)$ loop model we will discuss in Chapter 3— are deeply related with bidimensional walks confined in a quadrant. One of the first to realize the importance of this idea is Sheffield in his "hamburger-cheeseburger bijection" [She16] which motivated the "mating-of-trees" approach to Liouville quantum gravity [DMS14]. There are several known bijections of this style —see the references given in the last section of [Sch15]— and the list keeps growing [KMSW19, Bud17a, GKMW18, BHS18]. I mention a possible connection with slice decomposition in Section 2.4.

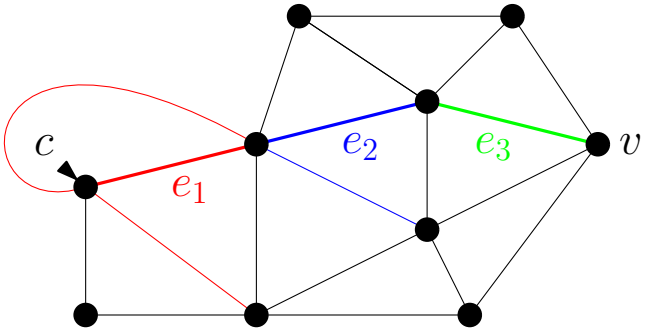

Figure 2.1 – Construction of the leftmost geodesic from the corner c to the vertex v. We start at the vertex incident to c, and consider all the incident edges leading to a vertex strictly closer to v (these edges are here shown in red). We pick e_1 as the leftmost one (i.e. e_1 is the first red edge encountered when turning clockwise around the vertex incident to c). We then move to the other endpoint of e_1, and consider again all the incident edges leading to a vertex strictly closer to v (these edges are here shown in blue). We pick e_2 as the leftmost one, using now e_1 as the reference, and so on until we reach v. The edges e_1, e_2, ..., form the wanted leftmost geodesic. Note that this construction only relies on the existence of a local orientation at each vertex.

2.2 General slices

The most important part of this section consists of definitions: what slices are and which operations we may perform on them. Let us first observe that, in a planar map, or more generally an orientable map, there is a well-defined notion of *leftmost geodesic* from a corner c to a vertex v. As illustrated on Figure 2.1, we may construct it step-by-step by starting from the vertex incident to c and by moving, at each step, to the leftmost adjacent vertex lying strictly closer to v, where we use the direction we are coming from as a reference. We now introduce slices and some related terminology.

Definition 2.1 (see Figure 2.2(a) for an illustration)**.** A *slice* is a planar map with a boundary, with three distinguished outer corners —denoted here A, B, and C— which appear in counterclockwise around the outer face and split its contour in three portions:

— the *left boundary* AB, which is a geodesic between A and B,

— the *right boundary* AC, which is the unique geodesic between A and C,

3. In this document I do not consider at all blossoming trees, though I also investigated them during my doctoral thesis and shortly after in [1]. I remain puzzled by the fact that the blossoming bijection of [BDFG02a] appears in the intersection of both unified constructions [BF12b, Section 7.3] [AP15, p. 14].

4. See also the recent paper [Lep19] which gives a blossoming bijection in any genus, building on Propp's theory of orientations [Pro93].

5. In [BF12b, Section 1.1], Bernardi and Fusy mention that their approach based on generalized mobiles may be extended to irreducible maps, but cite a paper which has not appeared yet.

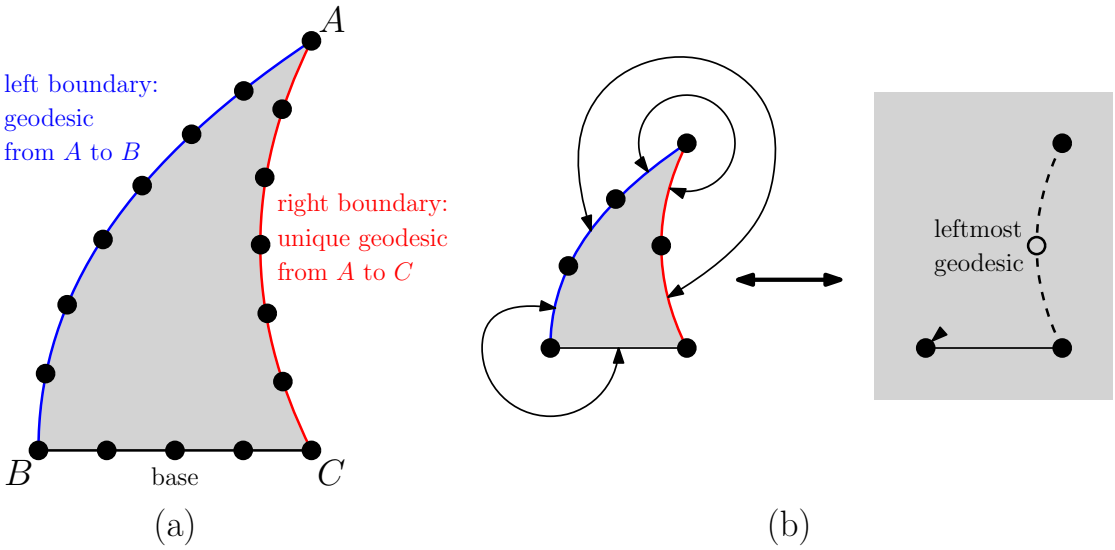

Figure 2.2 – (a) General structure of a slice. (b) The one-to-one correspondence between elementary slices and pointed rooted maps.

— and the *base* BC.

The vertex incident to A is called the *apex*, the *width* is the length of the base, the *depth* is the length of the left boundary, and the *tilt* is the depth minus the length of the right boundary. A slice of width 1 is said *elementary*, a slice of arbitrary width is said *composite*. The unique elementary slice of tilt -1 is the *trivial slice* reduced to a single edge whose two end corners are $A = B$ and C. It is different from the *empty slice*, which is the elementary slice of tilt $+1$ reduced to a single edge whose two end corners are B and $A = C$. Note that, by the triangular inequality, the tilt is smaller than or equal to the width, hence an nontrivial elementary slice may have tilt 0 or 1.

In [10, 16], it is assumed that all slices are elementary, but here we find convenient to also consider composite slices. Note that we impose no constraint on the base, it is not even assumed that it forms a simple path, and the graph distance from B to C may be smaller than the width.

For simplicity, we restrict from now on on to bipartite maps, and only briefly discuss the general case in Remark 2.1 at the end of this section. Bipartiteness implies that the width and the tilt have the same parity, in particular a nontrivial elementary slice has tilt 1.

It was noted in [10] that there is a one-to-one correspondence between elementary slices and pointed rooted maps: we go from an elementary slice to a pointed rooted map by identifying the boundary edges together as illustrated on Figure 2.2(b). We must exclude the trivial and empty slices which are pathological. After the identification, the base becomes the root edge and the apex becomes the origin. The correspondence is one-to-one because the merged boundaries form the leftmost geodesic going from the root to

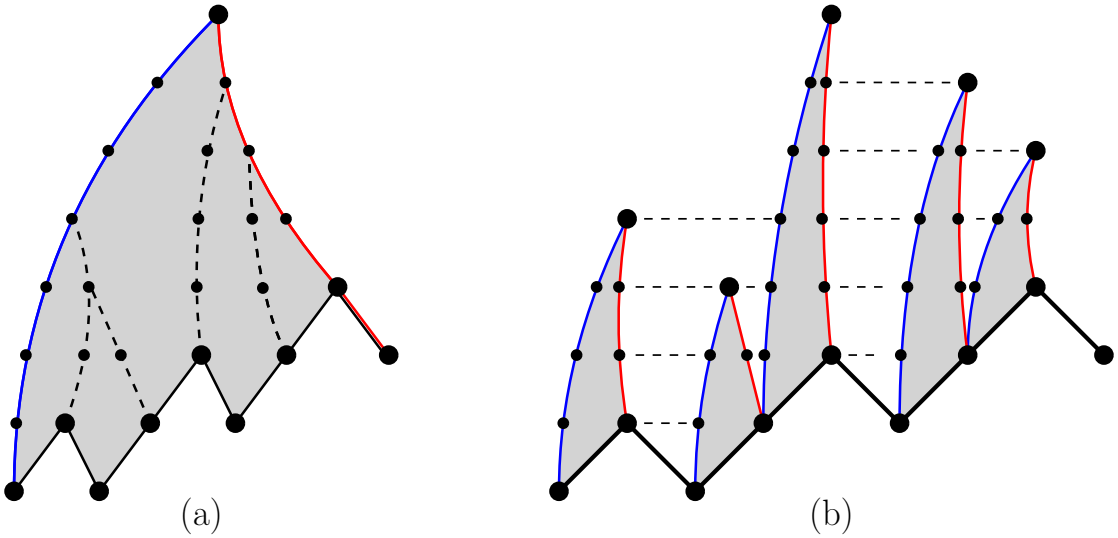

Figure 2.3 – (a) The decomposition of a composite slice into elementary slices, by cutting along the leftmost geodesics from the base vertices. (b) The corresponding "path of elementary slices".

the origin, which can be recovered canonically from the pointed rooted map structure [6]. From this correspondence, we deduce that the generating functions of elementary slices of tilt 1, weighted by the Boltzmann weight (1.14) —where we do not include the outer face in the product— is equal to R as defined in Section 1.4. Note that R has constant term 1, corresponding to the empty slice. The generating function of elementary slices of depth at most d is nothing but the two-point function R_d.

We now consider composite slices and describe the important operation of decomposing them into elementary slices. See the illustration on Figure 2.3(a). We start from a composite slice with apex A and base BC, and denote by $v_0, v_1, \dots, v_n$ the base vertices read from B to C. To the base vertex v_i we associate a label $\ell_i := d(v_0, A) - d(v_i, A)$, where d denotes the graph distance in the slice. Note that n is the width, $d(v_0, A)$ is the depth, ℓ_n is the tilt, and we have $|\ell_i - \ell_{i-1}| = 1$ for any $i = 1, \dots, n$. We now cut the slice along each leftmost geodesic from a base vertex to the apex A. This has the effect of cutting the composite slice into elementary slices. More precisely, if we denote by v_i' the first vertex common to the leftmost geodesics started at v_{i-1} and v_i, then these two geodesics delimit a slice of width 1, base $v_{i-1}v_i$, apex v_i' and tilt $\ell_i - \ell_{i-1}$. If $\ell_i - \ell_{i-1} = -1$, the slice is trivial. If $\ell_i - \ell_{i-1} = 1$, we obtain a nontrivial slice, which is possibly empty if the geodesic from v_{i-1} starts with the base edge $v_{i-1}v_i$. To summarize, we end up with a label sequence $0 = \ell_0, \ell_1, \dots, \ell_n$ with increments ± 1, and a nontrivial elementary slice for each up-step of the label sequence (and the trivial slice for each down-step). We

6. In all rigor, we only consider here pointed rooted maps such that the leftmost geodesic from the root to the origin starts with the edge immediately left of the root corner. In the bipartite case, these form precisely half of all pointed rooted maps (just reverse the direction of the root edge to obtain the others). Note that this remark was already made in Section 1.4 when defining the two-point function.

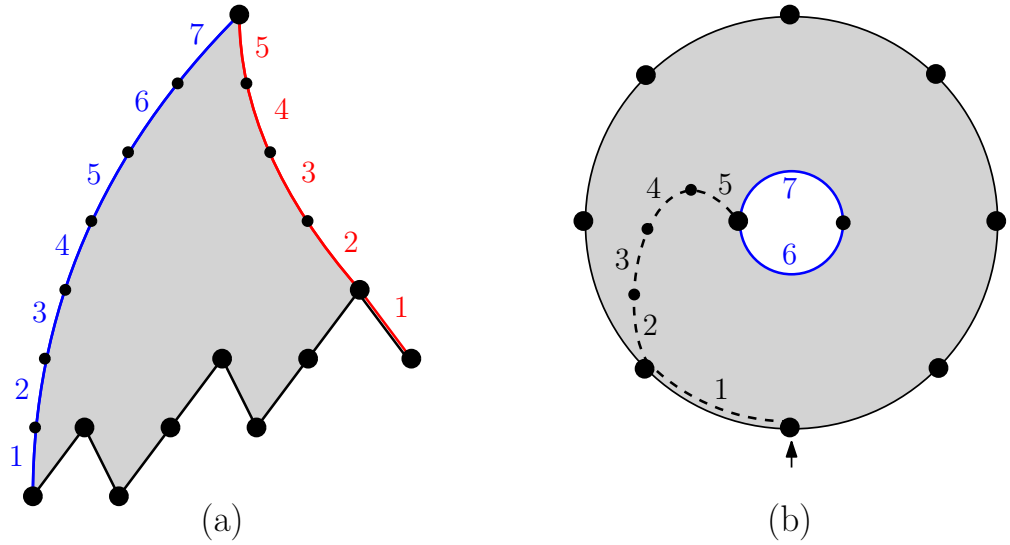

Figure 2.4 – (a) Wrapping a composite slice of tilt +2: pairs of edges with the same label are identified. They become a path joining the outer face to the central face (formed by the 2 unmatched left boundary edges) in the resulting 2-annular map (b).

may call such object a "path of elementary slices", and it is not difficult to check that the correspondence is one-to-one as we may reconstruct the composite slice by gluing back the elementary slices together as shown on Figure 2.3(b). An immediate consequence of the decomposition is that the generating function of composite slices of width n and tilt ℓ is equal to $\binom{n}{\frac{n+\ell}{2}} R^{\frac{n+\ell}{2}}$. It is possible to keep track of the depth of the composite slice, by expressing it in terms of the labels and the depths of the elementary slices, but we will not enter into such considerations here.

As an application of this decomposition, we easily recover the equation (1.15) satisfied by R: the term 1 on the right-hand side corresponds to the empty slice, and the term of index k in the sum corresponds to elementary slices where the base edge is incident to an inner face of degree $2k$. Indeed, for such a slice, removing the base edge yields a composite slice of width $2k-1$ and tilt 1.

We now describe another important operation on composite slices called *wrapping*, which we illustrate on Figure 2.4. It consists in identifying boundary edges as in the procedure of Figure 2.2(b), but the identifications are different. Namely, we only identify together the left and right boundaries, starting from the base. When the tilt is nonzero, some edges of the longer boundary remain unmatched, and they delimit a new face which we call the *central* face. The unmatched base edges delimit another new face which we consider as the outer face, and which we root at the former position of the base endpoints. When the tilt is zero, there is no central face but an origin which is the former apex. Before stating the conclusion as a theorem, we first need to characterize the resulting maps.

Definition 2.2. Given a positive integer ℓ, a *ℓ-annular map* is a rooted map with an extra distinguished face of degree ℓ, called the *central* face, such that any cycle winding around the central face has length at least ℓ. A *ℓ-strict-annular map* is a ℓ-annular map such that the contour of the central face is the unique winding cycle of length ℓ.

Note that we allow for odd values of ℓ, which corresponds to the "quasi-bipartite" case where both the central and the outer face have odd degrees (but all other faces have even degrees as usual). Pointed rooted maps may be thought as the case $\ell = 0$.

Theorem 2.1 (see [10] and [16])**.** *The wrapping operation is a one-to-one correspondence between:*

— *composite slices of zero tilt and pointed rooted maps,*

— *composite slices of positive tilt ℓ and ℓ-annular maps,*

— *composite slices of negative tilt $-\ell$ and ℓ-strict-annular maps.*

In all cases, the width of the composite slice is equal to the degree of the outer face of the corresponding map. The corresponding generating functions for a prescribed width/outer degree n are respectively $\binom{n}{n/2}R^{n/2}$, $\binom{n}{(n+\ell)/2}R^{(n+\ell)/2}$ and $\binom{n}{(n-\ell)/2}R^{(n-\ell)/2}$, where R is determined by (1.15)*.*

The case of zero tilt is rather straightforward and was given in [10]. The case of nonzero tilt is more involved and requires an argument which was first given in [16, Section 7.2] for the case of irreducible maps considered in the next section. As observed by the anonymous referee —which I would like to thank again for his/her most insightful report— the argument is actually more general, and I will now sketch it in the simpler current setting.

The main difficulty consists in defining the inverse operation of wrapping, i.e. reconstructing a composite slice from a map. The basic idea is that, as before, the left and right boundaries of the slice should somehow correspond to a "leftmost geodesic" in the map. This works straightforwardly for a pointed rooted map, where we have to consider the leftmost geodesic from the root to the origin. For a ℓ-(strict-)annular map, we actually have to introduce the *lift* of the map, which may be seen as its preimage through the exponential mapping $z \mapsto \exp(2i\pi z)$, assuming that the map is drawn on the complex plane with the point $z = 0$ within the central face. The lift is an infinite but periodic map, so its properties remain manageable. We then consider the leftmost geodesic going from (a preimage of) the root to $+\infty$ (for a ℓ-annular map) or to $-\infty$ (for a ℓ-strict-annular map). It follows from Definition 2.2 that such geodesic is indeed well-defined, and that it eventually reaches the central face and continues following its contour forever. See Figure 2.5 for an illustration, and [16] for more details. We now simply have to cut along the finite portion of the geodesic between the root and the coalescence point to obtain a composite slice, and it is now elementary to check that this is indeed the inverse operation of wrapping.

Theorem 2.1 may be seen as a first illustration of the relevance of slice decomposition. Its enumerative consequences can also be obtain as a particular case of [BF12b, Theorem 34] which relies on so-called "b-dibranching mobiles", but I consider the present

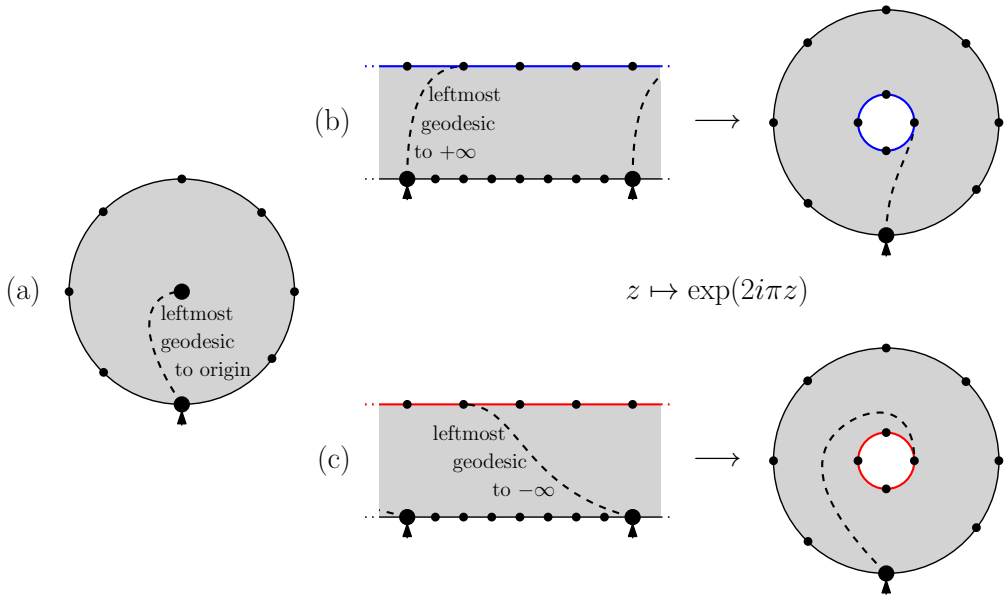

Figure 2.5 – Selecting a suitable leftmost geodesic in (a) a pointed rooted map, (b) a ℓ-annular map and (c) a ℓ-strict-annular map. In the annular cases, the leftmost geodesics are actually constructed on the "lift".

approach to be more transparent. Slice decomposition is actually able to treat the general setting of [BF12b] as we will see in the next section. But let us now finish this section with some remarks.

First, notice that the generating function of ℓ-annular slices is equal to R^ℓ times that of ℓ-strict-annular slices, for any outer degree n. This calls for a combinatorial explanation, which is as follows: given a ℓ-annular slice, we may decompose it bijectively along its *outermost* winding cycle of length ℓ, to obtain a ℓ-strict-annular slice (the exterior of the cycle) and a ℓ-annular slice of outer degree ℓ (the interior of the cycle). The latter slices have generating function R^ℓ, as seen by taking $n = \ell$ in Theorem 2.1.

Elaborating on this idea, we may enumerate general annular maps with prescribed boundary lengths —i.e. quasi-bipartite maps with two marked corners incident to distinct faces of respective prescribed degrees m and n, with $m+n$ even and no constraint on the winding cycles— through the generating function

$$\begin{aligned} A_{m,n} :&= \sum_{\substack{0\le\ell\le\min(m,n)\\ \ell+m \text{ even}}} \ell \times \binom{m}{(m-\ell)/2} R^{(m-\ell)/2} \times \binom{n}{(n+\ell)/2} R^{(n+\ell)/2} \\ &= \frac{2}{m+n} \cdot \frac{m!}{\lfloor \frac{m}{2} \rfloor! \lfloor \frac{m-1}{2} \rfloor!} \cdot \frac{n!}{\lfloor \frac{n}{2} \rfloor! \lfloor \frac{n-1}{2} \rfloor!} \cdot R^{(m+n)/2}. \end{aligned} \tag{2.1}$$

Indeed, considering such an annular map and treating the face of degree m as the outer face, we may decompose it along the outermost cycle of minimal length, which we denote by ℓ, and obtain a ℓ-strict-annular map of outer degree m (the exterior of the cycle)

and a ℓ-annular map of outer degree n (the interior of the cycle, after inversion). This decomposition is ℓ-to-one because there are ℓ ways to glue back the two pieces together. This explains the first line of (2.1) and we pass to the second line by a simple identity on binomial numbers. Note that the formula remains meaningful in the case $m = 0$, where we recover the generating function of pointed rooted maps with outer degree n.

The formula (2.1) appears in [Eyn16, Corollary 3.1.2] under different notations. A more general formula of Collet and Fusy [CF12] counts quasi-bipartite maps with an arbitrary number of boundaries of prescribed lengths: it may be obtained from (2.1) by taking derivatives with respect to the face weights $(g_{2k})_{k\geq 0}$ and by using (1.15), or by integrating in the case of one boundary to recover the formula (1.23).

Remark 2.1. The discussion of this section extends naturally to the nonbipartite case, up to some complications which we list here. First, the tilt of a slice is no longer necessarily of the same parity as the width. Therefore, there exists another type of elementary slice which has zero tilt. The generating function of such slices with depth at most d is nothing but the quantity S_d mentioned in Remark 1.4. Pairs of such slices may be glued to obtain a pointed rooted map where the root edge is frustrated, see [10, Figure 17]. The decomposition of a composite slice now involves a label sequence with increments $-1, 0, +1$, and elementary slices of zero tilt are attached to the 0-increments. The wrapping operation works unchanged. Generating functions of composite slices and annular maps are now polynomials in R and $S := S_\infty$, whose expressions are elementary but longer than those of the bipartite case $S = 0$. We therefore leave them as exercises to the reader.

2.3 Irreducible slices

In this section we explain how to adapt the slice decomposition in the presence of "irreducibility" constraints. Our discussion follows for a good part that of the previous section, and emphasizes what the new phenomena related to irreducibility are. The presentation will therefore be different from [16]. But let us first define what an irreducible map is.

Definition 2.3. Given a nonnegative integer d, a map (resp. a map with a boundary) is said *d-irreducible* if it does not contain any cycle of length smaller than d, and any cycle of length d is the contour of a face (resp. is the contour of an inner face). An *irreducible d-angulation* is a d-irreducible map where every face has degree d.

Note that d is unrelated to the depth considered previously. The notion of irreducibility is closely related to the girth: a d-irreducible map has girth at least d, and a map of girth at least d is a $(d-1)$-irreducible map containing no face of degree $d-1$.

Irreducible triangulations and quadrangulations were first enumerated by respectively Tutte [Tut62a] and Mullin and Schellenberg [MS68]. Note that these authors do not use the word "irreducible" but "simple", which probably did not have its current acceptation in the sixties. Their approach is based on a substitution procedure —see for instance [FS09, I.6.2] for general background— by deducing the generating function of

irreducible tri- or quadrangulations from that of simple ones. In our initial investigation of irreducible maps, we actually followed their approach by devising an iterated substitution procedure for enumerating d-irreducible maps, with arbitrary d and prescribed face degrees. We do not enter into the details and refer the interested reader to [16, Sections 2 and 3]. But we then realized that some of the auxiliary quantities that we needed for our computations could be interpreted combinatorially as slice generating functions. This allowed us to rederive our enumerative results bijectively, and recover in particular the bijections of [Fus09, FSP08] for irreducible triangulations and quadrangulations. We note in passing that irreducible quadrangulations are the "medials" —recall Figure 0.3— of 3-connected maps [MS68, Section 5], which themselves correspond to convex three-dimensional polyhedra by Steinitz's theorem.

We now consider d-irreducible slices, defined by combining Definitions 2.1 and 2.3 (note that a slice has a boundary). The Boltzmann weight of a d-irreducible slice is defined as in (1.14), where as before we do not include the outer face in the product. Here the weight only involves the g_k's for $k \geq d$. We again restrict here to the bipartite case, so we take $d = 2b$ and $g_k = 0$ for k odd. We denote by $R^{(d)}$ the generating function of bipartite d-irreducible nontrivial elementary slices.

The first new phenomenon is that it is no longer possible to identify $R^{(d)}$ with the generating function of d-irreducible pointed rooted maps. Indeed, gluing the boundaries as in Figure 2.2(b) might create "short cycles" that wind around the origin.

Fortunately, d-irreducibility poses no problem for the decomposition of Figure 2.3: a composite slice is d-irreducible if and only if all the elementary slices appearing in its decomposition are d-irreducible. One direction is obvious, the other relies on the observation that, when gluing d-irreducible elementary slices along their left/right boundaries as on Figure 2.3(b), then we cannot create "short cycles". Indeed, since the glued boundaries are geodesics, and since every cycle in the composite map that crosses one of them must cross it another time, we see that for any cycle in the composite map there exists a shorter cycle in each elementary slice that it visits. We deduce that the generating function of d-irreducible composite slices of width n and tilt ℓ is $\binom{n}{\frac{n+\ell}{2}}(R^{(d)})^{\frac{n+\ell}{2}}$. That is, we only change R into $R^{(d)}$ with respect to the expression of Section 2.2.

The main complication arises when we attempt to find an analogue of equation (1.15) for $R^{(d)}$ by removing the base edge in a d-irreducible elementary slice. The composite slice we obtain by removing the base edge is still d-irreducible, but it satisfies extra constraints due to cycles going through the base edge in the elementary slice. We therefore have to find another decomposition, which may be done by introducing generalized elementary slices, which we called k-slices in [16] but which we call here quasi-slices.

A *quasi-slice* is defined as an elementary slice in Definition 2.1, with the sole difference that the left boundary is no longer assumed to be a true geodesic between A and B, but only a shortest path among paths *avoiding the base edge* BC. See Figure 2.6(a) for an illustration. The tilt may now take values other than ± 1. Since we have not changed the assumption on the right boundary, the tilt is still at least -1 with equality if and only if the quasi-slice is reduced to the trivial slice, but we may now have a tilt larger than 1. By bipartiteness, it must be an odd number, and we denote by $U_k^{(d)}$ the generating function

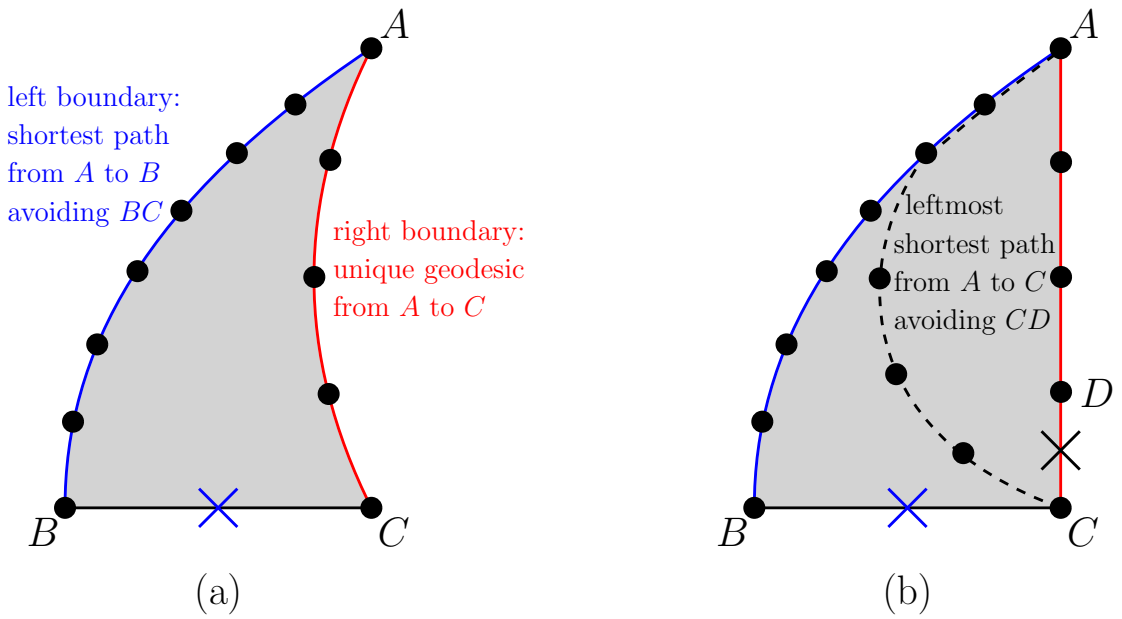

Figure 2.6 – (a) General structure of a quasi-slice. (b) The decomposition of a quasi-slice with "small" tilt: we cut along the leftmost shortest path from A to C avoiding the first vertex D of the right boundary.

of d-irreducible quasi-slices of tilt $2k+1$. We have $U_{-1}^{(d)} = 1$ and $U_0^{(d)} = R^{(d)} - 1$, as the empty slice should not be regarded as a quasi-slice. We now explain how to decompose a quasi-slice, which is done in two ways depending on k (recall that $d = 2b$).

— For $k \geq b$, the decomposition consists as before in removing the base edge. We obtain a d-irreducible composite slice of tilt $2k+1 \geq d+1$, and we easily check that the decomposition is now bijective because of the large tilt (in the reverse bijection we do not risk creating short cycles). We deduce that

$$U_k^{(d)} = \sum_{\ell \geq k+1} g_{2\ell} \binom{2\ell-1}{\ell+k} (R^{(d)})^{\ell+k}, \qquad k \geq b. \tag{2.2}$$

In particular this quantity vanishes in the case of irreducible d-angulations, since we shall take $g_{2\ell} = 0$ for all $\ell \geq b$.

— For $0 \leq k \leq b-1$, we have to consider a new decomposition illustrated on Figure 2.6(b). First, d-irreducibility implies that the length of the right boundary is positive (except in the case $k = b-1$ where the slice might also be reduced to a single d-gon). Hence, there is a first vertex D on the right boundary, and we now cut the quasi-slice along the leftmost shortest path from A to C avoiding CD. We obtain generically two quasi-slices, with respective bases BC and CD and tilts

$2i+1$ and $2j+1$, where $-1 \le i < k$ and $j = k-i$. We deduce that

$$U_k^{(d)} = g_{2b}\delta_{k,b-1} + U_{k+1}^{(d)} + \sum_{j=1}^{k} U_{k-j}^{(d)} U_j^{(d)}, \qquad 0 \le k \le b-1. \tag{2.3}$$

Note that, combining (2.2) and (2.3), we get a closed system of equations for $U_0^{(d)} = R^{(d)} - 1, U_1^{(d)}, \dots, U_b^{(d)}$. It is actually possible to eliminate the last b quantities, see [16, Section 5.4] for details, and we end up with the following explicit equation for $R^{(d)}$:

$$-\frac{1}{b}\sum_{p=1}^{b}\binom{b}{p}\binom{b}{p-1}\left(1-R^{(d)}\right)^p = g_{2b} + \sum_{\ell \ge k+1} g_{2\ell}\binom{2\ell-1}{\ell+k}(R^{(d)})^{\ell+k}. \tag{2.4}$$

It should be seen as the d-irreducible counterpart of (1.15). Let us mention that, in the decomposition of quasi-slices, it is possible to keep track of the depth and obtain refined generation functions that are essentially two-point functions of d-irreducible maps, see [16, Section 8].

We turn to the wrapping operation of Figure 2.4: it actually works without any modification once we realize that we should treat differently the winding and nonwinding cycles. This is the clever observation of our anonymous referee, which we mentioned above. Let us define the resulting objects.

Definition 2.4. Given two nonnegative integers d, ℓ, a (d,ℓ)-*quasi-irreducible annular map* is a rooted map, where the outer face is regarded as a boundary, and an extra distinguished *central* face of degree ℓ —or a marked central vertex if $\ell = 0$— such that:

— the length of any cycle not winding around the central face/vertex is at least d, with equality if and only if the cycle is the contour of a face,

— for $\ell > 0$, the length of any cycle winding around the central face is at least ℓ.

A (d,ℓ)-*irreducible annular map* is defined in the same way, with the extra condition that the only winding cycle of length ℓ is the contour of the central face.

For $d = 0$, we recover the notion of ℓ-(strict)-annular map of the previous section. For $d = \ell$, a (d,d)-irreducible annular map is nothing but a d-irreducible map with a boundary and an extra marked face of degree d. We again allow ℓ to be odd, which corresponds to the quasi-bipartite case where the central and outer faces are the only two faces of odd degree. We may now state the d-irreducible analogue of Theorem 2.1.

Theorem 2.2 (see [16, Section 9.3])**.** *The wrapping operation is a one-to-one correspondence between:*

— *d-irreducible composite slices of nonpositive tilt $-\ell$ and (d,ℓ)-irreducible annular maps,*

— *d-irreducible composite slices of nonnegative tilt ℓ and (d,ℓ)-quasi-irreducible annular maps.*

In all cases, the width of the composite slice is equal to the degree of the outer face of the corresponding map. The corresponding generating functions for a prescribed width/outer degree n are respectively $\binom{n}{(n-\ell)/2}(R^{(d)})^{(n-\ell)/2}$ and $\binom{n}{(n+\ell)/2}(R^{(d)})^{(n+\ell)/2}$, where $R^{(d)}$ is determined by (2.4).

As a consequence, the generating function $F^{(d)}_{2m}$ of d-irreducible maps with a boundary of degree $2m$ satisfies the "pointing" formula

$$\frac{\partial F^{(d)}_{2m}}{\partial g_d} = \binom{2m}{m-b}(R^{(d)})^{m-b}, \qquad d = 2b. \tag{2.5}$$

The proof is essentially the same as that of Theorem 2.1. The only new thing to check is that we cannot create "short" nonwinding cycles when identifying the left and right boundary as in Figure 2.4, but the reasoning is the same as for the decomposition of d-irreducible composite slices into elementary slices.

We now conclude this section by some remarks, several of which are direct adaptations of the remarks made after Theorem 2.1. The generating function of (d,ℓ)-quasi-irreducible annular maps is equal to $(R^{(d)})^\ell$ times that of (d,ℓ)-irreducible annular maps, for the same combinatorial reason as before. We may also enumerate d-irreducible quasi-bipartite annular maps with prescribed boundary lengths $m, n > d$ by decomposing along the outermost shorter cycle which must have a length $\ell > d$, to get the generating function

$$\begin{aligned} A^{(d)}_{m,n} :&= \sum_{\substack{2b<\ell\le\min(m,n)\\ \ell+m \text{ even}}} \ell \times \binom{m}{(m-\ell)/2}(R^{(d)})^{(m-\ell)/2} \times \binom{n}{(n+\ell)/2}(R^{(d)})^{(n+\ell)/2} \\ &= \frac{2}{m+n}\cdot\frac{m!}{\lfloor\frac{m+d}{2}\rfloor!\lfloor\frac{m-1-d}{2}\rfloor!}\cdot\frac{n!}{\lfloor\frac{n+d}{2}\rfloor!\lfloor\frac{n-1-d}{2}\rfloor!}\cdot(R^{(d)})^{(m+n)/2}. \end{aligned} \tag{2.6}$$

This is the d-irreducible analogue of the formula (2.1), which we recover for $d = 0$. By differentiating with respect to the face weights $(g_{2k})_{k>d}$, we obtain a d-irreducible analogue of the Collet-Fusy formula [CF12]. We actually adapted their bijective proof to the irreducible setting in [17], but we will not enter into the details here. Note that, to obtain the generating function $F^{(d)}_n$ of d-irreducible maps with a single boundary, we may either integrate (2.6) with respect to g_m for some $m > d$, or integrate (2.5) at $n = 2m$ with respect to g_d. The lengthy expression of $F^{(d)}_n$ is given at [16, Equation (3.21)], where we obtained it via substitution. To my knowledge, it still awaits a bijective interpretation.

So far we have enumerated d-irreducible maps with boundaries. Note that, by Definition 2.3, a d-irreducible map with a boundary of length d is reduced to either a tree or a single d-gon. But, if we do not regard the outer face as a boundary anymore, there may exist nontrivial rooted d-irreducible maps whose outer face has degree d, and we denote by H_d their generating function. In [16, Section 9.1], we computed H_d through substitution. We may also characterize it combinatorially as follows. Observe that $\frac{\partial H_d}{\partial g_d}$ counts d-irreducible maps with two marked faces of degree d, which are closely related with (d,d)-quasi-irreducible maps whose generating function is $(R^{(d)})^d$. Indeed, the latter are

essentially "sequences" formed by concatenating the former. There are small subtleties to be taken care of, and we obtain the relation

$$\frac{\partial H_d}{\partial g_d} = 2 + d g_d - \frac{d}{2} \cdot \frac{2g_d + g_d^2}{1 + 2g_d + g_d^2} - (R^{(d)})^{-d}, \tag{2.7}$$

see also [16, Equation (9.21)].

Again, all our discussion may be extended to the nonbipartite case, at the price of having to introduce another generating function $S^{(d)}$ counting d-irreducible elementary slices of tilt 0. The first part of Theorem 2.2 is unchanged, but the generating functions are now polynomials in $R^{(d)}$ and $S^{(d)}$.

Finally, let us observe that we may recover the enumerative results of [BF12b] for maps with prescribed girth, simply by setting the weight g_d to 0: as mentioned above a d-irreducible map without d-gons is nothing but a map of girth $d+1$ (or $d+2$ in the bipartite case).

2.4 Conclusion and perspectives

We now conclude this chapter by evoking some directions for future research.

A first immediate question is the connection between slice decomposition and the bijective canvas. There is such a close connection between the enumerative results of Section 2.3 and those of [BF12b] that we may wonder whether the two approaches are the two sides of the same coin. At the fundamental level it is however not clear how to relate orientations and geodesics, I currently do not understand the Bernardi-Fusy bijection between bioriented maps and generalized mobiles well enough to tell. Superficially, the fact that it is essential to consider orientations that are *accessible* suggests that one might associate with it a suitable generalized distance. Incidentally, we may wonder whether the bijection of Section 1.2 —that produces mobiles with several faces— might be extended in the Bernardi-Fusy framework to treat certain "partially accessible" orientations.

Another direction concerns the extension of slice decomposition to Eulerian maps, where we may distinguish two types of faces hence weight them differently. In view of the Eulerian version of the [BDFG04] bijection, it is natural not to consider true geodesics anymore, but instead shortest oriented paths with respect to the canonical orientation that alternates around each vertex. The fundamental ideas of slice decomposition seem to adapt to this setting, see [13, Section 4] for the case of constellations and [DPS16, Der18] for the case of corner triangulations, which are Eulerian triangulations subject to certain irreducibility constraints arising from their connection with corner polyhedra [EM14]. With Marie Albenque, we are currently investigating the general theory. One of our goals is to provide bijective proofs of the several beautiful formulas for bicolored (Ising) maps which may be found in [Eyn16, Chapter 8]. We already obtained several results which seemed out of reach using the Eulerian mobiles of [BDFG04] or the blossoming trees of [BMS02]. Our next challenge is the treatment of maps with "Dobrushin" boundary conditions, which seem naturally connected with bidimensional walks by keeping track of the boundary lengths of each color in some suitable (e.g. peeling) decomposition. See also

the recent preprint [CT18] of my former student Linxiao Chen [7] and Joonas Turunen, which enumerates Ising triangulations with Dobrushin boundary conditions via Tutte equations. We note that Eulerian maps with girth —and more generally cycle-length— constraints have been considered by Bernardi and Fusy in [BF14] under the name of hypermaps. Once again one may attempt to reproduce their results using slices. We speculate that the choice for the decomposition of a quasi-slice used in Section 2.3, where we may choose to either remove the base edge or cut as in Figure 2.6, might be made dependent on some varying parameter to accommodate for cycle-length constraints.

A third direction which I would like to investigate is the possible connection with topological recursion, see [Eyn16, Chapter 7] for an account of its map-related aspects. In topological recursion, a key role is played by the "Bergman kernel" which, in maps, is essentially the generating function of cylinders/annular maps. As we gave in Section 2.2 a new bijective derivation of this quantity, we might try to look for a slice decomposition of maps with more involved topologies. A first case to understand is that of "pants" or more generally planar maps with several boundaries, where we may for instance attempt to reinterpret the Collet-Fusy bijective derivation using slices.

Finally, let me mention some asymptotic questions. Since irreducible quadrangulations are in bijection with three-connected planar graphs —whose planar embedding is unique by Whitney's theorem— it is tempting to try studying their scaling limits, starting from quadrangulations using slices or the Fusy-Poulalhon-Schaeffer bijection [FSP08], and going to three-connected graphs possibly through an irreducible analogue of the Ambjørn-Budd bijection [AB13, BJM14]. Then, one might try to deduce results for general planar graphs [CFGN15]. Less speculatively, substitution schemes for planar maps lead to very interesting asymptotic phenomena [BFSS01] and it might be worthwhile to investigate the case of irreducible maps.

7. and the corresponding chapter of his thesis [Che18, Chapter V]

3 The $O(n)$ loop model on random planar maps

In this chapter we come closer to physics, by considering a model of statistical mechanics on random maps. The publications in this topic are [12,14,15,25]. Our initial interest came from the work of Le Gall and Miermont on scaling limits of maps with large faces, which differ from the Brownian map. We were particularly puzzled by the discussion in [LGM11, Section 8] which suggests a connection with the so-called $O(n)$ loop model. After some investigation we realized that the connection becomes much simpler when "loops are drawn on the dual", as we will explain in more detail below. This led us to introduce the gasket decomposition, which is an exact combinatorial relation between loop-decorated maps and Boltzmann maps (as defined in Section 1.4). The gasket decomposition allows to rederive and generalize in a transparent manner some functional equations for the partition function of the model, which were first derived using matrix models.

To simplify the presentation, I will focus on the specific case of the rigid $O(n)$ loop model on quadrangulations, whose analysis is easier. After recalling some context in Section 3.1, I define the model and present the gasket decomposition in Section 3.2. I then discuss the phase diagram of the model in Section 3.3. The material for these two sections comes mostly from the paper [12] written with Gaëtan Borot and Emmanuel Guitter. Section 3.4 is devoted to the statistics of nestings between loops, and is based on the more recent preprint [25] written with G. Borot and Bertrand Duplantier. Concluding remarks and perspectives are gathered in Section 3.5.

3.1 Context

Let me attempt to review the literature on models of statistical mechanics on random maps. Arguably, the most emblematic model is the Ising model, which was solved [1] by Kazakov [Kaz86] via a two-matrix integral in the case of "dynamical" random planar quartic maps. By dynamical it is meant that the model is annealed: the map and its *decorations* —here ± 1 spins— are drawn together at random, so that the marginal probability of drawing a given map is proportional to the partition function of the Ising model defined on it. This is the situation which is most relevant for 2D quantum gravity, where we want the geometry to be affected by the presence of the spins ("matter"). Quenched models have also been studied through scaling arguments and numerical simulations, see e.g. [JJ00] and references therein, but the results are much scarcer than in the annealed

1. In the usual sense in statistical mechanics: computation of the partition function.

case which we consider from now on.

The remarkable feature of Kazakov's solution is that it shows the existence of a phase transition and a critical point, as in the Ising model on regular bidimensional lattices. The universal critical exponents are however different from their regular lattice counterparts [BK87], but related via the Knizhnik-Polyakov-Zamolodchikov (KPZ) relations [KPZ88]. In fact, the Ising model was used as a testbed for the KPZ relations, see for instance [Dup04] for a review of this fascinating topic. What is most relevant for our discussion is that the "string susceptibility exponent" at the Ising critical point differs from that of pure gravity, which is why it is expected that the large-scale geometric properties of critical Ising maps are fundamentally different from those of usual undecorated maps.

Another, actually older, solvable model is that of maps decorated with a spanning tree [Mul67]. It was argued in [BKKM86] that this is equivalent to considering Gaussian embeddings of maps in "-2" dimensions (note that Boulatov *et al.* consider cubic maps, and do not seem to know about Mullin's formula). This yields yet another check of the KPZ relations, and yet another large-scale geometry.

A common generalization of these two models is the q-state Potts model [Kaz88]: Ising corresponds to the case $q = 2$ and spanning trees (or forests) to the $q \to 0$ limit. By the Fortuin-Kasteleyn (FK) random cluster representation, it makes sense to consider noninteger values of q. The case $q = 1$ corresponds to bond percolation, for which the geometry of maps is the same as in the pure gravity case (since the "partition function" of percolation is trivial). It is however very interesting to study the percolation transition and the geometry of interfaces, see e.g. [Ang03, AC15, CK15]. For any $q \in [0, 4]$, there is a continuous phase transition whose critical exponents vary with q. Consequently we expect a different large-scale geometry of the maps for each q. Much effort has been devoted to analyzing the Potts model on maps for general q, sometimes in different languages.

1. In its original formulation, the Potts model amounts to considering q-colorings of maps. This topic was considered by Tutte himself [Tut71]. In particular, he worked for more than ten years to solve some functional equations arising in the case of "chromatic sums" (i.e. of properly q-colored maps, obtained in the antiferromagnatic zero-temperature limit of the Potts model). See [Tut95] and references therein, and also [Bax01]. The combinatorial approach of Tutte, based on functional equations, has been recently generalized by Bernardi and Bousquet-Mélou to nonzero temperatures [BBM11, BBM17]. The main outcome is a characterization of the partition function of the q-state Potts model on random planar maps: it satisfies an explicit algebraic equation for q of the form $2 + 2\cos(\pi j/m)$ with j, m integers (and $q \neq 0, 4$), and it obeys an explicit nonlinear differential equation for general q. See also [BMC15] for the already nontrivial case $q \to 0$.

   Meanwhile, in theoretical physics, the matrix integral representation of the Potts model was studied in several papers [Dau95, Bon99, EB99, ZJ00a, GJSZJ12]. We note that there is not so far much connection between the two approaches: for instance the existence of "algebraic points" is known to theoretical physicists, but for

a slightly different notion of algebraicity (i.e. with respect to the parameter coupled to the boundary length in the disk generating function, while Tutte, Bernardi and Bousquet-Mélou consider the parameter coupled to the number of edges).

2. By a well-known construction, which we review in [15, Section 2.1], the q-state Potts model on a planar map may be reformulated in terms of loops on a derived map. In particular, at a "self-dual" point, we obtain precisely the fully-packed version of the $O(n)$ loop model with the relation $q = n^2$, and the general $O(n)$ loop model corresponds to the dilute Potts model. Here, the natural range for observing new geometries is $n \in [0, 2]$, or actually $[-2, 2]$ if we dare consider negative Boltzmann weights [CS05]. The $O(n)$ loop model on cubic maps turns out to be exactly solvable using matrix integrals and loop equations [Kos89, GK89, KS92, EZJ92, EK95, EK96] or the gasket decomposition [12, 14] presented in this chapter. The limit $n \to 0$, which describes polymers or self-avoiding walks, was first considered in [DK88]. The exact solvability of the $O(n)$ loop model allows to analyze completely its critical behavior and exponents, which again are consistent with the KPZ relations. More recently, the model was put into the framework of topological recursion [BE11].
3. The self-dual q-state Potts model/fully-packed $O(n)$ loop model appears under yet another language in the paper [She16], which we already mentioned in Section 2.1 and which led to many further developments [GMS19, BLR17, Che17, GS17, GS15, GKMW18] including the abelian sandpile model on random maps [SW15] and bipolar orientations [KMSW19]. Most of these papers deal with the scaling limits at critical points, using the "mating-of-trees" or "peanosphere" construction.
4. On the square lattice, there is a well-known correspondence between the Potts model and the ice or "six-vertex" model. This correspondence breaks down on a random quartic map, but still there is a three-to-one correspondence between 3-colorings of a planar quadrangulation and ice configurations/Eulerian orientations of its dual quartic map. The matrix integral representation of the six-vertex model on random quartic maps was studied in [Kos00, ZJ00b]. More recently, Eulerian orientations of both quartic and general Eulerian maps were considered in [BBMDP17, EPG18, BMEP18]. Here the results are mostly enumerative.

After this long list one may wonder if a model other than the Potts model has ever been considered on random maps. In 1989, Kazakov [Kaz89] realized that the one-matrix model, corresponding to the Boltzmann maps considered in Section 1.4, already allows to reach multicritical points different from pure gravity by fine-tuning the weight sequences $(g_k)_{k\geq 1}$. Unfortunately some of these weights are negative, which makes the probabilistic interpretation difficult and the conformal field theory "nonunitary", as realized by Staudacher who noted a connection with the dimer model on random quartic maps [Sta90]. More recently, Le Gall and Miermont proposed another way of escaping from pure gravity with Boltzmann maps, by considering a nonnegative weight sequence $(g_k)_{k\geq 1}$ with unbounded support and fine-tuned asymptotics [LGM11]. Interestingly, it appears that there exists a one-parameter family of weight sequences which interpolates between the cases considered by Kazakov and by Le Gall and Miermont [ABM16]. As we will explain in this chapter, Boltzmann maps with weight sequences satisfying the

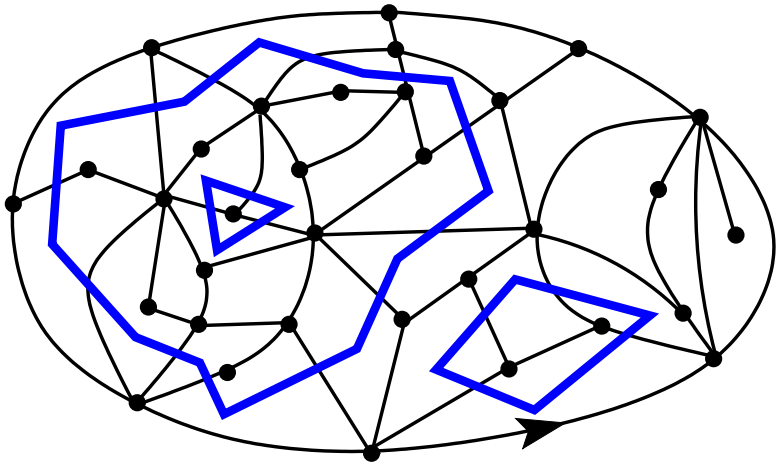

Figure 3.1 – A (non-rigid) loop configuration on a quadrangulation with a boundary.

assumptions of [LGM11] appear in the gasket decomposition of $O(n)$ loop configurations on random maps. So, the Potts model is still lurking in the background!

Still, a few models of statistical mechanics on random maps which are not (immediately) related to the Potts model have been considered, such as ADE height models [Kos92, Kos96] and hard particles [BDFG02b], which are both exactly solvable.

3.2 The gasket decomposition

The $O(n)$ loop model aims at describing a "gas of loops" on a lattice. By loop, we here mean a cycle (simple closed path), and not a loop in the graph theoretical sense. As usual in statistical mechanics, the model admits several different "microscopic" definitions, which are expected not to matter much at a macroscopic level. Their common feature is that n plays the role of a nonlocal weight per loop, which arises through high-temperature graphical expansions of models with $O(n)$ symmetry [DMNS81]. We note that the term "$O(n)$ loop model" is a misnomer since there is no action of the orthogonal group on the loops themselves, but this term is traditionally used in the literature so we will stick with it. We now provide the precise combinatorial (microscopic) definition on which we will concentrate.

A *loop configuration* is a collection of disjoint cycles (i.e. the loops are both self- and mutually avoiding). On planar maps, we find it convenient to think of loops as living on the dual map: they go through the faces and edges of the primal map. For simplicity, we restrict to the case of a quadrangulation with a boundary: the loops then live on the dual almost-quartic map, and we assume that no loop visits the outer face. See Figure 3.1 for an example.

A loop configuration on a quadrangulation with a boundary is said *rigid* if, in each visited face, the loop enters and exists through opposite edges. In other word, "turns" are forbidden, see Figure 3.2. The *rigid* $O(n)$ *loop model* is a measure on the set of

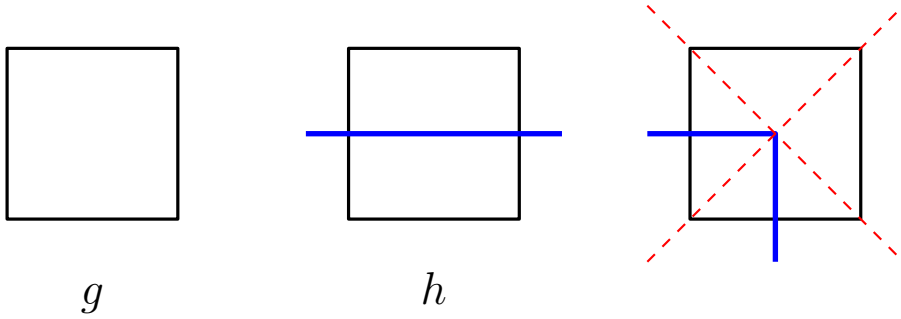

Figure 3.2 – The possible types of faces in the rigid $O(n)$ loop model, and their weights.

quadrangulations with a boundary which are endowed with a rigid loop configuration. It is defined by assigning to such a map m a weight

$$w(m) = n^{L(m)} g^{f_u(m)} h^{f_v(m)} \tag{3.1}$$

where n, g, h are nonnegative real parameters, and $L(m), f_u(m), f_v(m)$ denote respectively the number of loops, the number of unvisited inner faces and the number of visited faces of m. Note that taking $n = 0$ or $h = 0$ amounts to forbidding the loops, and we recover the natural weight function of quadrangulations considered in Section 1.3.

For p a positive even integer, we denote by Z_p the sum of the weights of all loop-decorated quadrangulations with a boundary of length p. We say that the triplet (n, g, h) is *admissible* if Z_p is finite. It is not difficult to check that the property of being admissible does not depend on p and that, for all n, it is satisfied for g and h small enough. We set by convention $Z_0 = 1$.

We now describe the gasket decomposition, which makes a link with the face-weighted Boltzmann maps defined in Section 1.4. The general idea of viewing Boltzmann maps as "gaskets" of $O(n)$ loop models actually appears already in [LGM11], but the precise connection proposed by Le Gall and Miermont poses some technical difficulties which we were able to circumvent with the idea of having the loops on the dual map, and introducing the rigid $O(n)$ loop model which makes the correspondence both exact and manageable.

Starting with a loop-decorated quadrangulation with a boundary, let us erase all the loops and their interiors (vertices and edges) as well as the edges they cross. See Figure 3.3. We call *gasket* the resulting object, it is a planar bipartite map without loops, but possibly with inner faces of high degree. In particular, it is not necessarily a quadrangulation. Note that the degree of the outer face is unchanged.

Of course, we lose information in the process so this correspondence is not bijective. But we can fix this by keeping track of the contents of the outermost loops, which turn into faces in the gasket. Let us consider such an outermost loop of length ℓ. Since we are considering a rigid loop configuration, it is not difficult to check that ℓ is necessarily even, and that the gasket face associated with the loop has degree ℓ. We now consider the *internal map* formed by the vertices, edges and loops inside the loop at hand: it is

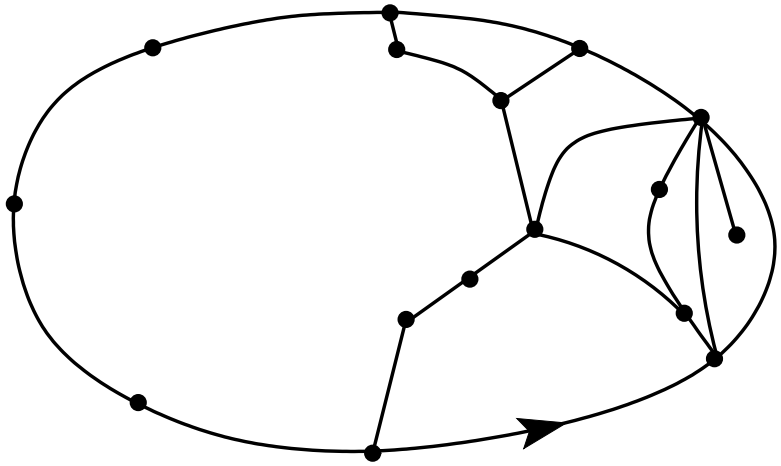

Figure 3.3 – The gasket of the loop-decorated map of Figure 3.1.

nothing but a loop-decorated quadrangulation with a boundary of length ℓ (as counted by Z_ℓ), with a rooting inherited from that of the original map. Therefore, to make the decomposition reversible, we need to attach to each face of the gasket coming from an outermost loop an internal map with matching outer degree. Note that the gasket may also have *regular* faces of degree 4, corresponding to the unvisited faces of the original quadrangulations which are not surrounded by loops. It is not difficult to check that the decomposition is now reversible and can be turned into a recursive bijective decomposition, which has the following consequences.

Theorem 3.1 (see [12]). *For $p \geq 2$ even, denote by $\mathcal{F}_p(g_2, g_4, g_6, \ldots)$ the generating function of rooted bipartite maps with a boundary of length p, with the Boltzmann weight* (1.14)*. Then, the sequence $(Z_p)_{p\geq 2}$ is solution of the fixed-point equation*

$$\begin{aligned} Z_p &= \mathcal{F}_p(z_2, z_4, z_6, \ldots) \\ z_p &= g\delta_{p,4} + nh^p Z_p. \end{aligned} \tag{3.2}$$

When (n, g, h) is admissible, the gasket is distributed as a Boltzmann bipartite map with the weight sequence $(z_k)_{k\geq 2}$.

Note that $\mathcal{F}_{2n}(g_2, g_4, g_6, \ldots)$ is the same quantity as that denoted by w_n in Section 1.4, we use here a different notation to emphasize its dependency on the weight sequence. It is clear that the fixed-point equation (3.2) uniquely determines Z_p and z_p as formal power series in n, g and h. The quantity z_p accounts for the possible ways to "fill" a face of degree p in the gasket: it may either be a regular face of weight g if $p = 4$, or arise from an outermost loop (weight n) covering p visited faces (h^p) and containing an internal map of outer degree p (Z_p).

Remark 3.1. The gasket decomposition may be adapted to situations which are more general than the rigid case presented here, at the price of making the fixed-point equation more complicated (as we have to correctly account for the different possible types of

"rings" formed by the faces visited by a given loop). We treated the case of quadrangulations (not necessarily rigid) in [12], then extended to general degrees in [14]. This allows to recover in particular the $O(n)$ loop on cubic maps, previously studied in the references given in Section 3.1. We may also incorporate an extra "bending energy" parameter. Finally in [15] we considered "twofold" loop models that arise from the correspondence with the Potts model outside the self-dual situation.

3.3 Exact solution and phase diagram

It turns out that the fixed-point equation (3.2) may be "solved", in the sense that we may rewrite it as a functional equation whose solution may be written in parametric form using the techniques from [Kos89, GK89, EK95]. But, before, it is instructive to have a qualitative discussion of the possible asymptotic behaviors of Z_p and z_p as $p \to \infty$, as it makes the connection with the work of Le Gall and Miermont [LGM11].

Consider a sequence $\underline{g} = (g_{2k})_{k\geq 1}$ of nonnegative weights and set

$$\varphi(x) := \sum_{k=1}^{\infty} \binom{2k-1}{k} g_{2k} x^k. \tag{3.3}$$

We saw in Section 1.4, precisely at (1.15), that the generating function R of pointed rooted bipartite maps with the Boltzmann weight (1.14) satisfies $R = 1 + \varphi(R)$. The weight sequence $\underline{g}$ is said *admissible* if R is finite and, in this case, we necessarily have $\varphi'(R) \leq 1$. We say that $\underline{g}$ is *subcritical* if $\varphi'(R) < 1$, and *critical* if $\varphi'(R) = 1$. This distinction plays a role when considering the probability that the Boltzmann map has a large number of vertices: it decays exponentially in the subcritical case, and as a power law in the critical case. Furthermore, a critical sequence $\underline{g}$ is said *generic* if R is strictly smaller than the radius of convergence of φ, and *nongeneric* otherwise. Le Gall and Miermont exhibited examples of nongeneric critical sequences for which

$$g_{2k} \sim c \frac{(4R)^{-k}}{k^a}, \qquad k \to \infty \tag{3.4}$$

where c is a fine-tuned positive constant, and the exponent a is comprised between $3/2$ and $5/2$. Note that the exponential decay factor $(4R)^{-k}$ is fixed by the requirement that φ has radius of convergence R. For such sequences, the law of the degree of a typical face has a heavy tail (while it has an exponential tail in the generic case), and we observe scaling limits different from the Brownian map [LGM11].

How do the weight sequence $\underline{z}$ solving the fixed point equation (3.2) fit into this classification? We cannot rule out the possibility that $\underline{z}$ is subcritical or generic critical. But, more interestingly, an elementary computation —see [12, Section 3.3] for details— shows that for a nongeneric critical weight sequence satisfying (3.4) we have

$$\mathcal{F}_{2k}(g_2, g_4, g_6, \ldots) \sim \frac{c}{2\cos \pi a} \frac{(4R)^k}{k^a}, \qquad k \to \infty. \tag{3.5}$$

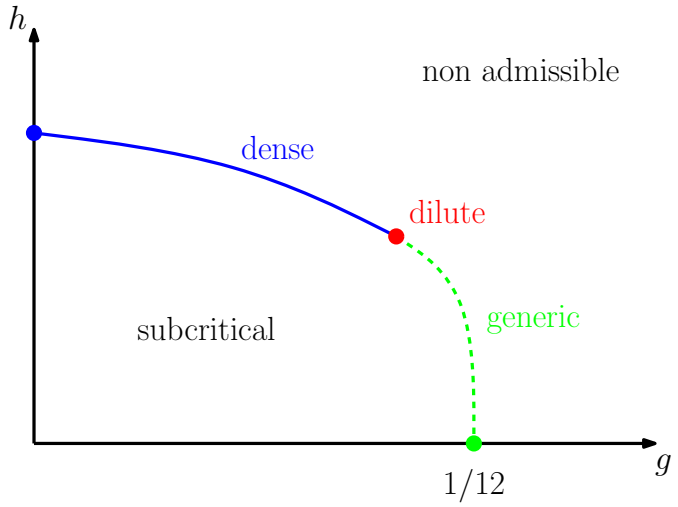

Figure 3.4 – Qualitative phase diagram of the rigid $O(n)$ model for fixed $n < 2$.

The only way to make such asymptotics compatible with the fixed-point equation (3.2) is to have the relations

$$n = 2\cos\pi a \tag{3.6}$$

and

$$h = \frac{1}{4R}. \tag{3.7}$$

Thus, for $n > 2$ we cannot obtain a nongeneric critical sequence in the rigid $O(n)$ model. For $n < 2$, there are two possible values of the exponent a in the allowed interval $[3/2, 5/2]$, namely

$$a = 2 \pm b, \qquad b := \frac{1}{\pi}\arccos(n/2) \in [0, 1/2]. \tag{3.8}$$

Following the physics terminology, the value $a = 2 - b \in [3/2, 2]$ is called *dense* and the value $a = 2 + b \in [2, 5/2]$ *dilute*. These two values coincide for $n = 2$. To summarize, for an admissible triplet of parameters (n, g, h), the weight sequence $\underline{z}$ governing the structure of the gasket in the rigid $O(n)$ model may either be subcritical, generic critical or nongeneric critical with the dense or dilute value of the exponent a. Correspondingly, we say that the model is at a *subcritical point*, a *generic critical point* or a dense or dilute *nongeneric critical point*. Which situation occurs in practice is encoded in the *phase diagram* of the model. Figure 3.4 displays the qualitative phase diagram for a fixed value of $n < 2$, which is expected from physical grounds and is confirmed by the exact solution, as we will explain now.

We start by recalling certain well-known analytical properties of the generating function of Boltzmann maps with a boundary, see for instance [14, Section 6] for more details. Let us introduce the *resolvent*

$$\mathcal{W}(\xi) := \frac{1}{\xi} + \sum_{k\geq 1} \frac{\mathcal{F}_{2k}(g_2, g_4, g_6, \ldots)}{\xi^{2k+1}} \tag{3.9}$$

which is closely related with the quantity W_0 considered in Section 1.4. The one-cut lemma states that, when the weight sequence $\underline{g}$ is admissible, the function $\xi \mapsto \mathcal{W}(\xi)$ is analytic in $\mathbb{C} \setminus [-\gamma, \gamma]$ with $\gamma := 2\sqrt{R}$ (which depends on $\underline{g}$), has singularities at $\pm\gamma$ and a cut on $[-\gamma, \gamma]$, with finite limits when one approaches the cut from the upper or the lower half-plane. For $\xi \in [-\gamma, \gamma]$, we denote these limits by $\mathcal{W}(\xi + i0)$ and $\mathcal{W}(\xi - i0)$ respectively. Note that, in the bipartite setting considered here, $\mathcal{W}$ is an odd function of ξ; in the general setting the cut may no longer be symmetric about 0. Furthermore, the *spectral density*

$$\rho(\xi) := \frac{\mathcal{W}(\xi - i0) - \mathcal{W}(\xi + i0)}{2i\pi} \tag{3.10}$$

is a nonnegative even function on $[-\gamma, \gamma]$, vanishing at $\pm\gamma$, and we have the functional relation

$$\mathcal{W}(\xi - i0) + \mathcal{W}(\xi + i0) = \xi - \sum_{k \geq 1} g_{2k} \xi^{2k-1}, \qquad \xi \in [-\gamma, \gamma]. \tag{3.11}$$

Let us now substitute $\underline{g} = \underline{z}$ the solution of the fixed point equation (3.2). Then, we get that

$$W(\xi) := \frac{1}{\xi} + \sum_{k \geq 1} \frac{Z_{2k}}{\xi^{2k+1}} \tag{3.12}$$

has a cut $[-\gamma, \gamma]$ depending on (n, g, h), and the functional relation becomes

$$W(\xi - i0) + W(\xi + i0) = \xi - g\xi^3 - \frac{n}{h\xi^2} W\left(\frac{1}{h\xi}\right) + \frac{n}{\xi}, \qquad \xi \in [-\gamma, \gamma]. \tag{3.13}$$

This equation is very similar to that for the $O(n)$ loop model on cubic maps, which was originally derived using matrix integrals, and which we recovered using the gasket decomposition in [14].

The functional equation (3.13) relates the values of W on the cut $[-\gamma, \gamma]$ to that on its image through the inversion $\xi \mapsto \frac{1}{h\xi}$. Admissibility entails that the cut and its image have disjoint interiors, but they can possibly meet at their endpoints when γ is equal to the fixed point $h^{-1/2}$ of the inversion. From the relation $\gamma = 2\sqrt{R}$, this happens precisely when the second condition (3.7) for nongeneric criticality is satisfied. As we shall see, the first condition (3.6) is then a consequence of the functional equation. In other words, we have $\gamma \leq h^{-1/2}$ with equality if and only if the model is a nongeneric critical point.

The key observation for solving the functional equation (3.13) is that, given the value of γ, it is an inhomogeneous *linear* equation in W. Therefore, we have

$$W(\xi) = W_{\mathrm{part}}(\xi) + W_{\mathrm{hom}}(\xi) \tag{3.14}$$

where

$$W_{\mathrm{part}}(\xi) := \frac{2(\xi - g\xi^3) - n\left(\frac{1}{h^2\xi^3} - \frac{g}{h^4\xi^5}\right)}{4 - n^2} + \frac{n}{(2+n)\xi} \tag{3.15}$$

is the particular solution of (3.13) which is a Laurent polynomial in ξ, and W_{hom} is an odd solution of the homogeneous linear equation

$$W_{\mathrm{hom}}(\xi - i0) + W_{\mathrm{hom}}(\xi + i0) + \frac{n}{h\xi^2} W_{\mathrm{hom}}\left(\frac{1}{h\xi}\right) = 0, \qquad \xi \in [-\gamma, \gamma]. \tag{3.16}$$

The set of meromorphic solutions of this equation is a certain infinite-dimensional vector space, and the precise solution W_{hom} which we should pick is determined by the analyticity properties of W. Indeed, we know that W cannot have poles, but W_{part} has poles at 0 and ∞: these should be therefore cancelled by W_{hom}. Also, by (3.12), we should moreover impose that $W(\xi) \sim \frac{1}{\xi}$ for $\xi \to \infty$. Such constraints turn out to be sufficient to fix completely W_{hom} given γ.

The actual value of γ is fixed by the *consistency condition* that the spectral density ρ is nonnegative on $[-\gamma, \gamma]$ and vanishes at $\pm\gamma$. All the nonlinearity of the problem is hidden in this condition, as the space of solutions of (3.16) depends on γ in an essential way.

Let us write the solution in the nongeneric critical case $\gamma = h^{-1/2}$, which is both easier and more interesting. In this case the solution of (3.16) takes the form

$$W_{\mathrm{hom}}(\xi) = \left(B(\xi) - \tfrac{\gamma^2}{\xi^2} B\left(\tfrac{\gamma^2}{\xi}\right)\right)\left(\frac{\xi-\gamma}{\xi+\gamma}\right)^b - \left(B(-\xi) - \tfrac{\gamma^2}{\xi^2} B\left(-\tfrac{\gamma^2}{\xi}\right)\right)\left(\frac{\xi+\gamma}{\xi-\gamma}\right)^b \quad (3.17)$$

where the exponent b is as in (3.8), and B is a meromorphic function which, from the analyticity requirements on W, is equal to

$$B(\xi) = \frac{g}{4-n^2}\left(\xi^3 + 2b\gamma\xi^2 + 2b^2\gamma^2\xi + \frac{2}{3}(b+2b^3)\gamma^3\right) - \frac{1}{4-n^2}(\xi + 2b\gamma). \quad (3.18)$$

Finally, the consistency condition yields a relation between the parameters n, g and h of the model, which is nothing but the equation for the nongeneric critical line.

Theorem 3.2 (see [12, Section 6.2] and [Bud18, Section 1.2.1])**.** *For $n \in [0,2]$, the nongeneric critical points of the rigid $O(n)$ loop model are obtained for parameters (g,h) such that*

$$g = \frac{3}{2+b^2}\left(h - \frac{2-n}{2b^2}h^2\right) \quad (3.19)$$

and $g \le g^*$, $h \ge h^*$, with

$$g^* := \frac{3b^2(2-b)^2}{2(2-n)(b^2-2b+3)^2}, \qquad h^* := \frac{b^2(2-b)^2}{(2-n)(b^2-2b+3)} \quad (3.20)$$

and b as in (3.8)*. The point (g^*, h^*) is a dilute critical point, and all the other points are dense critical points, including the "full-packed" critical point $(0, \frac{2b^2}{2-n})$.*

Identifying the dilute and dense critical exponents is rather straightforward from (3.17), as it yields the expansion of W around the singularities at $\pm\gamma$, which are related with the asymptotic behavior of Z_{2k} for $k \to \infty$.

It is also possible to obtain a parametrization for the generic critical line displayed on Figure 3.4, which connects the point $(g,h) = (1/12, 0)$ to the dilute critical point. It is more complicated since, for $\gamma < h^{-1/2}$, the solution of the functional equation (3.16) passes through the use of an elliptic parametrization, see [12, Sections 6.3 and 6.4] for details.

Let me mention that the derivation of Theorem 3.2 which we gave in [12] was based on numerical evidence which we did not fully justify. More precisely, we assumed that the consistency condition, which we use to identify the correct value of γ, is not only necessary but also sufficient. This has been proved rigorously by Timothy Budd and Linxiao Chen in [Bud18, Theorems 1 and 2]. In a nutshell, the first theorem, due to T. Budd, asserts that the model is admissible if the fixed-point equation (3.2) admits a solution in the space of nonnegative real sequences (which is then unique), while the second theorem, due to L. Chen, asserts that such solution exists if the functional equation (3.13) admits a solution satisfying the consistency condition [2] (which is then unique). See also the discussion in Linxiao's thesis [Che18, Chapter II].

In the papers [14] and [15], we follow a similar approach to analyze the phase diagrams of the $O(n)$ loop model on cubic maps with bending energy and of the "twofold" loop models, respectively. These are the most general models that we may solve by the techniques presented in this section. New insights are needed to solve models where the loops may visit faces of higher degree.

By combining Theorems 3.1 and 3.2 with the results from [LGM11], we obtain some interesting information about the geometry of the gasket in the rigid $O(n)$ loop model for $n < 2$: at the nongeneric critical points, whose existence has been shown, the gasket is distributed as a Boltzmann bipartite map with a nongeneric critical weight sequence $\underline{z}$ such that $z_{2k} \sim c\frac{\gamma^{-2k}}{k^{2\pm b}}$ where b is as in (3.8), and where the $+$ and $-$ sign is taken in the dilute and dense case respectively. Therefore, by the results of Le Gall and Miermont, if we condition the gasket to have a large number U of vertices, the typical distance between gasket vertices is of order $U^{3\pm 2b}$, and if we divide by this factor the gasket converges (at least along subsequences) in the Gromov-Hausdorff sense as $U \to \infty$ towards a random compact metric space of Hausdorff dimension $3 \pm b \in (2, 4)$. This limit is different from the Brownian map which has dimension 4.

3.4 Nesting statistics

So far we have obtained a relatively precise information about the structure of the gasket, but it is natural to ask also for geometric information about the full map with loops. It seems difficult to handle distances in the full map by our approach but, interestingly, we may obtain information about the *nestings* between loops.

Let us consider a loop-decorated quadrangulation with a boundary. The associated *nesting tree* is the graph whose edges and vertices (hereafter called *nodes*) correspond respectively to the loops and to the regions which they delimit on the underlying surface of the quadrangulation; the incidence relations in the nesting tree keep track of those in the surface. See Figure 3.5 for an illustration. The nesting tree is indeed a tree by the planarity of the surface [3] and by the fact the loops are disjoint cycles. The *root node*

2. In fact, L. Chen proved that it is sufficient to check the positivity of the spectral density in the vicinity of $\pm\gamma$, which is the actual criterion we used in [12].

3. The higher genus case, where the nesting graph is not necessarily a tree, has been considered in [BGF16].

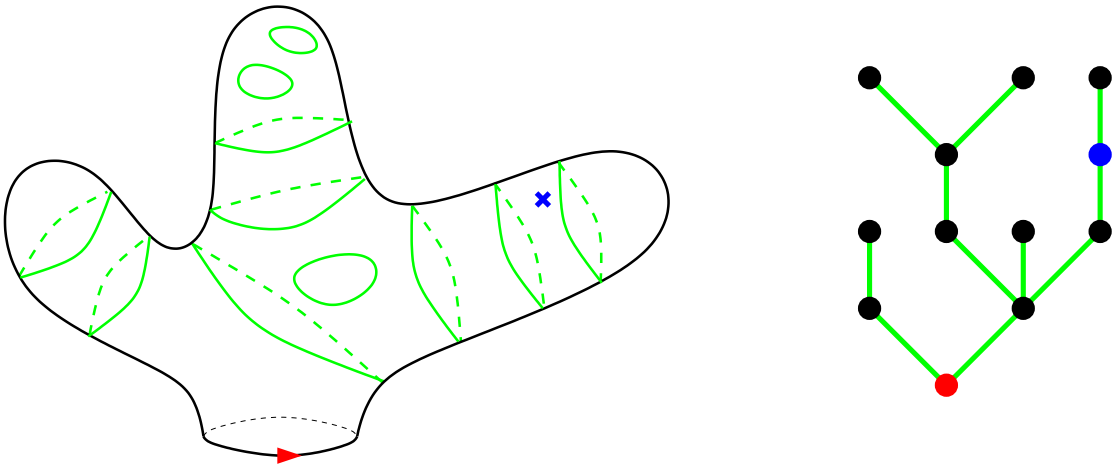

Figure 3.5 – Left: schematic representation of a pointed loop-decorated quadrangulation with a boundary (the red arrow and the blue cross represent respectively the root edge and the distinguished vertex). Right: the corresponding nesting tree.

of the nesting tree corresponds to the region incident to the boundary, which may be identified with the gasket. We are interested in understanding the structure of the nesting tree, especially at a nongeneric critical point where we expect it to have an nontrivial structure.

In the paper [25] we considered the situation where the loop-decorated map has an extra marking, such as a distinguished vertex or another boundary. The extra marking turns into a distinguished node in the nesting tree, which may differ from the root vertex. The *depth* is defined as the distance between the root and distinguished nodes in the nesting tree; it corresponds to the minimal number of loops that one must cross to go from the root to the extra marking in the loop-decorated map.

For simplicity I will restrict to the case where the extra marking is a vertex, which we pick uniformly at random in the loop-decorated map. Note that the corresponding node is in general *not* uniform in the nesting tree. If the loop-decorated map is itself picked at random, according to the rigid $O(n)$ loop model measure with a prescribed boundary length $2k$, the depth is a random variable which we denote by P_k.

Theorem 3.3 (see [25]). *At a nongeneric critical point of the rigid $O(n)$ loop model with $n \in (0,2)$, the depth P_k of a uniformly chosen vertex in a loop-decorated quadrangulation of boundary length $2k$ grows logarithmically with k as $k \to \infty$. More precisely, we have the convergence in distribution*

$$\frac{P_k - \frac{n}{\pi\sqrt{4-n^2}} \ln k}{\sqrt{\ln k}} \xrightarrow{d} N(0,\sigma^2) \qquad (k \to \infty) \tag{3.21}$$

where $N(0,\sigma^2)$ is the normal distribution with mean 0 and variance $\sigma^2 := \frac{4n}{\pi(4-n^2)^{3/2}}$,

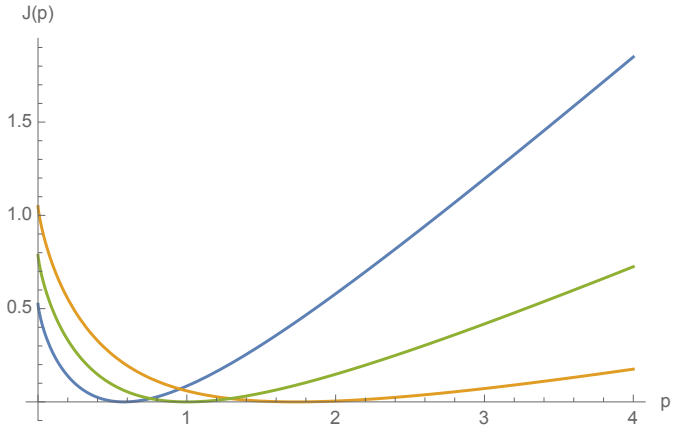

Figure 3.6 – A plot of the rate function J for $n = 1$ (blue), $n = \sqrt{2}$ (green) and $n = \sqrt{3}$ (yellow).

and we have the large deviation estimate

$$\ln \mathrm{Prob}\left(P_k = \left\lfloor \frac{p}{\pi} \ln k \right\rfloor\right) \sim -\frac{J(p)}{\pi} \ln k \qquad (k \to \infty,\ p \geq 0) \tag{3.22}$$

where the rate function J reads

$$J(p) := p \ln\left(\frac{2p}{n\sqrt{1+p^2}}\right) + \mathrm{arccot}(p) - \arccos(n/2). \tag{3.23}$$

The rate function J is plotted on Figure 3.6 for a few values of n. It is strictly convex—we have $J''(p) = \frac{1}{p(p^2+1)} > 0$—and attains it minimum at $p = \frac{n}{\sqrt{4-n^2}}$ consistently with (3.21). At $p = 0$ it takes the value $\arcsin(n/2)$. Note that, remarkably, the statement of the theorem does not depend on the dilute/dense nature of the nongeneric critical point.

Theorem 3.3 differs slightly from the results stated in [25]. First, we consider here the rigid $O(n)$ loop model instead of the $O(n)$ loop model on cubic maps with bending energy. This change is rather innocent since the computations are entirely similar. Second, we consider the asymptotics for a large perimeter $2k$ while, in [25], we condition the loop-decorated map to contain a fixed number V of vertices and consider the limit $V \to \infty$ (keeping either the perimeter $2k$ finite, or having it grow with V in an appropriate "crossover" scaling). This change somewhat simplifies the proof of Theorem 3.3 which we will sketch in the remainder of this section (see Remark 3.3 for a discussion of the conditioning).

The key ingredient in the proof of Theorem 3.3 is an exact expression for a refined generating function keeping track of the depth of the marked vertex. More precisely, for k a nonnegative integer and s a formal or nonnegative real variable, we set

$$Z^{\bullet}_{2k}[s] := \sum_{m} w(m) s^{P(m)} \tag{3.24}$$

where the sum runs over all *pointed* loop-decorated quadrangulations m with a boundary of length $2k$, the weight $w(m)$ is as in (3.1), and $P(m)$ denotes the depth of the distinguished vertex. The probability generating function of P_k is then given by

$$\mathbb{E}\left(s^{P_k}\right) = \frac{Z^\bullet_{2k}[s]}{Z^\bullet_{2k}} \tag{3.25}$$

where the unrefined generating function $Z^\bullet_{2k} = Z^\bullet_{2k}[1]$ is related to the generating function Z_{2k} considered in the previous sections by

$$Z^\bullet_{2k} = \left(g\frac{\partial}{\partial g} + h\frac{\partial}{\partial h} + k + 1\right) Z_{2k}. \tag{3.26}$$

Indeed, by Euler's relation, the number of vertices of a loop-decorated quadrangulation m with a boundary of length $2k$ is equal to $f_u(m) + f_v(m) + k + 1$.

Now, by differentiating the fixed point equation (3.2), we find that $Z^\bullet_{2k}$ satisfies the relation

$$Z^\bullet_{2k} = \mathcal{F}^\bullet_{2k}(z_2, z_4, z_6, \ldots) + n\sum_{\ell=0}^{\infty} h^{2\ell}\mathcal{F}^\circ_{2k,2\ell}(z_2, z_4, z_6, \ldots)Z^\bullet_{2\ell} \tag{3.27}$$

where $\mathcal{F}^\bullet_{2k}(g_2, g_4, g_6, \ldots)$ denotes the generating function of pointed rooted bipartite maps with a boundary of length $2k$, and $\mathcal{F}^\circ_{2k,2\ell}(g_2, g_4, g_6, \ldots) = \frac{\partial}{\partial g_{2\ell}}\mathcal{F}_{2k}(g_2, g_4, g_6, \ldots)$ that of annular bipartite maps with boundaries of lengths $2k$ and 2ℓ, the boundary of length $2k$ being rooted [4]. The combinatorial meaning of (3.27) is the following. The first term in the right-hand side corresponds to the case where the marked vertex belongs to the gasket. The second term corresponds to the opposite case: then, we consider the outermost loop that separates the marked vertex from the boundary. Denoting the length of this loop by 2ℓ, we find that, in the gasket decomposition, the gasket has a distinguished face of degree 2ℓ, inside which we find a pointed internal map with outer degree 2ℓ. This explains the different factors appearing in the sum over ℓ.

We then claim that the refined generating function $Z^\bullet_{2k}[s]$ satisfied the modified equation

$$Z^\bullet_{2k}[s] = \mathcal{F}^\bullet_{2k}(z_2, z_4, z_6, \ldots) + ns\sum_{\ell=0}^{\infty} h^{2\ell}\mathcal{F}^\circ_{2k,2\ell}(z_2, z_4, z_6, \ldots)Z^\bullet_{2\ell}[s] \tag{3.28}$$

where the weight sequence $\underline{z}$ does not depend on s, and is still given by the fixed point equation (3.2). Indeed, if we consider a map m contributing to $Z^\bullet_{2k}[s]$, it contributes to the first term of the right-hand side if $P(m) = 0$, and to the second term if $P(m) \geq 1$. In this latter case, we have $P(m) = P(m') + 1$, where m' is the internal map containing the marked vertex.

We now form the series

$$W^\bullet_s(\xi) := \frac{1}{\xi} + \sum_{k\geq 1} \frac{Z^\bullet_{2k}[s]}{\xi^{2k+1}}. \tag{3.29}$$

4. If we choose to also root the other boundary for symmetry, then we have to divide the term of index ℓ in (3.27) by 2ℓ. This is the convention that we follow in [25], where the cylinder generating function $\mathcal{F}^{(2)}$ which we consider is related to the current $\mathcal{F}^\circ$ by $\mathcal{F}^{(2)}_{2k,2\ell} = 2\ell\mathcal{F}^\circ_{2k,2\ell}$.

For $|s| \leq 1$, it is analytic in the same domain as the series $W(\xi)$ considered in Section 3.3, namely $\mathbb{C} \setminus [-\gamma, \gamma]$ (γ being independent of s). The equation (3.28) then translates into the functional equation

$$W_s^\bullet(\xi - i0) + W_s^\bullet(\xi + i0) = -\frac{ns}{h\xi^2} W_s^\bullet\left(\frac{1}{h\xi}\right) + \frac{ns}{\xi}, \qquad \xi \in [-\gamma, \gamma], \tag{3.30}$$

see [25, Section 4] for details. This functional equation may be solved along the same lines as (3.13). In particular, the homogeneous linear equation is the same as (3.16), except that n is replaced by ns. At a nongeneric critical point, the solution takes the form

$$W_s^\bullet(\xi) = \frac{ns}{(2+ns)\xi} + \frac{1}{2(2+ns)b(s)\gamma}\left(\left(\frac{\xi+\gamma}{\xi-\gamma}\right)^{b(s)} - \left(\frac{\xi-\gamma}{\xi+\gamma}\right)^{b(s)}\right) \tag{3.31}$$

with

$$b(s) := \frac{1}{\pi}\arccos(ns/2). \tag{3.32}$$

Note that the expression for $W_s^\bullet(\xi)$ is much more compact than that for $W(\xi)$, cf (3.17) and (3.18). This is again a manifestation of the general principle that the generating functions of pointed rooted maps are simpler than those of maps which are just rooted [5]. Close to the endpoints of the cut, we have the asymptotic equivalent

$$W_s^\bullet(\xi) \sim \pm\frac{2^{b(s)-1}}{(2+ns)b(s)\gamma} \cdot (1 \mp \gamma/\xi)^{-b(s)} \qquad (\xi \to \pm\gamma) \tag{3.33}$$

which implies (using the analyticity of $W_s^\bullet$ in $\mathbb{C} \setminus [-\gamma, \gamma]$) the asymptotics

$$Z_{2k}^\bullet[s] \sim \frac{4^{b(s)}}{2(2+ns)\Gamma(1+b(s))} \cdot \frac{\gamma^{2k}}{k^{1+b(s)}} \qquad (k \to \infty). \tag{3.34}$$

Note that this asymptotic behavior does not depend on the dense/dilute nature of the nongeneric critical point, and that the subleading exponent $1 + b(s)$ takes the value $3/2$ at $s = 0$ regardless of n. By (3.25), we find that the probability generating function of P_k satisfies

$$\mathbb{E}\left(s^{P_k}\right) \sim \mathrm{cst} \cdot k^{b-b(s)}. \tag{3.35}$$

Theorem 3.3 follows by standard arguments of analytic combinatorics: the asymptotic normality (3.21) follows from the quasi-powers theorem [FS09, Theorem IX.8], and the large deviation estimate (3.22) is given by considering the Legendre transform of the function $t \mapsto b - b(e^t)$, which is nothing but

$$\frac{J(p)}{\pi} = \inf_{t \in (-\infty, \ln(2/n))} \left(b - b(e^t) - \frac{p}{\pi}t\right). \tag{3.36}$$

5. In particular, for $s = 0$—which amounts to forcing the marked vertex to be in the gasket—we have $W_0^\bullet(\xi) = \frac{1}{\xi\sqrt{1-(\gamma/\xi)^2}}$ consistently with the universal form of the series $\mathcal{W}^\bullet(\xi)$ of pointed rooted Boltzmann maps.

Remark 3.2. Outside the nongeneric critical situation, it should be possible to obtain an expression for $W_s^\bullet(\xi)$ using the same elliptic parametrization as for $W(\xi)$. We expect to find an asymptotic behavior of the form $Z_{2k}^\bullet[s] \sim C(s)\frac{\gamma^{2k}}{k^{3/2}}$ for $k \to \infty$, with only the constant depending on s. This would imply that P_k has a discrete limit law as $k \to \infty$.

Remark 3.3. Conditioning on having a fixed number V of vertices, as we do in [25], is more involved since we need to extract from the refined generating function $Z_{2k}^\bullet[s]$ the contribution of maps with V vertices, which may be done by introducing an auxiliary weight per vertex and performing a contour integral. The limit $V \to \infty$ may then be studied by a bivariate saddle-point analysis. Remarkably, we find that Theorem 3.3 holds with very little modification in this setting: set $c = 1$ if we are at a dilute critical point, and $c = 1/(1-b)$ otherwise. Then, in the regime $V \to \infty$ with k fixed, we simply have to replace $\ln k$ by $c \ln V$ in (3.21) and (3.22). And in the crossover regime $V \to \infty$ with $k \propto V^{c/2}$, the statements hold without modification.

Interestingly, we found that the rate function J of Theorem 3.3 also appears when considering the so-called Conformal Loop Ensembles (CLE) coupled to Liouville quantum gravity. More precisely, our starting point was the expression of the *multifractal spectrum of extreme nesting in CLE* which has been computed by Miller, Watson and Wilson [MWW16]. In a nutshell, it is the function that associates to $\nu > 0$ the Hausdorff dimension of the set of points $z \in \mathbb{C}$ such that the number of CLE loops surrounding the ball $B(z, e^{-r})$ grows as νr for $r \to \infty$. To obtain our J, we need to replace the Euclidean radius e^{-r} of the ball by its *Liouville quantum measure*. This is done by applying a functional version of the KPZ relations, see [25, Section 2.6] for details.

To conclude this section, let me mention that our results have been complemented by Chen, Curien and Maillard [CCM17]—see also [Che18, Chapter III]—who showed that, when the perimeter $2k$ of the loop-decorated map tends to infinity, the nesting tree may be described by a certain *multiplicative cascade*. Their approach consists in keeping track of the lengths of the longest outermost loops, and showing that they scale linearly with k, with random proportionality constants whose law is explicit.

3.5 Conclusion and perspectives

In this chapter we have presented the gasket decomposition and some of its applications to the study of the $O(n)$ loop model on random maps. Many other results on this model have been obtained recently by Timothy Budd [Bud17a, Bud17b, Bud18]. In particular, while studying the peeling process of loop-decorated random maps, he uncovered a surprising connection with walks on the square lattice, which allows to study their winding angles around the origin.

Let me now list a few directions for future research. First, it would be interesting to make a connection between our approach and that developed by Bernardi and Bousquet-Mélou (recall that the $O(n)$ loop model is intimately connected with the Potts model, as mentioned in Section 3.1). Do the techniques discussed in this chapter allow to recover the same algebraicity results as those [BBM11]? And how does differential algebraicity [BBM17] arise in this context? Another challenging question is to extend the gasket

decomposition in the presence of degree constraints on the vertices. In particular, the results from [EB99] still await a combinatorial explanation.

The topic of maps with large faces, which was my initial motivation for considering the $O(n)$ loop model, is still a very active domain of research [BC17, Ric18, CR18, Mar18a]. From the point of view of statistical physics, it is still not completely understood how the phase transition between the dense and dilute regimes manifests itself at the geometric level. More precisely, in the qualitative discussion at the beginning of Section 3.3, the phase transition occurs when the exponent a appearing in (3.4) takes the value 2. The dense and dilute phases corresponds to the respective cases $a < 2$ and $a > 2$. By analogy with the $O(n)$ loop model on regular lattices (whose scaling limit at a critical point is believed to be a conformal loop ensemble), we expect the contours of the faces to be simple in the scaling limit for $a \geq 2$, and nonsimple for $a < 2$. Some results in that direction were obtained in [Ric18] but, to my knowledge, the question is not settled. A very interesting duality between the dense and dilute regimes has been studied in [CR18].

Finally, I would like to extend the gasket decomposition to other models of statistical physics on random maps such as the six-vertex model—see the references given in Section 3.1 and the recent preprint [BMEPZJ19]—and the ADE height model [Kos92,Kos96]. Some preliminary investigation shows that our approach may indeed be adapted to this setting, with new technical challenges to be overcome. For instance, loop representations of the six-vertex model typically involve complex weights, whose probabilistic interpretation is unclear. The primary motivation is to gain geometric insight on these models.

4 Schur processes

In this chapter, we leave the the realm of planar maps and enter that of Schur processes. They are certain measures over sequences of partitions, with deep connections with models of statistical mechanics such as lozenge or domino tilings, last passage percolation (LPP) and the totally asymmetric simple exclusion process (TASEP). The publications closest to this topic are [21, 22, 24, 26–28]. In this chapter I will present my contributions from a personal perspective.

After recalling some context in Section 4.1, I discuss in Section 4.2 how Schur processes arise in connection with a family of domino tilings called *steep tilings* [21], that are equivalent to dimer coverings of *rail yard graphs* [24]. In Section 4.3, I explain how to compute the correlation functions in the presence of periodic or free boundary conditions using the free fermion formalism. Then, in Section 4.4, I discuss the corresponding asymptotics. The material for these two sections comes from [26, 27]. I conclude with some perspectives in Section 4.5.

4.1 Context

Let me start by telling how I became interested in the subject: in 2011-2012 I was spending the academic year at LIAFA [1], and participating in their *groupe de lecture de combinatoire* which that year was on the topic of integrable hierarchies, following the book by Miwa, Jimbo and Date [MJD00]. The initial motivation was to understand their connection with map generating functions, but I actually did not pursue further work in that direction [2]. However, in Spring 2012 I also visited the Mathematical Sciences Research Institute in Berkeley during the program *Random spatial processes*, where I learnt about the work of Benjamin Young on pyramid partitions [You09]. Back in Paris, together with Guillaume Chapuy and Sylvie Corteel, we were struck that the fact that the *vertex operator formalism*, that plays a key role in integrable hierarchies, is also useful for the study of pyramid partitions [You10]. Also, we were puzzled by the similarity between the expression of the generating function of pyramid partitions and that of domino tilings of the Aztec diamond [EKLP92a, EKLP92b]. This led us to introduce the notion of steep tilings [21], which encompasses both families and may be enumerated by the vertex operator formalism. After Sylvie presented our work at Aléa, we were joined by Cédric Boutillier and Sanjay Ramassamy, with whom we introduced rail yard graphs [24]. Dimer models on rail yard graphs are essentially equivalent to steep tilings,

1. Laboratoire d'informatique algorithmique : fondements et applications, now merged into IRIF (Institut de recherche en informatique fondamentale)
2. Unlike my colleague Guillaume Chapuy [CC15, ACEH18, Cha18]

as we shall see in Section 4.2, but they come with a coordinate system which is more convenient for expressing the so-called correlation functions. These models are, in some sense, the most general combinatorial realizations of Schur processes.

Schur processes were introduced by Okounkov and Reshetikhin [OR03, OR07] as a generalization of Okounkov's Schur measures [Oko01]. They also appear, more or less implicitly, in the works of Johansson [Joh02, Joh03, Joh05]. Together with their nondeterminantal generalization called Macdonald processes [BC14], they are central models in the field known as *integrable probability* [Bor14, BG16]. I will not attempt to review the abundant literature in this field but, besides the references cited in the previous papers, point to the book by Romik [Rom15]. It gives a nice account of the story of the *Ulam–Hammersley problem*, which consists in studying the asymptotic distribution of the length of a longest increasing subsequence of a random permutation, and which is intimately connected with the *Plancherel measure on integer partitions* [BDJ99, BOO00, Joh01], the simplest instance of a Schur measure.

The vertex operator formalism, also known as the free fermion formalism, the (semi) infinite wedge, the fermionic Fock space, the boson-fermion correspondence, etc, is a classical topic in mathematical physics, see e.g. [JM83, MJD00, AZ13], [Kac90, Chapter 14] or [ZJ08, Chapter 1]. Its probabilistic application for the study of Schur measures and processes was pioneered by Okounkov [Oko01, Appendix A], see also [PS02]. In contrast, other authors such as Johansson [Joh01] and Borodin–Rains [Rai00, BR05, Bor07] used variants of the orthogonal polynomial method developed in random matrix theory.

Since my own entry in the subject was through the vertex operator formalism, I found it natural to continue using it. In our work on steep tilings [21], we understood how to apply it to enumerate tilings with periodic or free boundary conditions. But it was unclear how to extend the approach to handle the correlation functions. This is the problem that we solved in the papers [26, 27], which will be reviewed in Section 4.3.

4.2 From domino tilings to Schur processes

In this section we explain how Schur processes arise in connection with a certain family of domino tilings, that we call *steep tilings*, and that are in bijection with *dimer coverings of rail yard graphs*. The definitions in this section differ slightly from those in [21] and [24], see Remark 4.1. The term "steep" comes from the fact that the associated height function, which we will not discuss here for brevity, has eventually the maximal possible slope in two opposite directions.

Consider the domino tiling represented on the left of Figure 4.1, which we call the *fundamental tiling*. We choose the Cartesian coordinate system (x, y) such that the corners of dominoes belong to the lattice $\mathbb{Z}^2$ and, by convention, the origin $(0, 0)$ is the point at the center of the figure (hence is a corner common to four different dominoes). A point of $\mathbb{Z}^2$ is said *odd* or *even* depending on the parity of the sum of its coordinates. Parity allows to distinguish four types of dominoes: a horizontal (resp. vertical) domino is said *north* (resp. *east*) if its top-left corner is odd, and *south* (resp. *west*) otherwise. In the fundamental tiling, the region $x + y \geq 1$ contains only north and east dominoes,

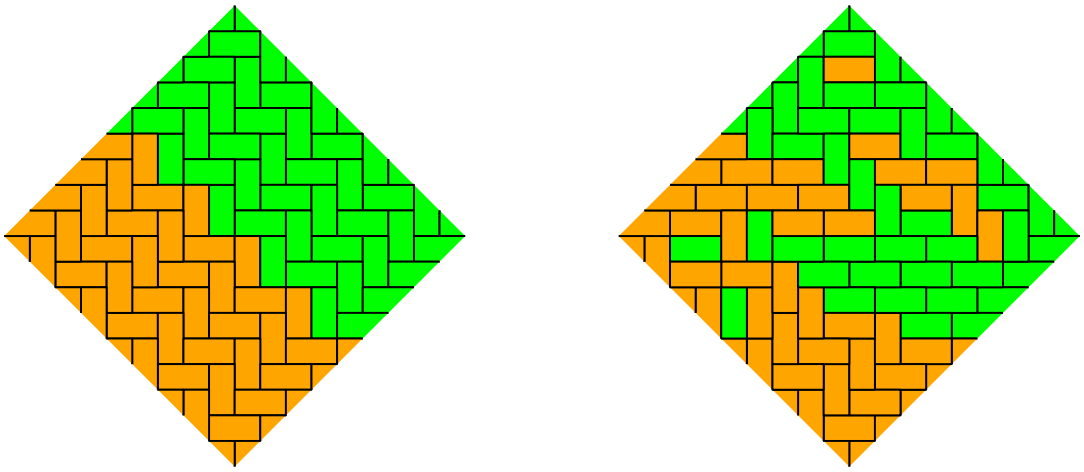

Figure 4.1 – A portion of the fundamental tiling (left), and a pure steep tiling (right) corresponding to a perturbation of it by finitely many "flips". North and east (resp. south and west) dominoes are represented in green (resp. orange). The fundamental tiling is periodic along the north-west to south-east direction, along the perpendicular direction it is almost periodic (notice the "zig-zag" pattern gets shifted at the green-orange interface, which is the only place where we can perform initial flips). A general steep tiling coincides with the fundamental tiling far away from the interface.

while the region $x + y \geq -1$ contains only south and west dominoes.

A general *steep tiling* is obtained from the fundamental tiling by performing flips. A *flip* is the elementary operation which consists in replacing a pair of parallel dominoes forming a 2×2 block by a pair of dominoes with the opposite orientation. Note that, initially in the fundamental tiling, the only flippable blocks are centered at the positions (n, n) with n an odd integer. But, after such flips have been performed, new flippable blocks appear. An example of steep tiling is represented on the right of Figure 4.1. A steep tiling is said *pure* if it may be obtained from the fundamental tiling by finitely many flips, hence it coincides with it outside a finite region. For a general steep tiling, we require that the number of flips centered on the line $x - y = n$ be finite for each n, but the total number of flips may be infinite. Informally this says that a steep tiling coincides with the fundamental tiling sufficiently far away from the line $x + y = 0$. Such more general setting is necessary when considering periodic steep tilings, for instance. Keeping track of the number of flips on each line amounts to putting certain weights on dominoes, but these weights are easier to define in the language of rail yard graphs, which we now present.

Steep tilings are in bijection with certain *dimer coverings* of the (universal) *rail yard graph*, obtained as follows. Given a steep tiling, the first step consists in passing to the dual picture, namely to the corresponding dimer covering of the dual graph, as displayed on the left of Figure 4.2. The vertex set of the dual graph may be thought as $(\mathbb{Z}')^2$,

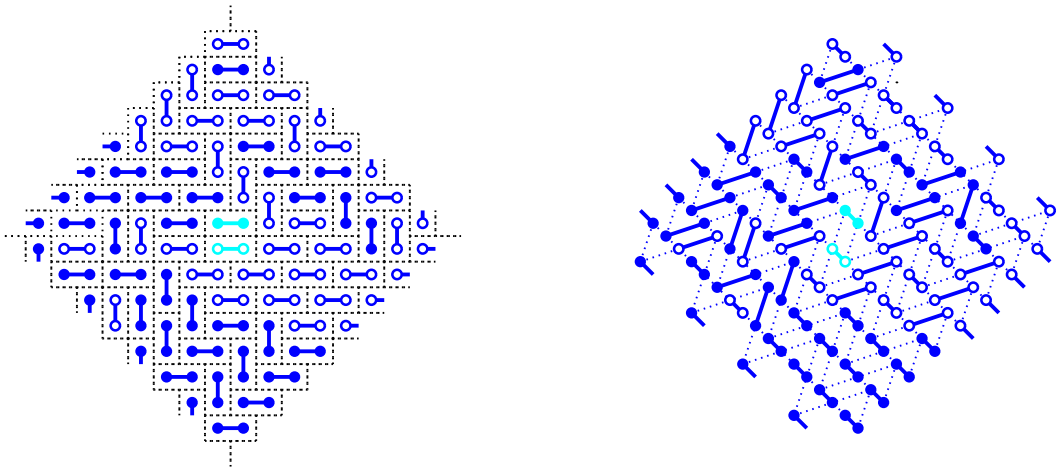

Figure 4.2 – Left: the dimer covering on $(\mathbb{Z}')^2$ corresponding to the steep tiling displayed on the right of Figure 4.1. To facilitate the further identification with a sequence of interlaced partitions, south and west (resp. north and east) dimers are represented with solid (resp. hollow) endpoints, that indicate the presence of a particle (resp. of a hole). Right: the same dimer covering, now represented on the "universal" rail yard graph. To help visualize the deformation, we represent in lighter color the dimers close to the origin. There are finitely many dimers on the longer edges, and the weights are associated with them.

where $\mathbb{Z}' := \mathbb{Z} + \frac{1}{2}$ is the set of half-integers. Next, we slightly deform the dual graph as follows: given a vertex $(x, y) \in (\mathbb{Z}')^2$

— we leave it at the same position if $x - y$ is even,

— we translate it by $(\frac{1}{2}, \frac{1}{2})$ if $x - y \equiv 1 \mod 4$,

— we translate it by $(-\frac{1}{2}, -\frac{1}{2})$ if $x - y \equiv -1 \mod 4$.

See the right of Figure 4.2 for an illustration. A more convenient choice of coordinates [24] for the vertices of the deformed graph, which we call the *universal rail yard graph* (URYG), is to set

$$x = \frac{X}{2} + Y, \quad y = -\frac{X}{2} + Y \tag{4.1}$$

where $X \in \mathbb{Z}$ and $Y \in \mathbb{Z}'$. Thus, the vertex set of the URYG may be thought as $\mathbb{Z} \times \mathbb{Z}'$ in terms of the (X, Y) coordinates. There are two types of edges: *shorter* edges connecting vertices with the same value of Y, and *longer* edges connecting vertices whose values of Y differ by ± 1. We do not detail here the full characterization of dimer coverings corresponding to steep tilings, but simply note that the finiteness condition on the number of flips along a line $x - y = n$ implies that the number of longer edges covered by dimers, hereafter called *covered longer edges*, is finite along each such line. In particular *pure* dimer coverings, corresponding to pure steep tilings, have finitely many covered longer

edges, but the converse is not true [3]. To a dimer covering C with finitely many covered longer edges, we assign a weight

$$w(C) := \prod_{i \in \mathbb{Z}'} u_i^{n_i(C)} \tag{4.2}$$

where $n_i(C)$ is the number of covered longer edges connecting vertices with abscissas $i - \frac{1}{2}$ and $i + \frac{1}{2}$ in the URYG coordinates (so their middles have abscissa $i \in \mathbb{Z}'$), and the u_i's are arbitrary variables. By working out the correspondence backwards, we see that the weight $w(C)$ corresponds to putting certain weights on dominoes in the steep tiling picture. Details are left to the reader. The only pure tiling with weight 1 (i.e. containing no covered longer edge in the dimer picture) is the fundamental tiling.

Remark 4.1. The original definition of steep tilings in [21] involves the so-called asymptotic data, which is a binary word on the alphabet $\{+, -\}$. Here we consider only steep tilings with asymptotic data $\cdots + + - - + + - - + + - - \cdots$. There is no loss of generality in doing so, as arbitrary asymptotic data may be "emulated" by setting appropriate variables u_i in (4.2) to zero. Similarly the original definition of rail yard graphs in [24] involves the so-called LR and sign sequences, and here we consider the case where these are respectively $\cdots LRLRLRLR \cdots$ and $\cdots + + - - + + - - + + - - \cdots$ (again, without loss of generality, which is why we call this case "universal"). The URYG which we consider here corresponds actually to the contracted graph $\tilde{R}$ of [24, Section 5.2].

The main result of [21] concerns the weighted enumeration of steep tilings subject to various kinds of boundary conditions (pure, periodic, free, etc), and the main result of [24] is an explicit expression for their so-called correlation functions in the *pure* case. So, let us first review the results for the pure case. We start with the enumerative result.

Theorem 4.1 (see [21, Theorem 3] and [24, Theorem 1])**.** *The* pure partition function Z*, defined as the sum of the weights* (4.2) *of all pure dimer coverings, is equal to*

$$Z = \prod_{\substack{(i,j) \in \mathbb{Z}^2 \\ i<j}} \frac{\left(1 + u_{4i+\frac{1}{2}} u_{4j-\frac{1}{2}}\right)\left(1 + u_{4i+\frac{3}{2}} u_{4j-\frac{3}{2}}\right)}{\left(1 - u_{4i+\frac{1}{2}} u_{4j-\frac{3}{2}}\right)\left(1 - u_{4i+\frac{3}{2}} u_{4j-\frac{1}{2}}\right)}. \tag{4.3}$$

It is clear that Z is a well-defined formal power series in the variables $(u_i)_{i \in \mathbb{Z}'}$, with nonnegative integer coefficients. Furthermore, it is analytically convergent when the u_i's are small enough and decay fast enough (e.g. exponentially) at $\pm\infty$.

We now discuss some examples, that are obtained by *reduction*, i.e. by setting some u_i's to zero, cf. Remark 4.1. Reduction amounts to forbidding certain types of dominoes/dimers at certain positions, such that the resulting subfamily is in bijection with another family of tilings. For brevity, we only write down the reduced formulas, and refer to the original papers for the combinatorial details of reduction.

3. Dimer coverings with finitely many covered longer edges may have different boundary conditions for $X \to \pm\infty$. A boundary condition corresponds to a partition, and the pure case corresponds to having the empty partition as boundary condition for both $X \to +\infty$ and $X \to -\infty$. Boundary conditions are analogous to the "asymptotics" for "3d partitions" (plane partitions) considered in [ORV06].

Example 4.2 (Domino tilings of the Aztec diamond). Take $u_{4i+\frac{3}{2}} = u_{4i-\frac{3}{2}} = 0$ for all $i \in \mathbb{Z}$, and set $u_{4i+\frac{1}{2}} = v_{2i+1}$, $u_{4i-\frac{1}{2}} = v_{2i}$. We get

$$Z_{\text{Aztec}} = \prod_{i<j}(1 + v_{2i+1}v_{2j}) \tag{4.4}$$

which corresponds to Stanley's weighting scheme for the Aztec diamond, see [21, Remark 2]. Taking further $v_i = 1$ for $1 \leq i \leq 2\ell$ and $v_i = 0$ otherwise, we recover the well-known fact that there are $2^{\binom{\ell+1}{2}}$ domino tilings of the Aztec diamond of order ℓ. Taking more generally $v_i = q^{(-1)^i i}$ for $1 \leq i \leq 2\ell$, we recover the q-series $\prod_{i=1}^{\ell}(1+q^{2i-1})^{\ell+1-i}$ [EKLP92a].

Example 4.3 (Pyramid partitions). For $i \geq 0$, take $u_{4i+\frac{1}{2}} = u_{4i+\frac{3}{2}} = 0$, $u_{4i+\frac{5}{2}} = v_{2i}$ and $u_{4i+\frac{7}{2}} = v_{2i+1}$. Similarly for $i \leq 0$, take $u_{4i-\frac{1}{2}} = u_{4i-\frac{3}{2}} = 0$, $u_{4i-\frac{5}{2}} = v'_{2|i|}$ and $u_{4i-\frac{7}{2}} = v'_{2|i|+1}$. We get

$$Z_{\text{pyramids}} = \prod_{i,j=0}^{\infty} \frac{(1 + v_{2i}v'_{2j})(1 + v_{2i+1}v'_{2j+1})}{(1 - v_{2i}v'_{2j+1})(1 - v_{2i+1}v'_{2j})}. \tag{4.5}$$

By taking $v_i = v'_i = q^{i+\frac{1}{2}}$ we obtain the q-series $\prod_{k\geq 1} \frac{(1+q^{2k-1})^{2k-1}}{(1-q^{2k})^{2k}}$ which is the generating function of pyramid partitions [You09, You10].

Example 4.4 (Plane partitions). For $i \geq 0$, take $u_{4i+\frac{1}{2}} = u_{4i+\frac{3}{2}} = u_{4i+\frac{7}{2}} = 0$ and $u_{4i+\frac{5}{2}} = v_i$. For $i \leq 0$, take $u_{4i-\frac{1}{2}} = u_{4i-\frac{3}{2}} = u_{4i-\frac{5}{2}} = 0$ and $u_{4i-\frac{7}{2}} = v'_{|i|}$. We get

$$Z_{\text{pp}} = \prod_{i,j=0}^{\infty} \frac{1}{1 - v_i v'_i}.$$

By taking $v_i = v'_i = q^{i+\frac{1}{2}}$ we obtain the q-series $\prod_{k\geq 1} \frac{1}{(1-q^k)^k}$ which is the well-known MacMahon generating function of unboxed plane partitions.

We now discuss the correlation functions. Here it is slightly easier to work in the dimer picture: suppose that the u_i's are nonnegative and such that the partition function Z is finite. Then, we may interpret $w(C)/Z$ as the probability of the pure dimer covering C in the *URYG dimer model*. For E a finite set of edges of the URYG, the *correlation function* $P(E)$ is defined as the probability that all the edges in E are covered by dimers. Since the URYG is bipartite, we expect [4] by the general Kasteleyn theory (see e.g. [dT15] and references therein) that $P(E)$ may be expressed in the form of a determinant of size $|E|$, which is a minor of the so-called inverse Kasteleyn matrix. This turns out to be the case, and we are furthermore able to give an explicit expression for the entries of the inverse Kasteleyn matrix.

4. Let us point out that we only "expect" and do not "know" a priori: since the URYG is infinite there are technical difficulties in applying the Kasteleyn theory. To my knowledge, the general theorems of Kenyon *et al.* [KOS06] need certain periodicity assumptions that are not satisfied for the URYG with general, non periodic, weights.

To state this expression, we need some further definitions and notations: for $X \in \mathbb{Z}$, we set

$$F_X(z) := \prod_{\substack{i \in 4\mathbb{Z}+\frac{1}{2} \\ i<X}} (1-u_i z)^{-1} \prod_{\substack{i \in 4\mathbb{Z}+\frac{3}{2} \\ i<X}} (1+u_i z) \prod_{\substack{i \in 4\mathbb{Z}+\frac{5}{2} \\ i>X}} (1-u_i z^{-1}) \prod_{\substack{i \in 4\mathbb{Z}+\frac{7}{2} \\ i>X}} (1+u_i z^{-1})^{-1}. \quad (4.6)$$

This quantity, and its inverse $F_X(z)^{-1}$, are to be interpreted as Laurent series in z, where the first two factors should be seen as power series in z, and the last two as power series in z^{-1}. If we assume, for simplicity, that all the u_i's are smaller than 1 and decay exponentially as $i \to \pm\infty$, then these Laurent series are convergent in an open annulus containing the unit circle (other cases may be treated by analytic continuation). Let (X, Y) and (X', Y') be the URYG coordinates of two vertices, with X odd and X' even. Then, we set

$$\mathcal{C}(X, Y; X', Y') := \begin{cases} [z^Y w^{-Y'}] \dfrac{F_X(z)}{F_{X'}(w)} \displaystyle\sum_{k=0}^{\infty} \left(\frac{w}{z}\right)^{k+\frac{1}{2}} & \text{if } X < X', \\ [z^Y w^{-Y'}] \dfrac{F_X(z)}{F_{X'}(w)} \displaystyle\sum_{k=0}^{\infty} \left(\frac{z}{w}\right)^{k+\frac{1}{2}} & \text{if } X > X', \end{cases} \quad (4.7)$$

where $[z^Y w^{-Y'}]$ means extraction of the coefficient of $z^Y w^{-Y'}$ in the bivariate Laurent series on the right (which may be represented as a double contour integral).

Theorem 4.2 (see [24, Theorem 5]). *$\mathcal{C}$ is an inverse Kasteleyn matrix for the URYG dimer model, in the sense that, for any finite set $E = \{e_1, \dots, e_n\}$ of edges, we have*

$$P(E) = \pm u_{i_1} \cdots u_{i_m} \det_{1 \le k, \ell \le n} \mathcal{C}(X_k, Y_k; X'_\ell, Y'_\ell). \quad (4.8)$$

where the edge e_k has endpoints (X_k, Y_k) and (X'_k, Y'_k) (with X_k assumed odd and X'_k even), and $i_1, \dots, i_m$ ($m \le n$) denote the abscissas of the longer edges in E.

The proofs of Theorems 4.1 and 4.2 rely on two ingredients:

— a bijection between steep tilings (or URYG dimer coverings) and *sequences of interlaced partitions* that form a *Schur process*;

— the vertex operator/free fermion formalism (plus some combinatorial tricks to make the connection with Kasteleyn theory).

In the remainder of this section, we will give the first ingredient, for the second we refer to the original papers.

Consider again Figure 4.2 and pay now attention to the endpoints of the dimers, which are represented either solid (•) or hollow (∘). These symbols form a *particle configuration*: the symbol • indicates the presence of a particle, and the symbol ∘ the absence of a particle, hence the presence of a *hole*. In detail, we put particles (resp. holes) on the endpoints of dimers corresponding to south or west (resp. north or east) dominoes. In terms of URYG coordinates, there are particles on the endpoints of a dimer covering an

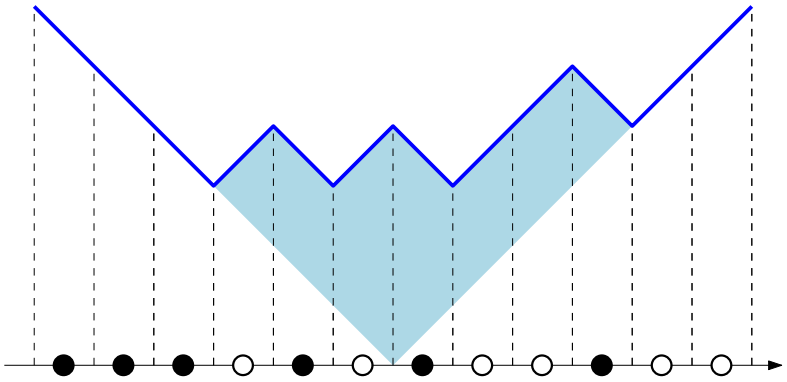

Figure 4.3 – The correspondence between Maya diagram and partitions. Here we consider the partition $\lambda = (4, 2, 1)$, whose parts give the displacements of the particles ($\bullet$) with respect to their "ground state". The parts of the conjugate partition $\lambda' = (3, 2, 1, 1)$ give the displacements of the holes ($\circ$).

edge between (X, Y) and $(X + 1, Y')$ if and only if X is even. Therefore, to each dimer covering we may associate a particle configuration on the URYG vertex set.

If we restrict to the vertices having a given abscissa $X \in \mathbb{Z}$, then we obtain a 1D particle configuration that is a *Maya diagram* [MJD00]. Such diagram is in bijection with a partition $\lambda(X)$: again we trust that Figure 4.3 is worth a thousand words. Therefore, a URYG dimer covering corresponds to a sequence of partitions $(\lambda(X))_{X\in\mathbb{Z}}$. This sequence satisfies the *interlacing property*

$$\lambda(4k) \prec \lambda(4k+1) \prec' \lambda(4k+2) \succ \lambda(4k+3) \succ \lambda(4k+4), \qquad 'k \in \mathbb{Z}. \tag{4.9}$$

This is a straightforward consequence of the URYG structure, of the coding of partitions by Maya diagrams, and of the characterization (0.5) of interlacing. For instance, the relation $\lambda(4k+1) \prec' \lambda(4k+2)$ is obtained by considering the dimers between vertices with abscissas $4k+1$ and $4k+2$: for each such dimer there are particles on the endpoints, whose ordinates differ by 0 or 1, so we conclude by (0.5) that $\lambda(4k+2)/\lambda(4k+1)$ is a vertical strip. Note that its size is equal to the number of covered longer edges with middle abscissas $4k + \frac{3}{2}$. Other cases are obtained by symmetry and "particle-hole duality".

The fundamental tiling corresponds to the constant sequence equal to the empty partition, and pure steep tilings map to sequences with finite support (i.e. equal to the empty partition except for finitely many terms). The weight $w(C)$ of a dimer covering may be rewritten in terms of partitions as

$$w(C) = \prod_{i\in\mathbb{Z}'} u_i^{||\lambda(i+\frac{1}{2})|-|\lambda(i-\frac{1}{2})||}. \tag{4.10}$$

Interestingly, both the interlacing property (4.9) and the weight (4.10) can be rewritten

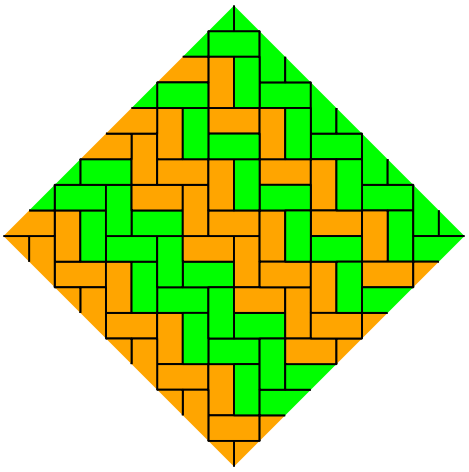

Figure 4.4 – The periodic steep tiling corresponding to the constant sequence of partitions equal to $(3, 2, 2)$.

in terms of *Schur functions* in one variable. More precisely, by (0.9), we have

$$w(\underline{\lambda}) := \prod_{k\in\mathbb{Z}} \left(s_{\lambda(4k+1)/\lambda(4k)}\left(u_{4k+\frac{1}{2}}\right) s_{\lambda'(4k+2)/\lambda'(4k+1)}\left(u_{4k+\frac{3}{2}}\right) \times \right.$$
$$\left. s_{\lambda(4k+2)/\lambda(4k+3)}\left(u_{4k+\frac{5}{2}}\right) s_{\lambda'(4k+3)/\lambda'(4k+4)}\left(u_{4k+\frac{7}{2}}\right)\right)$$
$$= \begin{cases} \prod_{i\in\mathbb{Z}'} u_i^{||\lambda(i+\frac{1}{2})|-|\lambda(i-\frac{1}{2})||} & \text{if (4.9) is satisfied,} \\ 0 & \text{otherwise.} \end{cases} \tag{4.11}$$

for any sequence of partitions $\underline{\lambda} = (\lambda(X))_{X\in\mathbb{Z}}$ which is eventually constant for $X \to \pm\infty$. If we restrict to sequences with finite support, corresponding to pure steep tilings, the form (4.11) tells that $\underline{\lambda}$ is a *Schur process* [OR03, OR07]. We then may reuse the results and methods of Okounkov and Reshetikhin, that are based on free fermions, to prove Theorem 4.1 and to characterize the correlation functions of the particle configuration (i.e., for any finite set F of vertices, the probability that there is a particle on each element of F). By relating the correlation functions of particles to those of dimers, we obtain Theorem 4.2.

4.3 Periodic and free boundary conditions: fermionic approach

In the paper [21], we did not restrict to pure steep tilings, which coincide with the fundamental tiling outside a finite region (see again Figure 4.1), but we also considered other types of "boundary conditions".

For instance, we may consider *periodic* steep tilings, that have a period $(2T, -2T)$ in the (x, y) coordinates for some positive integer T (note that the fundamental tiling

has period $(2,-2)$). In terms of sequences of interlaced partitions, such periodic tilings correspond to sequences of the form (4.9) which have a period $4T$. A first caveat is that the sum of the weights (4.2) of all periodic steep tilings is ill-defined, since there are infinitely many periodic tilings C such that $w(C) = 1$, for instance the tiling displayed on Figure 4.4. Such tilings are in bijection with constant sequences of partitions, for which the product of Schur functions $w(\underline{\lambda})$ of (4.11) evaluates to 1. To fix this problem, we introduce the modified partition function

$$Z_{\text{per}} := \sum_{C \text{ periodic}} q^{|\lambda(0)|} w(C) \tag{4.12}$$

where q is an extra variable, which should be of modulus smaller than 1 to make the sum convergent, and where we restrict the range of i's in (4.2) to the interval $\mathbb{Z}' \cap [0, 4T]$ by periodicity. The variables q and u_i's may be related to the number of *periodic flips* that are needed to obtain the tiling C from the fundamental tiling (a periodic flip is the operation that consists in performing simultaneous flips at all translates of a given position, so as to preserve periodicity).

Theorem 4.3 (see [21, Theorems 5 and 12])**.** *The periodic partition function is given by*

$$Z_{\text{per}} = \prod_{k=1}^{\infty} \left(\frac{1}{1-q^k} \prod_{i,j=1}^{T} \frac{\left(1 + q^{k-\mathbb{1}_{i<j}} u_{4i+\frac{1}{2}} u_{4j-\frac{1}{2}}\right)\left(1 + q^{k-\mathbb{1}_{i<j}} u_{4i+\frac{3}{2}} u_{4j-\frac{3}{2}}\right)}{\left(1 - q^{k-\mathbb{1}_{i<j}} u_{4i+\frac{1}{2}} u_{4j-\frac{3}{2}}\right)\left(1 - q^{k-\mathbb{1}_{i<j}} u_{4i+\frac{3}{2}} u_{4j-\frac{3}{2}}\right)} \right) \tag{4.13}$$

where $\mathbb{1}_{i<j} = 1$ *if* $i < j$ *and* 0 *otherwise.*

In the same way that the sequence of partitions corresponding to a random pure steep tiling is a Schur process as defined in [OR03], the sequence $\underline{\lambda}$ corresponding to a random periodic steep tiling (with the weight $q^{|\lambda(0)|} w(\underline{\lambda})$) forms a *periodic Schur process*, as defined in [Bor07]. In fact, Theorem 4.3 follows from Borodin's results. In [21] we gave another derivation based on the vertex operator formalism. It might be possible to derive the periodic analogue of Theorem 4.2 using Borodin's expression for the correlation functions, but the main difficulty is that the periodic Schur process is *not* determinantal as soon as $q > 0$, i.e. the particle correlation function is not directly given by a determinant.

Borodin found that the process becomes determinantal if one performs "shift-mixing": in colloquial terms this corresponds to choosing some integer $c \in \mathbb{Z}$ independent of the tiling, with probability proportional to $q^{\frac{c^2}{2}} t^c$ where q is the same parameter as before and t is another arbitrary positive real parameter, and shifting the tiling by the vector (c, c). Then, for the shift-mixed tiling, the particle correlation function has determinantal form.

I became quite puzzled by Borodin's result. His proof was based on the so-called L-ensembles, and not the free fermion formalism (though he mentions that his original unpublished derivation was based on Fock space techniques). I therefore took it as a challenge to rederive his result using fermions. We solved this problem with Dan Betea in [27], using *finite temperature* ensembles of free fermions. The idea is of course rather natural in quantum statistical mechanics, where inverse temperature may be thought of

as an imaginary period, but some details are nontrivial. In particular, we understood that shift-mixing amounts in physical terms to passing to the grand canonical ensemble.

In parallel, in our work on steep tilings we also found expressions for the partition function of tilings with *free boundary conditions*, see [21, Theorem 4]. Intuitively this corresponds to not prescribing the boundary conditions [5] of the URYG dimer coverings at $X \to \pm\infty$. When there is only one free boundary, i.e. when the asymptotics at $X \to +\infty$ is free but the one at $X \to -\infty$ corresponds to the empty partition, the sequence of interlaced partitions forms a *pfaffian Schur process*, as defined in [BR05]. For such a process, there is an analogue of Theorem 4.2 where the determinant is replaced by a pfaffian. When there are two free boundaries, we obtain a variant of the Schur process that, to my knowledge, had not been considered before [21]. By analogy with the periodic case, I conjectured that the correlation functions are not pfaffian in general, but become so after performing a suitable shift-mixing. We proved this conjecture with Dan Betea, Peter Nejjar and Mirjana Vuletić in [26], using again fermionic techniques. The basic idea here is to perform a certain *Bogoliubov transformation*, which is another classical method in mathematical physics [BR86].

In the remainder of this section, I will sketch the basic ideas of [27] and [26]. I mostly focus on the partition picture, but the reader may keep in the back of her mind the tiling/dimer picture.

Let me start with the most elementary setting, which corresponds to plain random partitions. Consider the periodic partition function Z_{per} of Theorem 4.3, in which we set all u_i's to zero. It then reduces to the well-known generating function of partitions

$$Z_{\mathrm{par}} = \prod_{k=1}^{\infty} \frac{1}{1-q^k}. \tag{4.14}$$

Indeed, URYG dimer coverings without covered longer edges are in bijection with constant sequences of partitions. In probabilistic terms, we are considering the *canonical measure* on partitions, in which a given partition λ appears with probability $\frac{1}{Z_{\mathrm{par}}} q^{|\lambda|}$. To such a random partition we associate a random Maya diagram, via the bijection of Figure 4.3. In explicit terms, the positions of the particles form the set

$$S(\lambda) = \left\{ \lambda_1 - \frac{1}{2}, \lambda_2 - \frac{3}{2}, \lambda_3 - \frac{5}{2}, \dots \right\} \subset \mathbb{Z}' \tag{4.15}$$

where the origin is by convention at the "bottom corner" of the Young diagram. It is clear that, for different $s \in \mathbb{Z}'$, the events $\{s \in S(\lambda)\}$ cannot be independent, because there are as many positive elements in the set $S(\lambda)$ as negative elements in its complementary (in other words, the Maya diagram has *charge* zero). There is, however, a surprisingly simple way to obtain independence: consider a random integer taking value c with probability proportional to $q^{\frac{c^2}{2}} t^c$ (it is nothing but Borodin's shift-mixing parameter) and independent of λ. Then, consider the shifted set

$$S(\lambda) + c = \left\{ \lambda_1 - \frac{1}{2} + c, \lambda_2 - \frac{3}{2} + c, \lambda_3 - \frac{5}{2} + c, \dots \right\} \subset \mathbb{Z}'. \tag{4.16}$$

5. cf. footnote 3

It is not difficult [6] to see that the probability that this set is equal to a given $S \subset \mathbb{Z}'$ is proportional to

$$q^{|\lambda|+\frac{c^2}{2}} t^c = \prod_{s \in S \cap (0,\infty)} (q^s t) \prod_{s \in (\mathbb{Z}' \setminus S) \cap (-\infty,0)} (q^{-s} t^{-1}). \tag{4.17}$$

Here, it is understood that the right-hand side vanishes as soon as one of the sets of indices is infinite (since $0 < q < 1$). Summing (4.17) over all pairs (λ, c) or subsets $S \subset \mathbb{Z}'$ yields a classical combinatorial proof of the well-known Jacobi triple product identity. Moreover, it also implies that

$$\text{Prob}\,(s \in S(\lambda) + c) = \frac{q^s t}{1 + q^s t}, \qquad s \in \mathbb{Z}' \tag{4.18}$$

and that these events are independent for different s's. We recognize the *Fermi-Dirac distribution* describing a grand canonical ensemble of fermions, where q is related to the physical temperature ($q = 0$ is zero temperature, $q \to 1$ is the high-temperature limit) and t to the chemical potential. Asymptotics will be discussed in Section 4.4.

We now turn to the general setting of the periodic Schur process, corresponding to taking nonzero u_i's in the partition function Z_{per} of Theorem 4.3. In other words, we are consider a random $4T$-periodic sequence of integer partitions, which is equal to $\underline{\lambda} = (\lambda(X))_{X \in \mathbb{Z}}$ with probability proportional to $q^{\lambda(0)}$ times the Schur weight (4.11) (with the range of indices in the product restricted to a period). At this stage, we make some use of the free fermion formalism: for brevity we will not include the definitions here, but refer instead to the relevant sections of the original papers, namely [26, Section 3] and [27, Appendix B], and references therein.

We are interested in the particle correlation function which, as mentioned at the end of the previous section, is defined as the probability that there are particles on all sites of a given finite set F. More precisely, let $F = \{(X_1, Y_1), \dots, (X_n, Y_n)\} \subset \mathbb{Z} \times \mathbb{Z}'$ be such a finite set, written in URYG coordinates. We assume that the abscissas are ordered ($X_1 \leq \cdots \leq X_n$) and, by periodicity, that all of them belong to a same period, say $\{1, \dots, 4T\}$. The correlation function $\rho(F)$ is defined explicitly in terms of $\underline{\lambda}$ as

$$\rho(F) := \text{Prob}\,(Y_k \in S(\lambda(X_k)) \text{ for all } k = 1, \dots, n)\,. \tag{4.19}$$

The free fermion formalism allows, after some manipulations, to write this correlation function in the form

$$\rho(F) = \langle \Psi(X_1, Y_1) \Psi^*(X_1, Y_1) \cdots \Psi(X_n, Y_n) \Psi^*(X_n, Y_n) \rangle \tag{4.20}$$

where the $\Psi(X_i, Y_i)$ are certain *fermionic creation operators* acting on the *fermionic Fock space*, the $\Psi^*(X_1, Y_1)$ are their dual *annihilation operators*, and $\langle \cdot \rangle$ denotes a certain *expectation value* (or state) on the corresponding operator algebra. See [24, Section 4.3] for

6. Consider first the case where $\lambda = \emptyset$, where the formula (4.17) is easy. Then, consider the effect of "creating" the parts of λ one at a time: to add the part λ_k we remove the element $-k + \frac{1}{2} + c$ from S, then add the element $\lambda_k - k + \frac{1}{2} + c$ to it. Observe that both sides of (4.17) get multiplied by q^{λ_k}. This establishes the formula for any partition λ.

a relatively detailed discussion of the way to arrive at the form (4.20) in the nonperiodic case. In the periodic case, the expectation value of an operator $\mathcal{O}$ reads

$$\langle \mathcal{O} \rangle = \frac{\mathrm{Tr}(\mathcal{O} q^H \Pi_0)}{\mathrm{Tr}(q^H \Pi_0)} \tag{4.21}$$

where H is the energy operator, and Π_0 the projector on the subspace of charge 0.

For $q = 0$ (zero temperature), the expectation value reduces to the *vacuum expectation value*. In this case, *Wick's lemma* entails that the correlation function reads

$$\begin{aligned} \rho(F) &= \det_{1 \le k,\ell \le n} K(X_k, Y_k; X_\ell, Y_\ell), \\ K(X, Y; X', Y') &:= \begin{cases} \langle \Psi(X,Y) \Psi^*(X',Y') \rangle & \text{if } X \le X', \\ -\langle \Psi^*(X',Y') \Psi(X,Y) \rangle & \text{if } X > X'. \end{cases} \end{aligned} \tag{4.22}$$

This says that the particle configuration is a *determinantal point process*, and K is its correlation kernel. In fact, in the case $q = 0$ the correlation kernel has essentially the same expression as the inverse Kasteleyn matrix $\mathcal{C}$ of the previous section.

In the case $q > 0$, the difficulty is that Wick's lemma does not hold anymore for the expectation value (4.21). Hence, the process is nondeterminantal. But the solution to this problem is the same as for the canonical measure on partitions, namely we shall pass to the *grand canonical ensemble* for which the expectation value reads

$$\langle \mathcal{O} \rangle = \frac{\mathrm{Tr}(\mathcal{O} q^H t^C)}{\mathrm{Tr}(q^H t^C)} \tag{4.23}$$

where C is the charge operator. This is nothing but the operator version of the Fermi-Dirac distribution (4.18). Passing to it amounts to considering the "shift-mixed" correlation function

$$\tilde{\rho}(F) := \mathrm{Prob}\left(Y_k - c \in S(\lambda(X_k)) \text{ for all } k = 1, \dots, n\right) \tag{4.24}$$

with c independent of the Schur process and distributed as above. The correlation function $\rho(F)$ may be recovered through a simple contour integration on t. For the expectation value (4.23), Wick's lemma holds for any q and t (the fundamental reason being that $q^H t^C$ is the exponential of a "free Hamiltonian", namely a quadratic form in the creation/annihilation operators), so we find that $\tilde{\rho}(F)$ admits the same determinantal expression as in (4.22), with $\langle \cdot \rangle$ the grand canonical expectation value. This was, in a nutshell, the idea of our rederivation of Borodin's correlation function, see [27, Sections 3 and 4].

We now discuss the free boundary case. We again find an expression of the form (4.20) for the correlation function $\rho(F)$, where the expectation value is now

$$\langle \mathcal{O} \rangle = \frac{\langle \underline{u} | \mathcal{O} | \underline{v} \rangle}{\langle \underline{u} | \underline{v} \rangle} \tag{4.25}$$

with $\langle \underline{u}|$, $|\underline{v}\rangle$ certain *free boundary states* depending on positive parameters u, v such that $uv < 1$ (the product uv plays a role similar to the q of the periodic case). We have

the same issue that Wick's lemma does not hold for this expectation value. In view of the periodic case, it is natural to try to fix this problem by modifying the expectation value. After some efforts, we were able to identify the appropriate modification, which consists in replacing the free boundary states $\langle \underline{u}|$, $|\underline{v}\rangle$ by some *extended free boundary states* $\langle \underline{u,t}|$, $|\underline{v,t}\rangle$ that are obtained by performing a certain Bogoliubov transformation on the vacuum, see [26, Section 3.2.1] for the details. Here, t is a positive real parameter playing a role similar to the periodic case. In terms of correlation functions, passing to the extended free boundary states amounts to replacing the original correlation function $\rho(F)$ by its shift-mixed variant $\tilde{\rho}(F)$ as in (4.24), with c now an *even* random integer independent of the Schur process (its law is obtained by conditioning the c of the periodic case to be even, with $q = uv$).

A peculiar property of the extended free boundary states is that they are *not* eigenvectors of the charge operator. As a consequence, for the corresponding expectation value we have

$$\big\langle \Psi(X,Y)\Psi(X',Y') \big\rangle \neq 0. \tag{4.26}$$

This says that, when we apply Wick's lemma to evaluate the correlation function (4.20), we shall not ignore the "contractions" between two Ψ's, or between two Ψ^*'s. The outcome is that the shift-mixed correlation function takes the pfaffian form

$$\tilde{\rho}(F) = \mathrm{pf}_{1\leq k,\ell\leq n} K(X_k, Y_k; X_\ell, Y_\ell) \tag{4.27}$$

where K is now a 2×2 *matrix-valued kernel*

$$K(X,Y;X',Y') := \begin{pmatrix} K_{1,1}(X,Y;X',Y') & K_{1,2}(X,Y;X',Y') \\ K_{2,1}(X,Y;X',Y') & K_{2,2}(X,Y;X',Y') \end{pmatrix} \tag{4.28}$$

with

$$\begin{aligned} K_{1,1}(X,Y;X',Y') &:= \big\langle \Psi(X,Y)\Psi(X',Y') \big\rangle \\ K_{2,2}(X,Y;X',Y') &:= \big\langle \Psi^*(X,Y)\Psi^*(X',Y') \big\rangle \\ K_{1,2}(X,Y;X',Y') &:= \begin{cases} \langle \Psi(X,Y)\Psi^*(X',Y') \rangle & \text{if } X \leq X' \\ -\langle \Psi^*(X',Y')\Psi(X,Y) \rangle & \text{if } X > X' \end{cases} \\ &=: -K_{2,1}(X',Y';X,Y). \end{aligned} \tag{4.29}$$

Here, the meaning of (4.27) is that we form the $2n\times 2n$ matrix made of the blocks $K(X_k,Y_k;X_\ell,Y_\ell)$, and we take its pfaffian (the matrix is indeed antisymmetric by properties of the kernel). The conclusion is that the shift-mixed process is a *pfaffian point process*. In the case of one free boundary ($u = 0$ or $v = 0$), the shift-mixed process is identical to the original process, and we recover the result of Borodin and Rains [BR05] regarding the correlation functions of the pfaffian Schur process. For two free boundaries ($uv > 0$), our result was new, see [26, Theorem 2.5].

4.4 Periodic and free boundary conditions: asymptotics

Beyond the technical challenge of adapting the free fermion formalism, our motivation for studying the Schur process with periodic and free boundary conditions is that it

allows to observe different large-scale behaviors from the usual Schur process with empty boundary conditions.

In random partitions, one distinguishes two types of scaling limits, called the *bulk* and *edge* scaling limits. Following [27, Section 2], let us illustrate the distinction in the case of a random partition λ distributed according to the canonical measure. From the expression (4.14) of the partition function, a second moment calculation shows that we have the convergence in probability

$$r^2|\lambda| \xrightarrow{\mathbb{P}} \frac{\pi^2}{6}, \qquad \text{where } q = e^{-r},\ r \to 0^+. \tag{4.30}$$

In particular, r^{-1} plays not only the role of a temperature, but also of a length scale for the Young diagram of λ (since its area $|\lambda|$ is of order r^{-2}), hence for its associated Maya diagram. This suggests to take $s = \lfloor xr^{-1} \rfloor$ in (4.18), for some fixed $x \in \mathbb{R}$, with the immediate result

$$\text{Prob}\left(s \in S(\lambda) + c\right) \to \frac{e^{-x+\ln t}}{1 + e^{-x+\ln t}}. \tag{4.31}$$

In fact, the same result holds without the $+c$ shift, with $t = 1$. The right-hand side gives the slope of Vershik's limit shape for uniform partitions [Ver96] [7]. Also, for $i \in \mathbb{Z}$, the indicators $\mathbb{1}_{s+i \in S(\lambda)}$ become asymptotically i.i.d. Bernoulli random variables: this is Okounkov's observation that "a typical (canonical) partition is locally a random walk" [Oko01, Section 3.4]. Such a result describes the *bulk scaling limit* of canonical partitions. We now turn to the *edge scaling limit* which corresponds to studying the distribution of the first part(s) of λ, or equivalently the position of the rightmost particle(s) in the Maya diagram. By the independence property of the Fermi-Dirac distribution (4.18), it is not difficult to check that, for any $x \in \mathbb{R}$, we have

$$\text{Prob}\left(\lambda_1 \leq r^{-1} \ln r^{-1} + xr^{-1}\right) \to e^{-e^{-x}}. \tag{4.32}$$

In other words, the rescaled fluctuations of the first part λ_1 are governed by the Gumbel distribution, consistent with the result of Erdős and Lehner [EL41]. More generally, the rescaled positions of the k first parts $\lambda_1, \ldots, \lambda_k$ converge to the positions of the k rightmost points in a Poisson point process with intensity $e^{-x}dx$.

Let us now discuss the periodic Schur process. The bulk scaling limit has been studied in great generality by Borodin [Bor07], but he did not consider the edge scaling limit. We addressed this question with Dan Betea [27], in the context of the *cylindric Plancherel measure/process* (CPM/CPP). The CPP corresponds to some sort of "poissonian" limit of periodic steep tilings, but we will not enter into details here. The CPM is a marginal of the CPP, and it may be defined as the measure on partitions

$$p(\lambda) = \frac{1}{Z_{\text{CPM}}} \sum_{\mu \subset \lambda} q^{|\mu|} (s_{\lambda/\mu}(\text{ex}_y))^2 \tag{4.33}$$

7. To recover Vershik's result, we should prove concentration, and that the limit of canonical partitions for $q \to 1$ is the same as the limit of uniform random partitions of size $n \to \infty$ ("equivalence of ensembles").

where q and y are nonnegative real parameters with $q < 1$, $s_{\lambda/\mu}(\mathrm{ex}_y)$ is the exponential specialization of the skew Schur function as defined in (0.12), and the partition function Z_{CPM} is equal to $e^{y^2/(1-q)} \prod_{k=1}^{\infty}(1-q^k)^{-1}$. The CPM interpolates between the canonical measure, recovered for $y = 0$, and the Plancherel measure, recovered for $q = 0$.

Let λ denote a random partition distributed according to the CPM. We are interested in the limit $q \to 1$ and/or $y \to \infty$ where $|\lambda|$ gets large, and we consider the largest part λ_1. We set as before $q = e^{-r}$. Since the CPM interpolates between canonical and Plancherel, we intuitively expect to observe at least two different regimes:

— when we let $r \to 0$ keeping y "small", λ_1 should have Gumbel-type fluctuations as in the canonical measure,

— when we let $y \to \infty$ keeping r finite, the fluctuations of λ_1 should be of the same nature as in the Plancherel measure which, as shown by Baik, Deift and Johansson [BDJ99], are governed by the Tracy–Widom GUE distribution.

In fact, there exists a *crossover* regime where the rescaled fluctuations of λ_1 follow a distribution that interpolates between Gumbel and Tracy–Widom. This interpolating distribution was first encountered by Johansson [Joh07] in a random matrix model. It depends on a positive parameter α and may be defined as the Fredholm determinant

$$F_\alpha(x) := \det(I - M_\alpha)_{L^2(x,\infty)} \tag{4.34}$$

where M_α is the *finite-temperature Airy kernel*

$$M_\alpha(x, x') := \int_{-\infty}^{\infty} \frac{e^{\alpha u}}{1 + e^{\alpha u}} \operatorname{Ai}(x + u) \operatorname{Ai}(x' + u) du \tag{4.35}$$

with Ai the Airy function. For $\alpha = \infty$, M_α reduces to the usual Airy kernel, hence (4.34) reduces to the classical expression for the Tracy–Widom GUE distribution as a Fredholm determinant. We may now state our main result.

Theorem 4.4 (see [27, Theorems 1 and 2])**.** *Consider the cylindric Plancherel measure* (4.33) *with $q = e^{-r}$, and suppose that $r \to 0$ and/or $y \to \infty$ in such a way that $r^2 y \to \alpha$, where $\alpha \in [0, \infty]$ is fixed.*

— *In the* low-temperature *regime $\alpha = \infty$ or the crossover regime $0 < \alpha < \infty$, we have for all $x \in \mathbb{R}$*

$$\operatorname{Prob}\left(\frac{\lambda_1 - 2L}{L^{1/3}} \leq x\right) \to F_\alpha(x), \qquad L := \frac{y}{1-q}. \tag{4.36}$$

— *In the* high-temperature *regime $\alpha = 0$, we have for all $x \in \mathbb{R}$*

$$\operatorname{Prob}\left(\frac{\lambda_1 - r^{-1} \ln(r^{-1} I_0(2y + ry))}{r^{-1}} \leq x\right) \to e^{-e^{-x}} \tag{4.37}$$

where $I_0(z) := \frac{1}{2\pi} \int_{-\pi}^{\pi} e^{z \cos\phi} d\phi$ is the modified Bessel function of the first kind and order zero.

Our theorem encompasses the canonical case $y = 0$, for which we recover (4.32), and the Plancherel case $q = 0$ for which we recover the result of Baik, Deift and Johansson [BDJ99]. The physical intuition behind our theorem is the following. In the CPM the fluctuations of λ_1 have two origins: *thermal* fluctuations of order r^{-1}, governed by the Gumbel distribution, and *quantum* fluctuations of order $L^{1/3}$, governed by the Tracy–Widom GUE distribution. In the high-temperature regime ($r^{-1} \gg L^{1/3}$) the former wins, hence we observe the Gumbel distribution. In the low-temperature regime ($r^{-1} \ll L^{1/3}$) the latter wins, hence we observe the Tracy–Widom GUE distribution. Finally in the crossover regime ($r^{-1} \propto L^{1/3}$) both have the same order of magnitude, hence we observe the interpolating distribution. Note that, in the high-temperature regime, the parameter y actually affects the deterministic first-order asymptotics of λ_1. This may be related to the bulk asymptotics of the CPM, see the discussion in [27, Section 5]. We have also studied the crossover edge asymptotics of the cylindric Plancherel process, and shown that it involves the *finite-temperature extended Airy kernel* previously introduced by Le Doussal, Majumdar and Schehr [LDMS17] in the context of the equilibrium dynamics of noninteracting fermions in a harmonic trap. See [27, Section 6] for more details.

While we have not considered the edge asymptotics of periodic steep tilings in our paper, we believe that, by universality, Theorem 4.4 should hold with little modifications for generic edge points. In fact, our approach based on saddle-point computations should be easy to adapt to this situation.

Finally, let us briefly discuss the free boundary Schur process. In the paper [26], we considered the asymptotics in the case of one free boundary, corresponding to the pfaffian Schur process of Borodin and Rains [BR05]. We discussed the bulk asymptotics for two instances of the process, namely symmetric plane partitions and plane overpartitions. It should not be difficult to extend our results to the case of steep tilings. Regarding the edge asymptotics, we considered its application to *last passage percolation*, and encountered a limiting distribution that interpolates between the three Tracy–Widom GOE/GUE/GSE distributions.

The case of two free boundaries is still pretty much work in progress. We have announced some of our results in the extended abstract [28], where we establish a convergence in distribution similar to (4.36) for some free boundary analogues of the CPM. The corresponding limiting distributions are expressed in terms of certain *Fredholm pfaffians*, and appear not to have been considered before. Together with Dan Betea, Peter Nejjar and Mirjana Vuletić, we are currently writing the long journal paper that will be the sequel of [26], and which will treat both bulk and edge asymptotics in the presence of two free boundaries.

4.5 Conclusion and perspectives

In this chapter I have explained how, starting from the question of finding a general family of tilings encompassing both domino tilings of the Aztec diamond and pyramid partitions, I was led to study various aspects of Schur processes and join the very active field of integrable probability.

One paper left out of this chapter is [22], where we revisit the Robinson-Schensted-Knuth correspondence and its growth diagram formulation [Fom95], from the point of view of its applications to the sampling of Schur processes. In particular, we found an unexpected connection with the famous domino shuffling algorithm [EKLP92b].

Let me now list some of the questions I would like to address from now on. In the immediate future, I am eager to explore further the applications of the periodic and free boundary Schur processes to last passage percolation and exclusion processes. A particularly tantalizing question is the connection with the $(1+1)$-dimensional Kardar-Parisi-Zhang (KPZ) equation: as noted for instance in [DLDMS15], the finite-temperature Airy kernel which we encountered in (4.35) also appears in the KPZ context. To our knowledge, the fundamental origin of this coincidence is yet to be found. Also, we would like to investigate whether a similar connection exists for the kernels which we encounter in [28].

The approach of Baik, Deift and Johansson [BDJ99] for studying the edge asymptotics of the Plancherel measure on partitions was based on Riemann-Hilbert techniques. It would be interesting to extend this approach to the CPM, as our derivation of Theorem 4.4 was based rather different methods, namely determinantal point processes in the spirit of [BOO00, Joh01]. The Riemann-Hilbert approach seems better suited to analyze the asymptotics of the distribution F_α, as was done in the very recent preprint [CC19] which complements the probabilistic approach of [CG18]. Also, this might shed light on the free boundary case for which everything is open.

The next direction of research is the extension to nondeterminantal models such as Macdonald processes [BC14]. These processes have been recently related to the six vertex model by graphical methods [BBW16] and the approach was extended to the case of one free boundary [BBCW18]. It is then natural to ask whether periodic and (two) free boundary versions of the processes may be considered.

Finally, it seems that we left random maps out of this chapter, but a connection with them was made in [Oko00]: in this paper Okounkov uses an interplay between maps on surfaces and ramified coverings of the sphere, to give the first proof of a conjecture left by Baik, Deift and Johansson regarding the asymptotic joint distribution of the first parts $\lambda_1, \lambda_2, \lambda_3, \dots$ of a Plancherel random partition (subsequent proofs were given in [BOO00, Joh01] by determinantal point process techniques). I have just started supervising the M2 internship of Alejandro Caicedo who will study Okounkov's paper, and look for possible extensions to related models of random partitions.

General bibliography

[AB13] J. Ambjørn and T. G. Budd. Trees and spatial topology change in causal dynamical triangulations. *J. Phys. A*, 46(31):315201, 33, 2013, arXiv:1302.1763 [hep-th].

[AB16] J. Ambjørn and T. G. Budd. Multi-point functions of weighted cubic maps. *Ann. Inst. Henri Poincaré D*, 3(1):1–44, 2016, arXiv:1408.3040 [math-ph].

[ABA17] L. Addario-Berry and M. Albenque. The scaling limit of random simple triangulations and random simple quadrangulations. *Ann. Probab.*, 45(5):2767–2825, 2017, arXiv:1306.5227 [math.PR].

[ABM16] J. Ambjørn, T. Budd, and Y. Makeenko. Generalized multicritical one-matrix models. *Nuclear Physics B*, 913:357 – 380, 2016, arXiv:1604.04522 [hep-th].

[Abr16] C. Abraham. Rescaled bipartite planar maps converge to the Brownian map. *Ann. Inst. Henri Poincaré Probab. Stat.*, 52(2):575–595, 2016, arXiv:1312.5959 [math.PR].

[AC15] O. Angel and N. Curien. Percolations on random maps I: Half-plane models. *Ann. Inst. Henri Poincaré Probab. Stat.*, 51(2):405–431, 2015, arXiv:1301.5311 [math.PR].

[ACEH18] A. Alexandrov, G. Chapuy, B. Eynard, and J. Harnad. Weighted Hurwitz numbers and topological recursion: an overview. *J. Math. Phys.*, 59(8):081102, 21, 2018, arXiv:1305.1312 [math.CO].

[Ang03] O. Angel. Growth and percolation on the uniform infinite planar triangulation. *Geom. Funct. Anal.*, 13(5):935–974, 2003, arXiv:math/0208123 [math.PR].

[AP15] M. Albenque and D. Poulalhon. A generic method for bijections between blossoming trees and planar maps. *Electron. J. Combin.*, 22(2):Paper 2.38, 44, 2015, arXiv:1305.1312 [math.CO].

[Arq86] D. Arquès. Les hypercartes planaires sont des arbres très bien étiquetés. *Discrete Math.*, 58(1):11–24, 1986.

[AS03] O. Angel and O. Schramm. Uniform infinite planar triangulations. *Comm. Math. Phys.*, 241(2-3):191–213, 2003, arXiv:math/0207153 [math.PR].

[AW95] J. Ambjørn and Y. Watabiki. Scaling in quantum gravity. *Nuclear Phys. B*, 445(1):129–142, 1995, arXiv:hep-th/9501049.

[AZ13] A. Alexandrov and A. Zabrodin. Free fermions and tau-functions. *J. Geom. Phys.*, 67:37–80, 2013, arXiv:1212.6049 [math-ph].

[Bax82] R. J. Baxter. *Exactly solved models in statistical mechanics*. Academic Press, Inc. [Harcourt Brace Jovanovich, Publishers], London, 1982.

[Bax01] R. J. Baxter. Dichromatic polynomials and Potts models summed over rooted maps. *Ann. Comb.*, 5(1):17–36, 2001, arXiv:cond-mat/0011400 [cond-mat.stat-mech].

[BBCW18] G. Barraquand, A. Borodin, I. Corwin, and M. Wheeler. Stochastic six-vertex model in a half-quadrant and half-line open asymmetric simple exclusion process. *Duke Math. J.*, 167(13):2457–2529, 2018, arXiv:1704.04309 [math.PR].

[BBM11] O. Bernardi and M. Bousquet-Mélou. Counting colored planar maps: algebraicity results. *J. Combin. Theory Ser. B*, 101(5):315–377, 2011, arXiv:0909.1695 [math.CO].

[BBM17] O. Bernardi and M. Bousquet-Mélou. Counting coloured planar maps: differential equations. *Comm. Math. Phys.*, 354(1):31–84, 2017, arXiv:1507.02391 [math.CO].

[BBMDP17] N. Bonichon, M. Bousquet-Mélou, P. Dorbec, and C. Pennarun. On the number of planar Eulerian orientations. *European J. Combin.*, 65:59–91, 2017, arXiv:1610.09837 [math.CO].

[BBW16] A. Borodin, A. Bufetov, and M. Wheeler. Between the stochastic six vertex model and Hall-Littlewood processes, 2016, arXiv:1611.09486 [math.PR].

[BC11] O. Bernardi and G. Chapuy. A bijection for covered maps, or a shortcut between Harer-Zagier's and Jackson's formulas. *J. Combin. Theory Ser. A*, 118(6):1718–1748, 2011, arXiv:1001.1592 [math.CO].

[BC14] A. Borodin and I. Corwin. Macdonald processes. *Probab. Theory Related Fields*, 158(1-2):225–400, 2014, arXiv:1111.4408 [math.PR].

[BC17] T. Budd and N. Curien. Geometry of infinite planar maps with high degrees. *Electron. J. Probab.*, 22:Paper No. 35, 37, 2017, arXiv:1602.01328 [math.PR].

[BDFG02a] J. Bouttier, P. Di Francesco, and E. Guitter. Census of planar maps: from the one-matrix model solution to a combinatorial proof. *Nuclear Phys. B*, 645(3):477–499, 2002, arXiv:cond-mat/0207682.

[BDFG02b] J. Bouttier, P. Di Francesco, and E. Guitter. Critical and tricritical hard objects on bicolourable random lattices: exact solutions. *J. Phys. A*, 35(17):3821–3854, 2002, arXiv:cond-mat/0201213.

[BDFG03a] J. Bouttier, P. Di Francesco, and E. Guitter. Geodesic distance in planar graphs. *Nuclear Phys. B*, 663(3):535–567, 2003, arXiv:cond-mat/0303272.

[BDFG03b] J. Bouttier, P. Di Francesco, and E. Guitter. Statistics of planar graphs viewed from a vertex: a study via labeled trees. *Nuclear Phys. B*, 675(3):631–660, 2003, arXiv:cond-mat/0307606.

[BDFG04] J. Bouttier, P. Di Francesco, and E. Guitter. Planar maps as labeled mobiles. *Electron. J. Combin.*, 11(1):Research Paper 69, 27, 2004, arXiv:math/0405099.

[BDJ99] J. Baik, P. Deift, and K. Johansson. On the distribution of the length of the longest increasing subsequence of random permutations. *J. Amer. Math. Soc.*, 12(4):1119–1178, 1999, arXiv:math/9810105 [math.CO].

[BE11] G. Borot and B. Eynard. Enumeration of maps with self-avoiding loops and the $O(n)$ model on random lattices of all topologies. *J. Stat. Mech. Theory Exp.*, (1):P01010, 62, 2011, arXiv:0910.5896 [math-ph].

[Ber07] O. Bernardi. Bijective counting of tree-rooted maps and shuffles of parenthesis systems. *Electron. J. Combin.*, 14(1):Research Paper 9, 36 pp. (electronic), 2007, arXiv:math/0601684 [math.CO].

[Bet10] J. Bettinelli. Scaling limits for random quadrangulations of positive genus. *Electron. J. Probab.*, 15:no. 52, 1594–1644, 2010, arXiv:1002.3682 [math.PR].

[Bet12] J. Bettinelli. The topology of scaling limits of positive genus random quadrangulations. *Ann. Probab.*, 40(5):1897–1944, 2012, arXiv:1012.3726 [math.PR].

[Bet15] J. Bettinelli. A bijection for nonorientable general maps. arXiv:1512.02208 [math.CO], 2015, arXiv:1512.02208 [math.CO].

[BF12a] O. Bernardi and E. Fusy. A bijection for triangulations, quadrangulations, pentagulations, etc. *J. Combin. Theory Ser. A*, 119(1):218–244, 2012, arXiv:1007.1292 [math.CO].

[BF12b] O. Bernardi and E. Fusy. Unified bijections for maps with prescribed degrees and girth. *J. Combin. Theory Ser. A*, 119(6):1351–1387, 2012, arXiv:1102.3619 [math.CO].

[BF14] O. Bernardi and E. Fusy. Unified bijections for planar hypermaps with general cycle-length constraints, 2014, arXiv:1403.5371 [math.CO].

[BF18] O. Bernardi and E. Fusy. Bijections for planar maps with boundaries. *J. Combin. Theory Ser. A*, 158:176–227, 2018, arXiv:1510.05194 [math.CO].

[BFSS01] C. Banderier, P. Flajolet, G. Schaeffer, and M. Soria. Random maps, coalescing saddles, singularity analysis, and Airy phenomena. *Random Structures Algorithms*, 19(3-4):194–246, 2001. Analysis of algorithms (Krynica Morska, 2000).

[BG16] A. Borodin and V. Gorin. Lectures on integrable probability. In *Probability and statistical physics in St. Petersburg*, volume 91 of *Proc. Sympos. Pure Math.*, pages 155–214. Amer. Math. Soc., Providence, RI, 2016, arXiv:1212.3351 [math.PR].

[BGF16] G. Borot and E. Garcia-Failde. Nesting statistics in the $O(n)$ loop model on random maps of arbitrary topologies, 2016, arXiv:1609.02074 [math-ph].

[BHS18] O. Bernardi, N. Holden, and X. Sun. Percolation on triangulations: a bijective path to Liouville quantum gravity, 2018, arXiv:1807.01684 [math.PR].

[BJM14] J. Bettinelli, E. Jacob, and G. Miermont. The scaling limit of uniform random plane maps, *v*ia the Ambjørn-Budd bijection. *Electron. J. Probab.*, 19:no. 74, 16, 2014, arXiv:1312.5842 [math.PR].

[BK87] D. V. Boulatov and V. A. Kazakov. The Ising model on a random planar lattice: the structure of the phase transition and the exact critical exponents. *Phys. Lett. B*, 186(3-4):379–384, 1987.

[BKKM86] D. V. Boulatov, V. A. Kazakov, I. K. Kostov, and A. A. Migdal. Analytical and numerical study of a model of dynamically triangulated random surfaces. *Nuclear Phys. B*, 275(4):641–686, 1986.

[BLG13] J. Beltran and J.-F. Le Gall. Quadrangulations with no pendant vertices. *Bernoulli*, 19(4):1150–1175, 2013, arXiv:1307.7524 [math.PR].

[BLR17] N. Berestycki, B. Laslier, and G. Ray. Critical exponents on Fortuin-Kasteleyn weighted planar maps. *Comm. Math. Phys.*, 355(2):427–462, 2017, arXiv:1502.00450 [math.PR].

[BM17] J. Bettinelli and G. Miermont. Compact Brownian surfaces I: Brownian disks. *Probab. Theory Related Fields*, 167(3-4):555–614, 2017, arXiv:1507.08776 [math.PR].

[BMC15] M. Bousquet-Mélou and J. Courtiel. Spanning forests in regular planar maps. *J. Combin. Theory Ser. A*, 135:1–59, 2015, arXiv:1306.4536 [math.CO].

[BMEP18] M. Bousquet-Mélou and A. Elvey Price. The generating function of planar Eulerian orientations, 2018, arXiv:1803.08265 [math.CO].

[BMEPZJ19] M. Bousquet-Mélou, A. Elvey Price, and P. Zinn-Justin. Eulerian orientations and the six-vertex model on planar map. In *31th International Conference on Formal Power Series and Algebraic Combinatorics (FPSAC 2019)*, Sém. Lothar. Combin. 82B, Art. 70. 2019, arXiv:1902.07369 [math.CO].

[BMJ06] M. Bousquet-Mélou and A. Jehanne. Polynomial equations with one catalytic variable, algebraic series and map enumeration. *J. Combin. Theory Ser. B*, 96(5):623–672, 2006, arXiv:math/0504018 [math.CO].

[BMR16] E. Baur, G. Miermont, and G. Ray. Classification of scaling limits of uniform quadrangulations with a boundary. arXiv:1608.01129 [math.PR], 2016, arXiv:1608.01129 [math.PR].

[BMS02] M. Bousquet-Mélou and G. Schaeffer. The degree distribution in bipartite planar maps: applications to the Ising model, 2002, arXiv:math/0211070 [math.CO].

[Bon99] G. Bonnet. Solution of Potts-3 and Potts-∞ matrix models with the equations of motion method. *Phys. Lett. B*, 459(4):575–581, 1999, arXiv:hep-th/9904058.

[BOO00] A. Borodin, A. Okounkov, and G. Olshanski. Asymptotics of Plancherel measures for symmetric groups. *J. Amer. Math. Soc.*, 13(3):481–515, 2000, arXiv:math/9905032 [math.CO].

[Bor07] A. Borodin. Periodic Schur process and cylindric partitions. *Duke Math. J.*, 140(3):391–468, 2007, arXiv:math/0601019 [math.CO].

[Bor14] A. Borodin. Integrable probability. In *Proceedings of the International Congress of Mathematicians—Seoul 2014. Vol. 1*, pages 199–216. Kyung Moon Sa, Seoul, 2014.

[Bou05] J. Bouttier. *Physique statistique des surfaces aléatoires et combinatoire bijective des cartes planaires.* Doctoral thesis, Université Pierre et Marie Curie – Paris 6, June 2005. `https://tel.archives-ouvertes.fr/tel-00010651`.

[BR86] J.-P. Blaizot and G. Ripka. *Quantum theory of finite systems.* MIT, 1986.

[BR05] A. Borodin and E. M. Rains. Eynard-Mehta theorem, Schur process, and their Pfaffian analogs. *J. Stat. Phys.*, 121(3-4):291–317, 2005, arXiv:math-ph/0409059.

[Bud17a] T. Budd. On a connection between planar map combinatorics and lattice walks. Talk at the Workshop on Large Random Structures in Two Dimensions, IHP, January 2017. Slides at `http://hef.ru.nl/~tbudd/docs/combi17-talk.pdf`.

[Bud17b] T. Budd. Winding of simple walks on the square lattice, 2017, arXiv:1709.04042 [math.CO].

[Bud18] T. Budd. The peeling process on random planar maps coupled to an O(n) loop model, 2018, arXiv:1809.02012 [math.PR]. With an appendix by Linxiao Chen.

[Car19] A. Carrance. *Random colored triangulations.* Doctoral thesis, Université Claude Bernard – Lyon 1, September 2019. `https://tel.archives-ouvertes.fr/tel-02338972`.

[CC15] S. R. Carrell and G. Chapuy. Simple recurrence formulas to count maps on orientable surfaces. *J. Combin. Theory Ser. A*, 133:58–75, 2015, arXiv:1402.6300 [math.CO].

[CC19] M. Cafasso and T. Claeys. A Riemann-Hilbert approach to the lower tail of the KPZ equation, 2019, arXiv:1910.02493 [math-ph].

[CCM17] L. Chen, N. Curien, and P. Maillard. The perimeter cascade in critical Boltzmann quadrangulations decorated by an $O(n)$ loop model, 2017, arXiv:1702.06916 [math.PR].

[CD17] G. Chapuy and M. Dołega. A bijection for rooted maps on general surfaces. *J. Combin. Theory Ser. A*, 145:252–307, 2017, arXiv:1501.06942 [math.CO].

[CF03] P. Chassaing and P. Flajolet. Hachage, arbres, chemins & graphes. *Gaz. Math.*, (95):29–49, 2003.

[CF12] G. Collet and E. Fusy. A simple formula for the series of bipartite and quasi-bipartite maps with boundaries. In *24th International Conference on Formal Power Series and Algebraic Combinatorics (FPSAC 2012)*, Discrete Math. Theor. Comput. Sci. Proc., AR, pages 607–618. Assoc. Discrete Math. Theor. Comput. Sci., Nancy, 2012, arXiv:1205.5215 [math.CO].

[CFGN15] G. Chapuy, E. Fusy, O. Giménez, and M. Noy. On the diameter of random planar graphs. *Combin. Probab. Comput.*, 24(1):145–178, 2015, arXiv:1203.3079 [math.CO].

[CG18] I. Corwin and P. Ghosal. Lower tail of the KPZ equation, 2018, arXiv:1802.03273 [math.PR].

[Cha09] G. Chapuy. Asymptotic enumeration of constellations and related families of maps on orientable surfaces. *Combin. Probab. Comput.*, 18(4):477–516, 2009, arXiv:0805.0352 [math.CO].

[Cha16] G. Chapuy. On tessellations of random maps and the t_g-recurrence. arXiv:1603.07714 [math.PR], 2016, arXiv:1603.07714 [math.PR]. Extended abstract in Séminaire Lotharingien de Combinatoire, 78B.79 (2017).

[Cha18] G. Chapuy. Rencontres autour de la combinatoire des cartes. Habilitation à diriger des recherches, Université Paris Diderot, 2018. `https://www.irif.fr/~chapuy/chapuyHabilitationWeb.pdf`.

[Che17] L. Chen. Basic properties of the infinite critical-FK random map. *Ann. Inst. Henri Poincaré D*, 4(3):245–271, 2017, arXiv:1502.01013 [math.PR].

[Che18] L. Chen. *Random Planar Maps coupled to Spin Systems*. Doctoral thesis, Université Paris-Saclay, April 2018. `https://tel.archives-ouvertes.fr/tel-01774839`.

[CK15] N. Curien and I. Kortchemski. Percolation on random triangulations and stable looptrees. *Probab. Theory Related Fields*, 163(1-2):303–337, 2015, arXiv:1307.6818 [math.PR].

[CLG15] N. Curien and J.-F. Le Gall. First-passage percolation and local modifications of distances in random triangulations, 2015, arXiv:1511.04264 [math.PR].

[CMS09] G. Chapuy, M. Marcus, and G. Schaeffer. A bijection for rooted maps on orientable surfaces. *SIAM J. Discrete Math.*, 23(3):1587–1611, 2009, arXiv:0712.3649 [math.CO].

[CR18] N. Curien and L. Richier. Duality of random planar maps via percolation, 2018, arXiv:1802.01576 [math.PR].

[CS04] P. Chassaing and G. Schaeffer. Random planar lattices and integrated superBrownian excursion. *Probab. Theory Related Fields*, 128(2):161–212, 2004, arXiv:math/0205226 [math.CO].

[CS05] S. Caracciolo and A. Sportiello. The $O(n)$ vector model at $n = -1, -2$ on random planar lattices: a direct combinatorial derivation. *J. Stat.*

Mech. Theory Exp., (2):L02002, 8, 2005, arXiv:cond-mat/0412327 [cond-mat.stat-mech].

[CT18] L. Chen and J. Turunen. Critical Ising model on random triangulations of the disk: enumeration and local limits, 2018, arXiv:1806.06668 [math.PR].

[Cur19] N. Curien. Peeling random planar maps. Lecture notes of the 2019 Saint-Flour Probability Summer School, preliminary version available at `https://www.math.u-psud.fr/~curien/enseignement.html`, 2019.

[CV81] R. Cori and B. Vauquelin. Planar maps are well labeled trees. *Canad. J. Math.*, 33(5):1023–1042, 1981.

[Dau95] J.-M. Daul. Q-states Potts model on a random planar lattice. arXiv:hep-th/9502014, 1995, arXiv:hep-th/9502014.

[Del03] J.-F. Delmas. Computation of moments for the length of the one dimensional ISE support. *Electron. J. Probab.*, 8(17):1–15, 2003.

[Der18] C. Dervieux. *Énumération de cartes planaires orientées*. Doctoral thesis, Université Paris Diderot – Paris 7, June 2018.

[DG19] J. Ding and E. Gwynne. The fractal dimension of Liouville quantum gravity: universality, monotonicity, and bounds. *Comm. Math. Phys.*, 2019, arXiv:1807.01072 [math.PR].

[DK88] B. Duplantier and I. Kostov. Conformal spectra of polymers on a random surface. *Phys. Rev. Lett.*, 61(13):1433–1437, 1988.

[DLDMS15] D. S. Dean, P. Le Doussal, S. N. Majumdar, and G. Schehr. Finite-temperature free fermions and the kardar-parisi-zhang equation at finite time. *Phys. Rev. Lett.*, 114:110402, Mar 2015, arXiv:1412.1590 [cond-mat.stat-mech].

[DLDRP00] A. Del Lungo, F. Del Ristoro, and J.-G. Penaud. Left ternary trees and non-separable rooted planar maps. *Theoret. Comput. Sci.*, 233(1-2):201–215, 2000.

[DMNS81] E. Domany, D. Mukamel, B. Nienhuis, and A. Schwimmer. Duality relations and equivalences for models with o(n) and cubic symmetry. *Nuclear Physics B*, 190(2):279 – 287, 1981.

[DMS14] B. Duplantier, J. Miller, and S. Sheffield. Liouville quantum gravity as a mating of trees, 2014, arXiv:1409.7055 [math.PR].

[DPS16] C. Dervieux, D. Poulalhon, and G. Schaeffer. The number of corner polyhedra graphs. In *28th International Conference on Formal Power Series and Algebraic Combinatorics (FPSAC 2016)*, Discrete Math. Theor. Comput. Sci. Proc., BC, pages 371–382. Assoc. Discrete Math. Theor. Comput. Sci., Nancy, 2016. `https://fpsac2016.sciencesconf.org/113744`.

[dT15] B. de Tilière. The dimer model in statistical mechanics. In *Dimer models and random tilings*, volume 45 of *Panor. Synthèses*, pages 1–45. Soc. Math. France, Paris, 2015.

[Dup04] B. Duplantier. Conformal fractal geometry & boundary quantum gravity. In *Fractal geometry and applications: a jubilee of Benoît Mandelbrot, Part 2*, volume 72 of *Proc. Sympos. Pure Math.*, pages 365–482. Amer. Math. Soc., Providence, RI, 2004, arXiv:math-ph/0303034.

[EB99] B. Eynard and G. Bonnet. The Potts-q random matrix model: loop equations, critical exponents, and rational case. *Phys. Lett. B*, 463(2-4):273–279, 1999, arXiv:hep-th/9906130.

[EG14] B. Eynard and E. Guitter. Distances sur les mobiles, et systèmes intégrables. Talk at the *Journées Cartes*, April 2014. Abstract at `http://cartaplus.math.cnrs.fr/JourneeCarte29avril2014#Eynard`.

[EK95] B. Eynard and C. Kristjansen. Exact solution of the $O(n)$ model on a random lattice. *Nuclear Phys. B*, 455(3):577–618, 1995, arXiv:hep-th/9506193.

[EK96] B. Eynard and C. Kristjansen. More on the exact solution of the $O(n)$ model on a random lattice and an investigation of the case $|n| > 2$. *Nuclear Phys. B*, 466(3):463–487, 1996, arXiv:hep-th/9512052.

[EKLP92a] N. Elkies, G. Kuperberg, M. Larsen, and J. Propp. Alternating-sign matrices and domino tilings. I. *J. Algebraic Combin.*, 1(2):111–132, 1992, arXiv:math/9201305 [math.CO].

[EKLP92b] N. Elkies, G. Kuperberg, M. Larsen, and J. Propp. Alternating-sign matrices and domino tilings. II. *J. Algebraic Combin.*, 1(3):219–234, 1992, arXiv:math/9201305 [math.CO].

[EL41] P. Erdős and J. Lehner. The distribution of the number of summands in the partitions of a positive integer. *Duke Math. J*, 8(2):335–345, 1941.

[EM14] D. Eppstein and E. Mumford. Steinitz theorems for simple orthogonal polyhedra. *J. Comput. Geom.*, 5(1):179–244, 2014.

[EPG18] A. Elvey Price and A. J. Guttmann. Counting planar Eulerian orientations. *European J. Combin.*, 71:73–98, 2018, arXiv:1707.09120 [math.CO].

[Eyn16] B. Eynard. *Counting surfaces*, volume 70 of *Progress in Mathematical Physics*. Birkhäuser/Springer, [Cham], 2016. CRM Aisenstadt chair lectures.

[EZJ92] B. Eynard and J. Zinn-Justin. The $O(n)$ model on a random surface: critical points and large-order behaviour. *Nuclear Phys. B*, 386(3):558–591, 1992, arXiv:hep-th/9204082.

[Fel04] S. Felsner. Lattice structures from planar graphs. *Electron. J. Combin.*, 11(1):Research Paper 15, 24, 2004.

[FG14] E. Fusy and E. Guitter. The three-point function of general planar maps. *J. Stat. Mech. Theory Exp.*, (9):p09012, 39, 2014, arXiv:1403.3514 [math.CO].

[Fla80] P. Flajolet. Combinatorial aspects of continued fractions. *Discrete Math.*, 32(2):125–161, 1980.

[Fom95] S. Fomin. Schur operators and Knuth correspondences. *J. Combin. Theory Ser. A*, 72(2):277–292, 1995.

[FS09] P. Flajolet and R. Sedgewick. *Analytic combinatorics*. Cambridge University Press, Cambridge, 2009. Available online at `http://algo.inria.fr/flajolet/Publications/books.html`.

[FSP08] E. Fusy, G. Schaeffer, and D. Poulalhon. Dissections, orientations, and trees with applications to optimal mesh encoding and random sampling. *ACM Trans. Algorithms*, 4(2):Art. 19, 48, 2008, arXiv:0810.2608 [math.CO].

[Fus07] E. Fusy. Straight-line drawing of quadrangulations. In *Graph drawing*, volume 4372 of *Lecture Notes in Comput. Sci.*, pages 234–239. Springer, Berlin, 2007.

[Fus09] E. Fusy. Transversal structures on triangulations: a combinatorial study and straight-line drawings. *Discrete Math.*, 309(7):1870–1894, 2009, arXiv:math/0602163 [math.CO].

[GHS17] E. Gwynne, N. Holden, and X. Sun. A mating-of-trees approach for graph distances in random planar maps, 2017, arXiv:1711.00723 [math.PR].

[GJSZJ12] A. Guionnet, V. F. R. Jones, D. Shlyakhtenko, and P. Zinn-Justin. Loop models, random matrices and planar algebras. *Comm. Math. Phys.*, 316(1):45–97, 2012, arXiv:1012.0619 [math.OA].

[GK89] M. Gaudin and I. Kostov. $O(n)$ model on a fluctuating planar lattice. Some exact results. *Phys. Lett. B*, 220(1-2):200–206, 1989.

[GKMW18] E. Gwynne, A. Kassel, J. Miller, and D. B. Wilson. Active spanning trees with bending energy on planar maps and SLE-decorated Liouville quantum gravity for $\kappa > 8$. *Comm. Math. Phys.*, 358(3):1065–1115, 2018, arXiv:1603.09722 [math.PR].

[GMS17] E. Gwynne, J. Miller, and S. Sheffield. The Tutte embedding of the mated-CRT map converges to Liouville quantum gravity, 2017, arXiv:1705.11161 [math.PR].

[GMS19] E. Gwynne, C. Mao, and X. Sun. Scaling limits for the critical Fortuin-Kasteleyn model on a random planar map I: Cone times. *Ann. Inst. Henri Poincaré Probab. Stat.*, 55(1):1–60, 2019, arXiv:1502.00546 [math.PR].

[GS15] E. Gwynne and X. Sun. Scaling limits for the critical Fortuin-Kasteleyn model on a random planar map III: finite volume case, 2015, arXiv:1510.06346 [math.PR].

[GS17] E. Gwynne and X. Sun. Scaling limits for the critical Fortuin-Kasteleyn model on a random planar map II: local estimates and empty reduced word exponent. *Electron. J. Probab.*, 22:Paper No. 45, 56, 2017, arXiv:1505.03375 [math.PR].

[Gui17] E. Guitter. On a conjecture by Chapuy about Voronoï cells in large maps. *J. Stat. Mech. Theory Exp.*, (10):103401, 33, 2017, arXiv:1703.02781 [math.CO].

[JJ00] W. Janke and D. A. Johnston. Ising and Potts models on quenched random gravity graphs. *Nuclear Phys. B*, 578(3):681–698, 2000, arXiv:hep-lat/9907026.

[JM83] M. Jimbo and T. Miwa. Solitons and infinite-dimensional Lie algebras. *Publ. Res. Inst. Math. Sci.*, 19(3):943–1001, 1983.

[Joh01] K. Johansson. Discrete orthogonal polynomial ensembles and the Plancherel measure. *Ann. of Math. (2)*, 153(1):259–296, 2001, arXiv:math/9906120 [math.CO].

[Joh02] K. Johansson. Non-intersecting paths, random tilings and random matrices. *Probab. Theory Related Fields*, 123(2):225–280, 2002, arXiv:math/0011250 [math.PR].

[Joh03] K. Johansson. Discrete polynuclear growth and determinantal processes. *Comm. Math. Phys.*, 242(1-2):277–329, 2003, arXiv:math/0206208 [math.PR].

[Joh05] K. Johansson. The arctic circle boundary and the Airy process. *Ann. Probab.*, 33(1):1–30, 2005, arXiv:math/0306216 [math.PR].

[Joh07] K. Johansson. From gumbel to tracy-widom. *Probability theory and related fields*, 138(1-2):75–112, 2007, arXiv:math/0510181 [math.PR].

[JS98] B. Jacquard and G. Schaeffer. A bijective census of nonseparable planar maps. *J. Combin. Theory Ser. A*, 83(1):1–20, 1998.

[Kac90] V. G. Kac. *Infinite-dimensional Lie algebras*. Cambridge University Press, Cambridge, third edition, 1990.

[Kaz86] V. A. Kazakov. Ising model on a dynamical planar random lattice: exact solution. *Phys. Lett. A*, 119(3):140–144, 1986.

[Kaz88] V. A. Kazakov. Exactly solvable Potts models, bond- and tree-like percolation on dynamical (random) planar lattice. *Nuclear Phys. B Proc. Suppl.*, 4:93–97, 1988. Field theory on the lattice (Seillac, 1987).

[Kaz89] V. A. Kazakov. The appearance of matter fields from quantum fluctuations of 2D-gravity. *Modern Phys. Lett. A*, 4(22):2125–2139, 1989.

[KMSW19] R. Kenyon, J. Miller, S. Sheffield, and D. B. Wilson. Bipolar orientations on planar maps and SLE_{12}. *Ann. Probab.*, 47(3):1240–1269, 2019, arXiv:1511.04068 [math.PR].

[Kos89] I. K. Kostov. $O(n)$ vector model on a planar random lattice: spectrum of anomalous dimensions. *Modern Phys. Lett. A*, 4(3):217–226, 1989.

[Kos92] I. K. Kostov. Gauge invariant matrix model for the $\hat{A}$-$\hat{D}$-$\hat{E}$ closed strings. *Phys. Lett. B*, 297(1-2):74–81, 1992, arXiv:hep-th/9208053.

[Kos96] I. K. Kostov. Solvable statistical models on a random lattice. *Nuclear Phys. B Proc. Suppl.*, 45A:13–28, 1996, arXiv:hep-th/9509124. Recent developments in statistical mechanics and quantum field theory (Trieste, 1995).

[Kos00] I. K. Kostov. Exact solution of the six-vertex model on a random lattice. *Nuclear Phys. B*, 575(3):513–534, 2000, arXiv:hep-th/9911023.

[KOS06] R. Kenyon, A. Okounkov, and S. Sheffield. Dimers and amoebae. *Ann. of Math. (2)*, 163(3):1019–1056, 2006, arXiv:math-ph/0311005.

[KPZ88] V. G. Knizhnik, A. M. Polyakov, and A. B. Zamolodchikov. Fractal structure of 2D-quantum gravity. *Modern Phys. Lett. A*, 3(8):819–826, 1988.

[KS92] I. K. Kostov and M. Staudacher. Multicritical phases of the $O(n)$ model on a random lattice. *Nuclear Phys. B*, 384(3):459–483, 1992, arXiv:hep-th/9203030.

[LDMS17] P. Le Doussal, S. N. Majumdar, and G. Schehr. Periodic Airy process and equilibrium dynamics of edge fermions in a trap. *Ann. Physics*, 383:312–345, 2017, arXiv:1702.06931 [cond-mat.stat-mech].

[Leh19] T. Lehéricy. First-passage percolation in random planar maps and Tutte's bijection, 2019, arXiv:1906.10079 [math.PR].

[Lep19] M. Lepoutre. Blossoming bijection for higher-genus maps. *J. Combin. Theory Ser. A*, 165:187–224, 2019, arXiv:1711.05606 [math.CO].

[LG07] J.-F. Le Gall. The topological structure of scaling limits of large planar maps. *Invent. Math.*, 169(3):621–670, 2007, arXiv:math/0607567 [math.PR].

[LG10] J.-F. Le Gall. Geodesics in large planar maps and in the Brownian map. *Acta Math.*, 205(2):287–360, 2010, arXiv:0804.3012 [math.PR].

[LG13] J.-F. Le Gall. Uniqueness and universality of the Brownian map. *Ann. Probab.*, 41(4):2880–2960, 2013, arXiv:1105.4842 [math.PR].

[LGM11] J.-F. Le Gall and G. Miermont. Scaling limits of random planar maps with large faces. *Ann. Probab.*, 39(1):1–69, 2011, arXiv:0907.3262 [math.PR].

[LGM12] J.-F. Le Gall and G. Miermont. Scaling limits of random trees and planar maps. In *Probability and statistical physics in two and more dimensions*, volume 15 of *Clay Math. Proc.*, pages 155–211. Amer. Math. Soc., Providence, RI, 2012, arXiv:1101.4856 [math.PR].

[LGP08] J.-F. Le Gall and F. Paulin. Scaling limits of bipartite planar maps are homeomorphic to the 2-sphere. *Geom. Funct. Anal.*, 18(3):893–918, 2008, arXiv:math/0612315 [math.PR].

[LZ04] S. K. Lando and A. K. Zvonkin. *Graphs on surfaces and their applications*, volume 141 of *Encyclopaedia of Mathematical Sciences*. Springer-Verlag, Berlin, 2004. With an appendix by Don B. Zagier, Low-Dimensional Topology, II.

[Mac95] I. G. Macdonald. *Symmetric functions and Hall polynomials*. Oxford Mathematical Monographs. The Clarendon Press, Oxford University Press, New York, second edition, 1995. With contributions by A. Zelevinsky, Oxford Science Publications.

[Mar18a] C. Marzouk. On scaling limits of planar maps with stable face-degrees. *ALEA Lat. Am. J. Probab. Math. Stat.*, 15(2):1089–1122, 2018, arXiv:1803.07899 [math.PR].

[Mar18b] C. Marzouk. Scaling limits of random bipartite planar maps with a prescribed degree sequence. *Random Structures & Algorithms*, 53(3):448–503, 2018, arXiv:1612.08618 [math.PR].

[Mie06] G. Miermont. An invariance principle for random planar maps. In *Fourth Colloquium on Mathematics and Computer Science Algorithms, Trees, Combinatorics and Probabilities*, Discrete Math. Theor. Comput. Sci. Proc., AG, pages 39–57. Assoc. Discrete Math. Theor. Comput. Sci., Nancy, 2006.

[Mie08] G. Miermont. On the sphericity of scaling limits of random planar quadrangulations. *Electron. Commun. Probab.*, 13:248–257, 2008, arXiv:0712.3687 [math.PR].

[Mie09] G. Miermont. Tessellations of random maps of arbitrary genus. *Ann. Sci. Éc. Norm. Supér. (4)*, 42(5):725–781, 2009, arXiv:0712.3688 [math.PR].

[Mie13] G. Miermont. The Brownian map is the scaling limit of uniform random plane quadrangulations. *Acta Math.*, 210(2):319–401, 2013, arXiv:1104.1606 [math.PR].

[Mie14] G. Miermont. Aspects of random maps. Lecture notes of the 2014 Saint-Flour Probability Summer School, preliminary version available at `http://perso.ens-lyon.fr/gregory.miermont/coursSaint-Flour.pdf`, 2014.

[MJD00] T. Miwa, M. Jimbo, and E. Date. *Solitons*, volume 135 of *Cambridge Tracts in Mathematics*. Cambridge University Press, Cambridge, 2000. Differential equations, symmetries and infinite-dimensional algebras, Translated from the 1993 Japanese original by Miles Reid.

[MM06] J.-F. Marckert and A. Mokkadem. Limit of normalized quadrangulations: the Brownian map. *Ann. Probab.*, 34(6):2144–2202, 2006, arXiv:math/0403398 [math.PR].

[MS68] R. C. Mullin and P. J. Schellenberg. The enumeration of c-nets via quadrangulations. *J. Combinatorial Theory*, 4:259–276, 1968.

[MS15a] J. Miller and S. Sheffield. An axiomatic characterization of the Brownian map, 2015, arXiv:1506.03806 [math.PR].

[MS15b] J. Miller and S. Sheffield. Liouville quantum gravity and the Brownian map I: The QLE(8/3,0) metric, 2015, arXiv:1507.00719 [math.PR].

[MS16a] J. Miller and S. Sheffield. Liouville quantum gravity and the Brownian map II: geodesics and continuity of the embedding, 2016, arXiv:1605.03563 [math.PR].

[MS16b] J. Miller and S. Sheffield. Liouville quantum gravity and the Brownian map III: the conformal structure is determined, 2016, arXiv:1608.05391 [math.PR].

[MS16c] J. Miller and S. Sheffield. Quantum Loewner evolution. *Duke Math. J.*, 165(17):3241–3378, 2016, arXiv:1312.5745 [math.PR].

[Mul67] R. C. Mullin. On the enumeration of tree-rooted maps. *Canad. J. Math.*, 19:174–183, 1967.

[MWW16] J. Miller, S. S. Watson, and D. B. Wilson. Extreme nesting in the conformal loop ensemble. *Ann. Probab.*, 44(2):1013–1052, 2016, arXiv:1401.0217 [math.PR].

[Nun16] F. Nunzi. *Autour de quelques chaînes de Markov combinatoires*. Doctoral thesis, Université Paris Diderot – Paris 7, December 2016. `https://www.theses.fr/fr/2016USPCC270`.

[Oko00] A. Okounkov. Random matrices and random permutations. *Internat. Math. Res. Notices*, (20):1043–1095, 2000, arXiv:math/9903176 [math.CO].

[Oko01] A. Okounkov. Infinite wedge and random partitions. *Selecta Math. (N.S.)*, 7(1):57–81, 2001, arXiv:math/9907127 [math.RT].

[OR03] A. Okounkov and N. Reshetikhin. Correlation function of Schur process with application to local geometry of a random 3-dimensional Young diagram. *J. Amer. Math. Soc.*, 16(3):581–603 (electronic), 2003, arXiv:math/0107056 [math.CO].

[OR07] A. Okounkov and N. Reshetikhin. Random skew plane partitions and the Pearcey process. *Comm. Math. Phys.*, 269(3):571–609, 2007, arXiv:math/0503508 [math.CO].

[ORV06] A. Okounkov, N. Reshetikhin, and C. Vafa. Quantum Calabi-Yau and classical crystals. In *The unity of mathematics*, volume 244 of *Progr. Math.*, pages 597–618. Birkhäuser Boston, Boston, MA, 2006, arXiv:hep-th/0309208.

[Pro93] J. Propp. Lattice structures for orientations of graphs, 1993, arXiv:math/0209005 [math.CO].

[PS02] M. Prähofer and H. Spohn. Scale invariance of the PNG droplet and the Airy process. *J. Statist. Phys.*, 108(5-6):1071–1106, 2002, arXiv:math/0105240 [math.PR]. Dedicated to David Ruelle and Yasha Sinai on the occasion of their 65th birthdays.

[PS03] D. Poulalhon and G. Schaeffer. A bijection for triangulations of a polygon with interior points and multiple edges. *Theoret. Comput. Sci.*, 307(2):385–401, 2003. Random generation of combinatorial objects and bijective combinatorics.

[PS06] D. Poulalhon and G. Schaeffer. Optimal coding and sampling of triangulations. *Algorithmica*, 46(3-4):505–527, 2006.

[Rai00] E. M. Rains. Correlation functions for symmetrized increasing subsequences, 2000, arXiv:math/0006097 [math.CO].

[Ric18] L. Richier. Limits of the boundary of random planar maps. *Probab. Theory Related Fields*, 172(3-4):789–827, 2018, arXiv:1704.01950 [math.PR].

[Rom15] D. Romik. *The surprising mathematics of longest increasing subsequences.* Institute of Mathematical Statistics Textbooks. Cambridge University Press, New York, 2015. `https://www.math.ucdavis.edu/~romik/book/`.

[Sch98] G. Schaeffer. *Conjugaison d'arbres et cartes combinatoires aléatoires.* Doctoral thesis, Université Bordeaux I, December 1998. `http://www.lix.polytechnique.fr/~schaeffe/Biblio/PhD-Schaeffer.pdf`.

[Sch07] O. Schramm. Conformally invariant scaling limits: an overview and a collection of problems. In *International Congress of Mathematicians. Vol. I*, pages 513–543. Eur. Math. Soc., Zürich, 2007, arXiv:math/0602151 [math.PR].

[Sch15] G. Schaeffer. Planar maps. In *Handbook of enumerative combinatorics*, Discrete Math. Appl. (Boca Raton), pages 335–395. CRC Press, Boca Raton, FL, 2015. `http://www.lix.polytechnique.fr/~schaeffe/Biblio/HB.pdf`.

[She16] S. Sheffield. Quantum gravity and inventory accumulation. *Ann. Probab.*, 44(6):3804–3848, 2016, arXiv:1108.2241 [math.PR].

[Sta90] M. Staudacher. The Yang-Lee edge singularity on a dynamical planar random surface. *Nuclear Phys. B*, 336(3):349–362, 1990.

[Sta99] R. P. Stanley. *Enumerative combinatorics. Vol. 2*, volume 62 of *Cambridge Studies in Advanced Mathematics*. Cambridge University Press, Cambridge, 1999. With a foreword by Gian-Carlo Rota and appendix 1 by Sergey Fomin.

[SW15] X. Sun and D. B. Wilson. Sandpiles and unicycles on random planar maps, 2015, arXiv:1506.08881 [math.PR].

[Tut62a] W. T. Tutte. A census of planar triangulations. *Canad. J. Math.*, 14:21–38, 1962.

[Tut62b] W. T. Tutte. A census of slicings. *Canad. J. Math.*, 14:708–722, 1962.

[Tut63] W. T. Tutte. A census of planar maps. *Canad. J. Math.*, 15:249–271, 1963.

[Tut71] W. T. Tutte. Dichromatic sums for rooted planar maps. In *Combinatorics (Proc. Sympos. Pure Math., Vol. XIX, Univ. California, Los Angeles, Calif., 1968)*, pages 235–245. Amer. Math. Soc., Providence, R.I., 1971.

[Tut95] W. T. Tutte. Chromatic sums revisited. *Aequationes Math.*, 50(1-2):95–134, 1995.

[Ver96] A. M. Vershik. Statistical mechanics of combinatorial partitions, and their limit shapes. *Functional Analysis and Its Applications*, 30(2):90–105, 1996.

[Vie84] X. Viennot. Une théorie combinatoire des polynômes orthogonaux. Notes from lectures given at LACIM, UQAM, Montréal, 1984. `http://www.xavierviennot.org/xavier/polynomes_orthogonaux.html`.

[You09] B. Young. Computing a pyramid partition generating function with dimer shuffling. *J. Combin. Theory Ser. A*, 116(2):334–350, 2009, arXiv:0709.3079 [math.CO].

[You10] B. Young. Generating functions for colored 3D Young diagrams and the Donaldson-Thomas invariants of orbifolds. *Duke Math. J.*, 152(1):115–153, 2010, arXiv:0802.3948 [math.CO]. With an appendix by Jim Bryan.

[ZJ00a] P. Zinn-Justin. The dilute Potts model on random surfaces. *J. Statist. Phys.*, 98(1-2):j10–264, 2000, arXiv:cond-mat/9903385 [cond-mat.stat-mech].

[ZJ00b] P. Zinn-Justin. The six-vertex model on random lattices. *Europhys. Lett.*, 50(1):15–21, 2000, arXiv:cond-mat/9909250 [cond-mat.stat-mech].

[ZJ08] P. Zinn-Justin. Six-vertex, loop and tiling models: integrability and combinatorics. Habilitation à diriger des recherches, Université Pierre et Marie Curie, 2008, arXiv:0901.0665 [math-ph].